LASER-INDUCED BREAKDOWN SPECTROSCOPY ON BACTERIAL SAMPLES

by

JONATHAN DIEDRICH

THESIS

Submitted to the Graduate School

of Wayne State University,

Detroit, Michigan

in partial fulfillment of the requirements

for the degree of

MASTER OF SCIENCE

2007

MAJOR: PHYSICS

Approved by:

_____

Advisor Date

_____

_____

_____

Table of Contents

List of Tables

List of Figures

Chapter 1 Introduction

1 Introduction

Bacterial identification has long been an interest for many fields of science. Microbiology, physics and medicine are just a few of the fields that have developed techniques for identifying bacteria. Just in the past three years, there have been several research efforts focused primarily on laser-based detection and identification of microbiological and pathogenic materials.[1-3] As could be imagined a lot of the research being done was to detect harmful biological agents that could be used in bioterrorism.[4-7] However; not all applications of bacterial identification were for military purposes. Identification of bacteria that can cause disease in civilian populations of humans is also of importance. The *Escherichia coli* bacterium is responsible for many diseases and illnesses in humans. Detection and identification of the different strains have been done through several different techniques. Many methods are time consuming and require a great deal of expertise to perform. A simple, quick, reliable method that could detect and identify *E. coli* would be a valuable tool.

1.1 Bacterial Detection

1.1.1 Non-optical methods

There are many methods that can be employed for identifying bacteria and to that extent to identify different strains of the same bacterial species. There are several methods that employ non-optical techniques. Genotyping, phenotyping, serotyping and gram staining are just of few of said techniques.

- **Genotyping**

A genotype describes the specific allelic constituents of an organism. Therefore genotyping is the identification of an organism's genotype. Typically this is done for identification purposes. Current methods of genotyping include polymerase chain reaction (PCR), DNA sequencing and hybridization to DNA micro arrays. Genotyping has been used for identification of microbial pathogens as well as bacteria including *E. coli*.[4, 9]

- **Phenotyping**

A phenotype is any detectable characteristic of an organism. This could be structural characteristics, biochemical signatures or behavioral tendencies. A phenotype is an organisms genotype responding to its environment. Thus when using phenotyping to identify bacteria, changes are made to the bacteria's environment and its response is studied and compared to know information.

- **Serotyping**

Serotype or serovar is a grouping of organisms based on their cell surface antigens. As such, it is particularly sensitive to the bacteria's surface or membrane chemistry and/or morphology. Serovars may be established based on virulence factors, lipopolysaccharides in Gram-negative bacteria, presence of an exotoxin (pertussis toxin in *Bordetella pertussis,* for example), plasmids, phages, or other characteristics which differentiate two members of the same species. [10, 11] Serotyping has been demonstrated to be effective in identification of *E. coli*. [12]

- **Gram Staining**

Gram staining can be used to identify bacteria based on the reaction of the bacteria to a stain applied to it. Based on the chemical and physical properties of the bacterial cell wall it is possible to divide bacteria into two large groups (Gram-negative or Gram-positive depending on the stain response) and to discriminate between types of bacteria. [20, 21]

1.1.2 Optical Methods

More recently, nano-biosensors and optical methods have also been used for bacterial detection. Nano-biosensors include the use of gold nano-wire arrays, fiber optic biosensors, Raman Spectroscopy and Laser-Induced Breakdown Spectroscopy (LIBS). [13-16]

- Optical Leaky Waveguide Sensors:

Optical leaky waveguide sensors have been used for the detection of pathogenic particles such as bacteria. These sensors utilize a waveguide through which a resonant laser beam is propagated and a biosensor chip with bacteria-specific antibodies to capture and "tag" the bacteria. The sensor chips are tailored to give the maximum extension of the evanescent field at the sensor surface in order to place the entire volume of the bacteria captured by immobilized antibodies on the chip surface within this field. This in turn increases the interaction of the light with the bacteria's bulk volume. These sensors have been characterized by detecting refractive index changes, scattering, and fluorescence from bacterial spores at the sensor surface when illuminated at the coupling angle. [17]

- Fiber Optic Biosensors

Fiber optic biosensors are a rapid, sensitive technology for *E. coli* detection.[18] It can be done in near real-time making it an attractive method for individuals in the food industry. The technique uses an immunoassay specific to the strain of *E. coli* as the principle detection method.[18] An immunoassay is a biochemical test that measures the amount of substance in a biological liquid. Immunoassay uses an antibody specific for the substance to be detected. If the substance, or antigen, is present it will interact with the antibody by binding to it.

There are two types of immunoassays, competitive and noncompetitive.[19] In the case of the fiber optical biosensors the noncompetitive immunoassay is used, this is said to be the standard "sandwich" technique. This method only allows binding if the unknown substance is present. [22] In the case of *E. coli* a dye-labeled antibody specific to *E. coli* is used to detect the *E. coli* cells by generating a fluorescent signal due to the laser energy incident upon the sample. Fluorescent molecules within several hundred nanometers of the fiber are excited by an evanescent wave, and a portion of the emission light from the fluorescent dye is transmitted by the fiber and collected by a photodetector at wavelengths of 670 to 710 nm. The immunosensor described was specific for *E. coli* O157:H7 but could be modified for other bacteria.[23-25] A schematic of an optical setup using a fiber-optic biosensor for collection of data is shown in Figure 1.

These methods can be very useful in their ability to detect bacteria given the right set of circumstances. However; the above methods do have some draw backs. First, they are pathogen specific: only the particular pathogen that responds to the antibody can be detected. Both Raman spectroscopy and LIBS do not suffer this short coming. Second,

they have a limited shelf life. Several use a chemical (antibodies) that don't keep forever. This in effect puts a shelf life on the ability to detect. Lastly, these techniques require contact with the pathogen; again LIBS and Raman, both optical techniques, allow testing at stand-off distances.

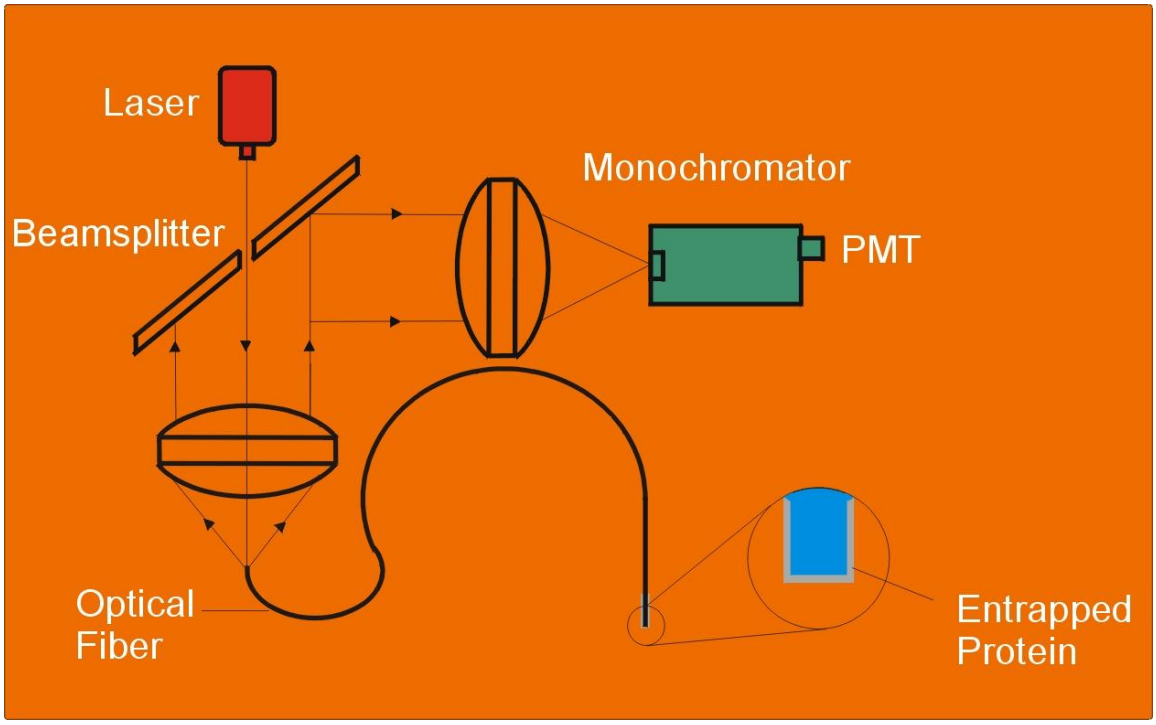

Figure 1. Fiber-optic biosensor experimental setup [26]

1.2 Laser-Induced Breakdown Spectroscopy

Another method used to detect bacteria is Laser-Induced Breakdown Spectroscopy (LIBS). LIBS is an all optical type of atomic emission spectroscopy. The LIBS experimental setup is simple. A high energy laser pulse is used as the excitation source. The laser pulse vaporizes a portion of the target (ablation) and creates a high-temperature microplasma containing atoms from that vapor. A spectrometer is used to disperse and analyze the light collected from the ablation sample. Finally, a computer is used as a

source of timing for the laser and spectrometer. A schematic of a generic LIBS experimental setup is shown in Figure 2. Since all elements emit light when excited to a sufficiently high energy state all elements can be analyzed using this technique.

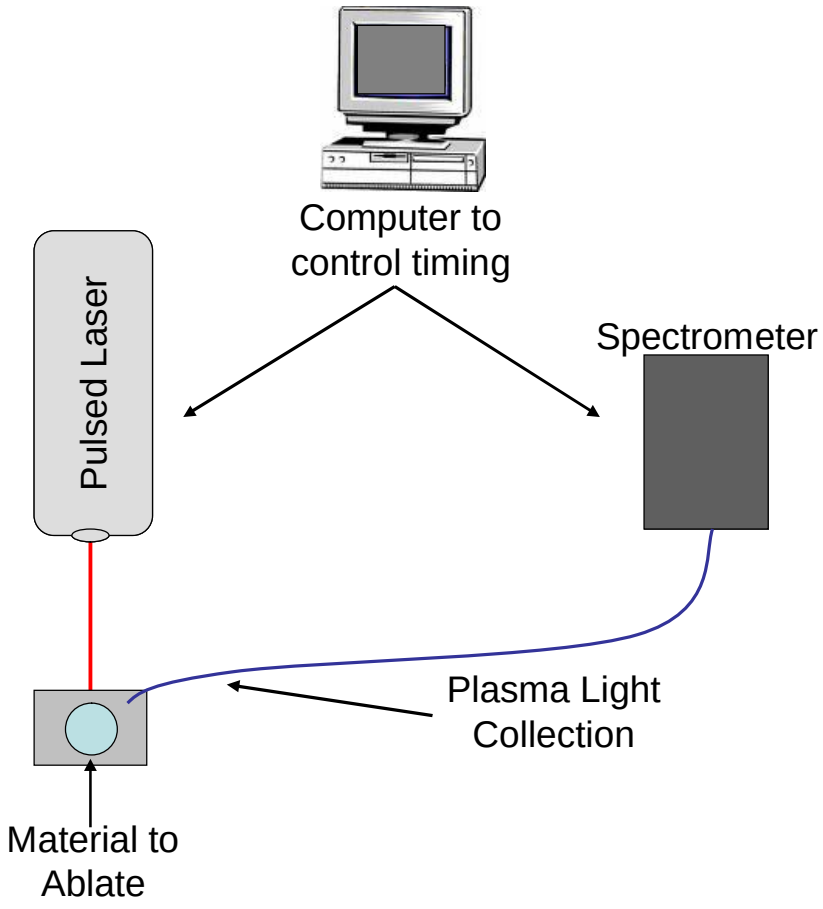

Figure 2. A generic bacterial ablation experimental setup

The principles are very straight forward and can be described in 4 steps.

1. A high-energy pulsed laser source is used to ablate a sample. LIBS is not contingent on the form of the material to be ablated. Liquid, solid, gas, aerosols, gels or just about any other form are suitable samples for LIBS. This ability to sample many different types of material is a big advantage of LIBS.

2. The laser is focused onto the sample causing a small amount to ablate. Ablation is a thermal process describing the rapid melting and vaporization or sublimation of the sample. The amount of sample ablated is extremely small, typically on the order of nanograms to picograms.

3. The ablation of the sample creates a super heated plasma ionizing the elements inside the plasma. The plasma formation occurs rapidly in a process called "breakdown". The "breakdown" process is described in detail in chapter 2. The excited atoms eventually de-excite and give off light (photons) as they decay to their ground states.

4. The light is collected into a spectrometer. Because at early times after the ablation pulse the plasma emission is dominated by broadband non-specific continuum emission it is important to temporally gate the detector. Once the spectrum is collected it can be analyzed to determine the elemental presence within the sample. The light collected by the spectrometer is incident upon a dispersion element such as a diffraction grating. The dispersed light is then incident upon a detector such as a charge-coupled device (CCD) camera. The detector collects the light into pixels which is saved as the intensity data, values for each pixel, from the detector. It is then possible to determine which wavelengths are present by the intensities. From these different wavelengths a spectrum is formed which shows the elemental composition of the plasma. The intensities from the detector can be used to measure the spectral line widths and intensities. Figure 3 shows a typical spectrum collected in the *E. coli* experiments to be described in this thesis. Note how the atoms present in the *E.*

coli give rise to narrow atomic emission lines from atoms and ions. Note that in this thesis we will use the spectroscopist's notation of X(II) or XII to denote singly-ionized element X. This could also be represented X^+.

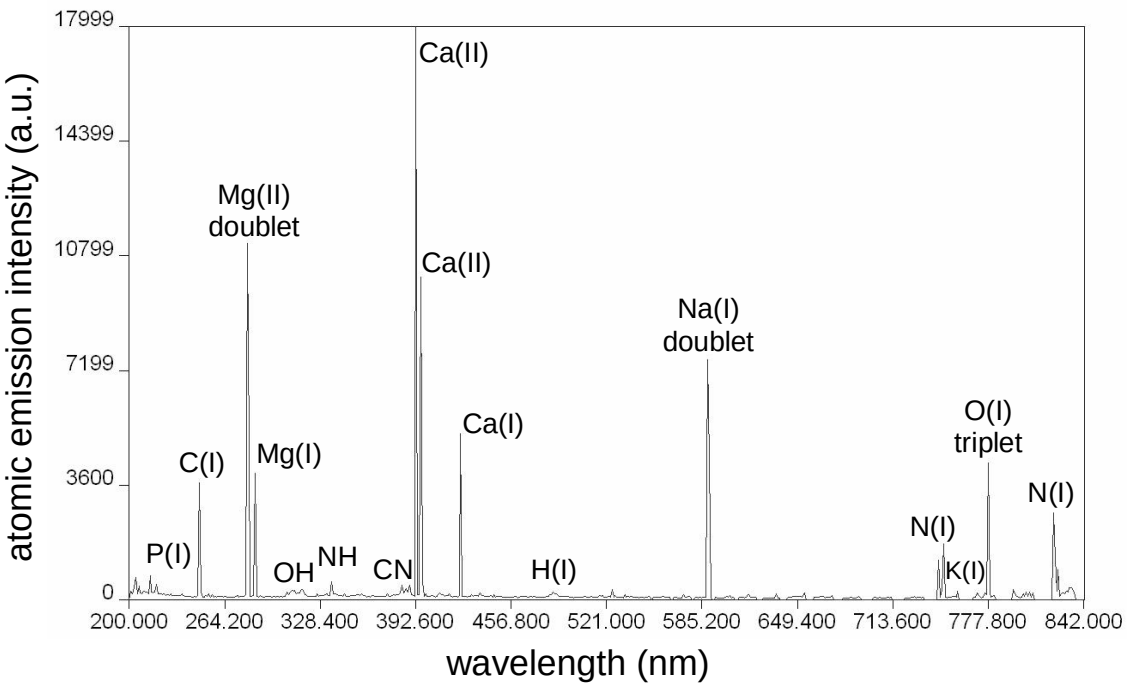

Figure 3 Spectrum of typical E. coli specimen

1.3 Applications of LIBS

LIBS has been used in many applications mainly due to its flexibility.[28, 29] Because LIBS can be utilized in many applications I have broken them into two categories, field applications and laboratory applications.

- Field users include military, geologists and first responders as well as many others who need rapid accurate detection and identification of unknown materials.[30-33] Field portable LIBS systems have been shown to be able to detect hazardous materials including bioaerosols.[6] They have also been used for detection of pollutants in soils and water.[32] One of the main advances in field portable

systems has been due to the advancement in laser technology in the past 20 years. The ability to package a high power energy source in a small form factor has allowed these systems to branch out where they were previously unable. Finally, in what could be an out of this world application, LIBS has been identified along with Raman spectroscopy as a fundamental, next-generation instrument for characterization of mineralogical and organic material on expeditions on the Martian surface. [34]

- Laboratory uses range from industrial use (e.g. as metallic alloy composition measurements, steel and glass melt testing, etc.[35-39]) to detection of bacteria and other pathogens.[4] As discussed in this thesis LIBS can be used to discriminate between different strains of the same bacteria. This work was done in the laboratory to allow greater control over the experiment and the materials to be analyzed. Experiments have a greater degree of control allowing for more precise results.

1.4 Experimental Samples

As mentioned earlier *E. coli* was used in the experiments for several reasons discussed below. It is appropriate to mention that in addition to *Escherichia coli* bacterium, other molds and pathogens were investigated as well. *Candida albicans* (a yeast), *Pseudomonas aeruginosa* (a bacteria) and other wild molds and bacteria were ablated using the LIBS technique described within. However; the main focus was on *E. coli*. *E. coli* has many strains, several are nonpathogenic but some are extremely harmful to humans.

Different *E. coli* strains can cause an impressive variety of diseases, including dysentery, hemolytic uremic syndrome (kidney failure), bladder infection, septicemia, pneumonia, and meningitis. In general, different strains are associated with different diseases. The ability to identify different strains will allow for the identification of specific diseases and possibly prevent outbreaks. Another advantage to using *E. coli* was in the preparation. This ease of preparation allowed the focus of this work to be on the spectral analysis and not on microbiological techniques. The *E. coli* was ablated without elaborate preparation techniques. Our technique was useful due to the fact that we were directly ablating the bacteria. There have been other studies of *E. coli* using LIBS but only one other directly ablated the *E. coli*.[27] Finally, and perhaps most important *E. coli* was used because of its know genetic characterization. With this we could fully investigate the results from LIBS with a known material allowing us to have a basis of comparison to vet the LIBS analysis results.

1.5 Benefits of LIBS

The benefits of using LIBS are numerous. Initially the advantage is in the experimental setup. The apparatus to setup a LIBS experiment can be very simple. This simplicity allows for LIBS systems to be field portable.[28] The ability to take the system into the field makes LIBS a candidate for first responders. In addition to the portability of the system the level of expertise needed to operate can be minimized easily with LIBS. Software can be easily designed to allow data collected in the field to be quickly compared to libraries of spectra. This rapid assessment can be critical in the field. From ablation to spectra, the time is not measured in seconds but fractions of a second. As in the case of a first responder the data is collected allowing it to be quickly

compared to a spectral library in order to ascertain the material in question. However; with speed of response LIBS does not sacrifice accuracy. As I will show in the chapter on results the experiments would yield accuracies in the upper eighty percentile using a discriminant function analysis.

1.6 Summary

In this thesis I report on the use of Laser-Induced Breakdown Spectroscopy on bacterial samples. In Chapter 2 I will discuss the physics behind the main principles of LIBS. There are four distinct parts to LIBS, I will discuss the physical processes going on in each. Chapter 3 details the experimental setup used to conduct the LIBS experiments on multiple bacterial strains. I will discuss the bacteria used, the laser, the fluorescence collection apparatus and the analysis software. Chapter 4 will present the statistical methods used to analyze the data. An introduction to the key statistical components used in the analysis and an in-depth explanation of Discriminant Function Analysis (DFA) will be presented. Chapter 5 presents the results from the LIBS experiments done on bacteria. I will show the first use of LIBS to discriminate among different strains of the same bacteria. Finally, Chapter 6 will present conclusions and suggestions for future work in this area.

Chapter 2 Principles of LIBS

In Chapter 1, LIBS was described as an atomic spectroscopic optical method for the elemental analysis of materials. LIBS, sometimes referred to as laser-induced plasma spectroscopy (LIPS) or laser spark spectroscopy (LSS), has advanced tremendously in the past two decades.[28] LIBS as an overall concept is very simple. 1) An energy source, the laser pulse, is incident upon a sample. 2) The incident energy vaporizes and ionizes the sample creating a plasma. 3) The light from the plasma is collected and disperse in a spectrometer. 4) The collected light is then analyzed to determine the elemental constituents of the material. Four discrete steps, however the physical and chemical processes occurring in each are not that simple. In this chapter I will describe in detail the four steps to LIBS.

1. LIBS Energy Source

In order to create a plasma, energy must be present to vaporize the sample material. Many LIBS experiments use a low-energy pulsed laser.[28] One such commonly used laser is the Nd:YAG laser in the near infrared range. Neodymium (chemical symbol: Nd) is a chemical element belonging to the group of rare-earth metals. In laser technology, it is widely used in the form of the trivalent ion Nd^{3+} as the laser-active dopant of gain media based on various host materials, including both crystals and glasses.[1] Nd:YAG is one of the most commonly used neodymium-doped media gained laser. $Y_3Al_5O_{12}$ (yttrium aluminum garnet, → YAG lasers): is the typical choice for 1064 nm, but is also usable at 946 nm and 1320 nm (and a few other lines) YAG is used most commonly in high power lasers and Q-switched lasers. [40, 41] A Nd:YAG laser

was also used in our LIBS experiments. In chapter 4 I will discuss the optical setup in detail. Pulsed lasers are used almost exclusively due to the very high peak energy present in the very short (nansosecond or femtosecond) laser pulses.

2. Ablation and plasma creation

Plasmas or ionized gasses are thought to be a distinct phase of matter. Their properties are distinct from solids, liquids and gases. Plasmas do however most resemble a gas. Unlike a gas though, they have a charge associated with them. Plasmas have a high electrical conductivity due to the presence of the charged particles within them. However; plasmas have a unique property called quasi-neutrality. Quasi-neutrality states that most of the negatively charged particles tend to cancel the positively charged particles, thus most of the plasma can be electrically neutral. Plasmas differ from gasses in that the electrons and ions are free to move about. In a gas they are bound to the atom. Ionization occurs when one or more electrons are dissociated from the atoms or molecules within the plasma. In order to create a plasma, energy is required to separate the electrons from the atoms. If the energy isn't sufficient enough the plasma will revert back to a normal gas. In most cases of plasma creation heat is the source of energy that creates the plasma. Plasmas are typically so hot and so high energy that they only consist of ions and electrons. Atoms are only present as the plasma cools. In section 2.4 it is discussed why this delay plays an important role in spectrometry. Plasmas have several properties. They are conductive so are susceptible to electric and magnetic fields. Because plasmas differ from gasses it is sometimes considered the fourth phase of matter. In fact, plasmas constitute most of the mater in the universe comprising nearly 99% of all mater. Examples of plasmas are listed below. Figure 4 shows different plasmas plotted

against electron density and temperature as all of these plasmas are a function of these two key parameters.

- Neon Signs
- Fluorescent lamps
- Lighting
- Welding torches
- Gas Nebulae
- Aurora Borealis

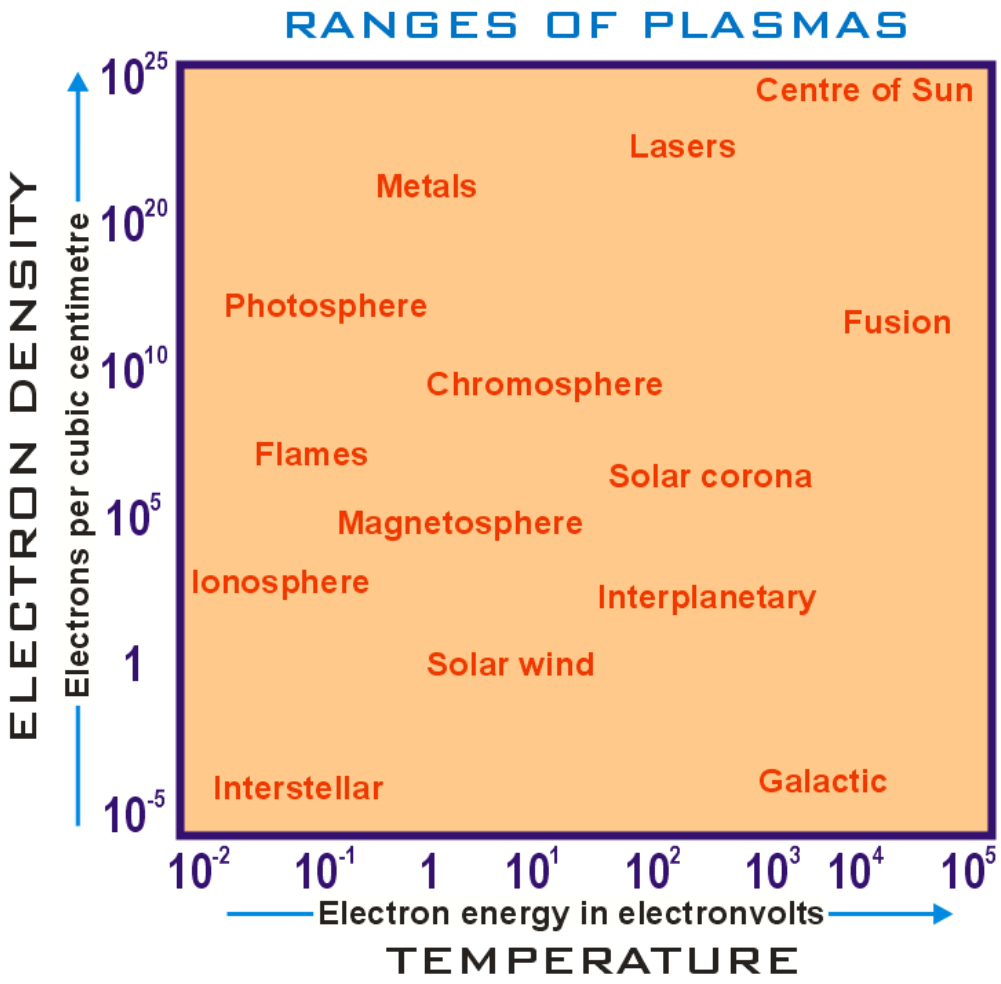

Figure 4 Examples of plasmas plotted temperature versus the electron density [49]

LIBS relies on the spectral analysis of plasmas. The laser initiates the plasma resulting in three stages to the plasma formation. First, the laser is incident upon the bacterial sample, or any other liquid, gas, or solid, vaporizing it and creating a vapor plume above the surface of the target. The timescale of this thermal process is shorter than the laser pulse duration so the plume is irradiated by the laser pulse. The plume begins to condense leading to further laser absorption and scattering within the plume. This absorption and scattering of the incident laser results in strong heating, ionization and plasma generation. What happens next can be broken into three stages. 1) The vapor plume and plasma generation is referred to as plasma ignition. 2) The next stage is plasma growth. 3) Finally, the plasma absorbs and scatters the incident beam. Each of these stages is described below.

2.1. Plasma Ignition

Now that we know what a plasma is let us now investigate the methods of generating a plasma. As stated above, plasmas can be created by supplying a sufficient amount of energy to a gas in order to separate the electrons from the atoms. It is possible to simply heat the gas to very high temperatures, but it would probably destroy the gas container first. It is useful to heat the gas initially. This can be done with a simple heat source such as a flame or even through adiabatic compression of the gas. Adiabatic heating works because the gas can be characterized by the relation $(T/T_0)^{3/2} = V_0/V$ which is derived from the ideal gas law. V is the volume of the gas and T is the temperature. As the gas is compressed, decreasing the volume, the temperature of the gas will also rise.[42] This is in contrast to the familiar cooling which accompanies the rapid expansion of gases. Once the gas is heated another process is used to add the additional energy to create the plasma.

Applying a current or the use of radio frequency are alternate typical methods to generate enough energy for ionization. Although plasmas are commonly produced by electric discharges in gases, plasma can also be obtained when sufficient energy is provided to a liquid or a solid to cause its vaporization and ionization.[43, 44]

The last method of plasma generation I will discuss is via laser. LIBS creates a plasma via laser. I will discuss the plasma generation of gases and apply this to solids and liquids. In order to breakdown a gas free electrons and sufficient ion and electron densities are needed. First, there must be some initial electrons to "start" the breakdown. These can be generated by the photons in the initial laser pulse. They can also be found from transient electrons liberated by cosmic rays or even the neutral radioactivity of the earth.[28] These electrons are needed to create a multiphoton effect in order to ionize some elements. Elements or molecules such as O_2 and N_2 have higher ionization energies than what is provided by the incident laser. The second requirement for plasma creation is achieving ion and electron densities that can sustain ionization of the gas. In order to achieve this, enough energy must be delivered to the gas. Typical LIBS irradiance is on the order of $10^8 – 10^{10}$ W/cm^2. At these irradiance levels electron and ion densities are achieved via cascade (avalanche) ionization. Cascade ionization occurs when free electrons are accelerated by the energy of the incident laser pulse, which leads to the generation of more free electrons. This causes a continuous increase of the electron density. Due to the lower energy of the incident laser the plasma is created by this cumulative growth of electrons and ions. This is in contrast to higher irradiances where the plasma creation is due to multiphoton ionization. Multiphoton ionization occurs as a function of the instantaneous laser intensity. Here the incident energy is high enough to

create the electron density needed to create the plasma.[28] The multiphoton effect can be described by equation 2.1, where m is the number of photons.

$$M + mh\nu \rightarrow M^{+} + \mathrm{e}^{-} \qquad \text{Equation 2.1}$$

2.2. Plasma Growth

Five different transitions in atoms and ions contribute to the radiation in the plasma. Bound-bound, free-bound, free-free, ionization from ground state, and ionization from an excited state are the five different transitions. Bremsstrahlung and recombination are free-free and free-bound transitions responsible for a large background continuum radiation emission in LIBS. Bremsstrahlung occurs when a photon is emitted by electrons that are accelerated or decelerated in collisions. In our case the plasma is heated, and efficiently, via inverse Bremsstrahlung. This means the slow electrons of the plasma interact with the photons, equation 2.2, to generate fast electrons. Once there is sufficient kinetic energy in the electrons they collide with other atoms, knocking off more electrons and creating more ions and more free electrons. This exponential increase in electrons is called avalanche or cascading. It occurs while the laser pulse is still incident.

Afterward, as the plasma cools, the ions start to fall back into neutral atoms. This is the continuum radiation (free bound). The electrons in the plasma slow down generating Bremsstrahlung radiation. These two sources are the broadband background radiation we see at short delay times (but after the laser pulse is gone.)

$$e^{-}(slow) + h\nu \longrightarrow e^{-}(fast) \qquad \text{Equation 2.2}$$

When an atom absorbs a photon it absorbs its energy and the electrons are pushed to a higher energy state. The energy of the photon, *hν,* allows the electron to move from E_1 to E_2 where $E_2 - E_1 = h\nu$. In order to better describe these transitions an explanation using a hydrogen atom will be described. Given a system of hydrogen atoms in any state, we can perturb the system which will cause an atom to transition to a different state. Let's assume our hydrogen atom is the in the n = 3 state. If the atom was to emit a photon and lose energy it would drop to a lower energy state n = 2. The frequency of the emitted photon can be found from:

$$\Delta E = h\nu \qquad \text{Equation 2.3}$$

Since the energy transition is quantized and *h* is a constant the frequency is known. This frequency corresponds to spectral lines viewed in the electromagnetic spectrum. To be more specific the frequency is related to the wavelength of the spectral line given by: $\lambda = c/\nu$. In our case of a transition from n = 3 to n = 2, this transition is called the H-alpha line. There are other lines, H-beta and H-gamma, that correspond to a spectral lines in the visible spectrum that also terminate in the n = 2 state.

The resulting spectral lines will have a certain radiance, the amount of light which is emitted from a given area per unit solid angle, associated with them. This can be described by Plank's law. Planck's law describes the spectral radiance of electromagnetic radiation at all wavelengths from a black body at temperature *T*. As a function of frequency ν, Planck's law is written as:

$$I(\nu,T) = \frac{2h\nu^3}{c^2}\frac{1}{e^{\frac{h\nu}{kT}} - 1} \qquad \text{Equation 2.4}$$

Plank discovered his law in an attempt to improve a formula proposed by colleague Wilhelm Wien. Wien's formula for spectral radiation worked well for short wavelengths but had problems at longer wavelengths. By distributing the energy over the different modes of charged oscillators in matter, Plank was able to develop his equation to fit all wavelengths. A discrete level of energy proportional to the fundamental unit energy of the atom was the key to his discovery. Although Plank saw his discovery as a mathematical way to describe blackbody radiation (consequently his discovery solved the ultraviolet catastrophe brought on by the Rayleigh-Jeans equation for electromagnetic radiation) it would revolutionize the landscape of physics.

2.3. Plasma Breakdown & Diagnostics

2.3.1. LIBS Plasma Breakdown

As the number of electrons increases during the plasma growth the plasma reaches a point of breakdown. This level of breakdown is defined as a measure of the electron density of the plasma. During the growth of the plasma, electron density is in the range of: n_e~1-10 cm^{-3}. As the plasma continues to absorb photons from the laser the electron density grows exponentially. When n_e~10^{13} cm^{-3} then breakdown occurs. This leads to significant absorption and scattering of the incident laser resulting in a fully developed plasma.

The goal of LIBS is to identify the material being ablated. To do this we investigate the plasma during the breakdown stage. Ideally, the plasma will be optically thin and in equilibrium. Optically thin refers to a plasma in which the emitted radiation traverses and escapes from the plasma without significant absorption or scattering. If the plasma is in equilibrium, then the plasma properties, such as the relative populations of

energy levels, and the distribution of the speed of the particles, can be described through the concept of temperature.[28] If this equilibrium condition can be achieved, we can through analysis of the plasma determine the elemental constituents of the plasma and thus the sample material. As stated above there are several types of plasmas and techniques for investigating them. Plasmas can be characterized by their ionization. LIBS plasmas tend to be weakly ionized. A weakly ionized plasma is one in which the ratio of electrons to other charged neutrals is less than 10%.[28] The ionization of the plasma is a function of time. Ionization is higher early in the plasma. At later times electron-ion recombination occurs followed by formation of molecules. Figure 5 is an overview of the temporal history of a single laser pulse initiated LIBS plasma, which plots the optical intensity emitted by the plasma as a function of time after the initiation of the laser pulse. Typically in LIBS experiments, since the early plasma times are dominated by non-elemental specific radiation (denoted “plasma continuum” in Figure 5), a specific observation window is used. This observation window starts at a time called the delay time, t_d, after the laser pulse and lasts for a time called the gate width, t_w.

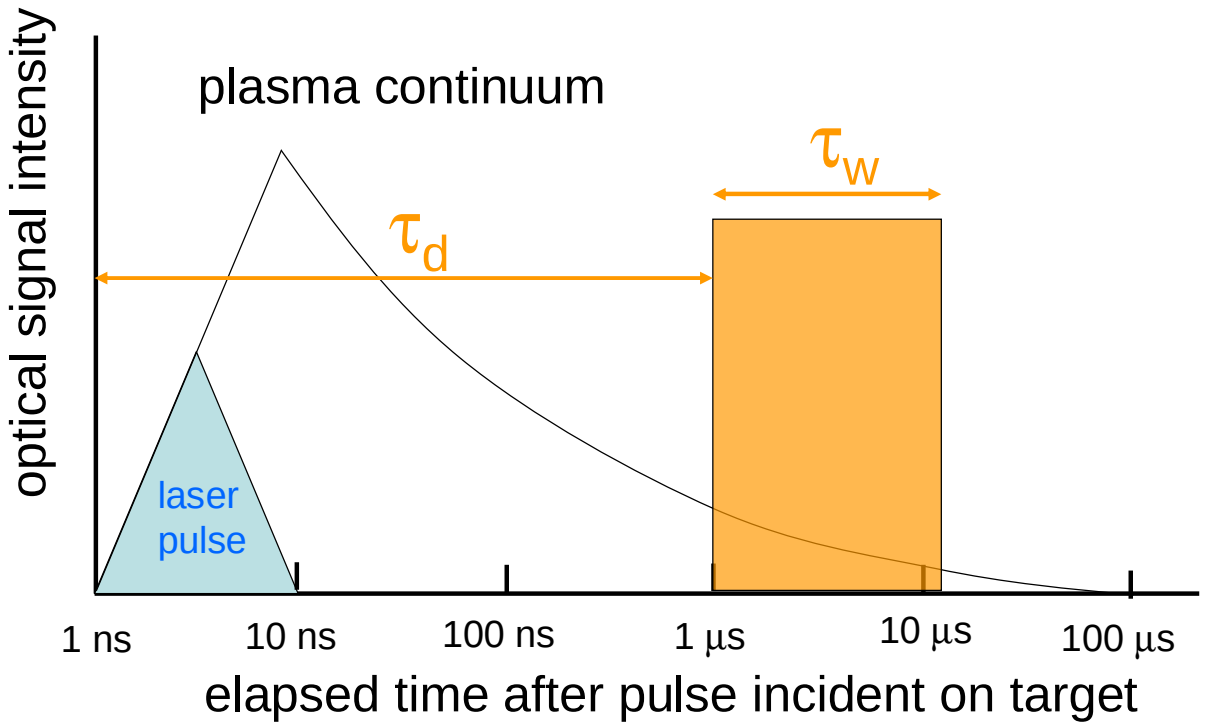

Figure 5 Temporal history of LIBS plasma [28]

As a result of the changes within the plasma due to time great detail was taken during the experiments to determine the ideal gate delay. Too early and the plasma will be entirely ions, too late the atomic signal will be too small and molecules will dominate the spectrum. However; as stated earlier the plasma is weakly ionized so less than 10% of the plasma will be ionized. Therefore the experiment tended to use earlier delay times to achieve the best results.

3. Plasma Light Collection

In order to analyze and employ some of the plasma diagnostic techniques the light from the plasma must be collected. To collect the light from the plasma, a fiber optic cable is used. It is setup in order to collect the most possible light. The exact mounting and positioning of the fiber is described in chapter 4. Here I will discus the fundamentals

of atomic spectroscopy as it is the fundamental technique used in the collection and analysis of the plasma light.

3.1. Frequency, wavelength and photon energy

As discussed earlier when an electron transitions from an upper energy state to a lower energy state it emits a photon. The frequency and wavelength of the photon can be determined from $\Delta E = E_k - E_i = h\nu = hc\sigma = hc/\lambda_{vac}$. This indicates that the change in energy from the upper level (k) and the lower level (i) is equal to the frequency times a constant. Thus the frequency of the photon is directly proportional to the difference in energy levels. From this we also see that the change in energy is proportional to the wavenumber and inversely proportional to the wavelength. If we can measure any of these properties we can determine the others. Optical wavelengths are typically measured in nanometers or micrometers. Different wavelengths correspond to different ranges of atomic spectra. Figure 6 shows defined wavelengths associated with the electromagnetic spectrum. As the plasma is created there are many such energy transitions taking place thus producing many photons and many wavelengths. As different elements transition from higher to lower energy states they emit photons. Different elements have different transition energies thus producing photons at different wavelengths producing a spectrum of wavelengths. Spectroscopy is defined to be the analysis of light to determine the composition of the thing emitting the light or to make accurate measurements of the light itself. This is precisely what LIBS is trying to do.

There are three basic types of spectroscopy: absorption, emission and scattering. LIBS is an emission technique. Emission spectroscopy uses the electromagnetic spectra emitted from the sample to determine the elemental constituents.

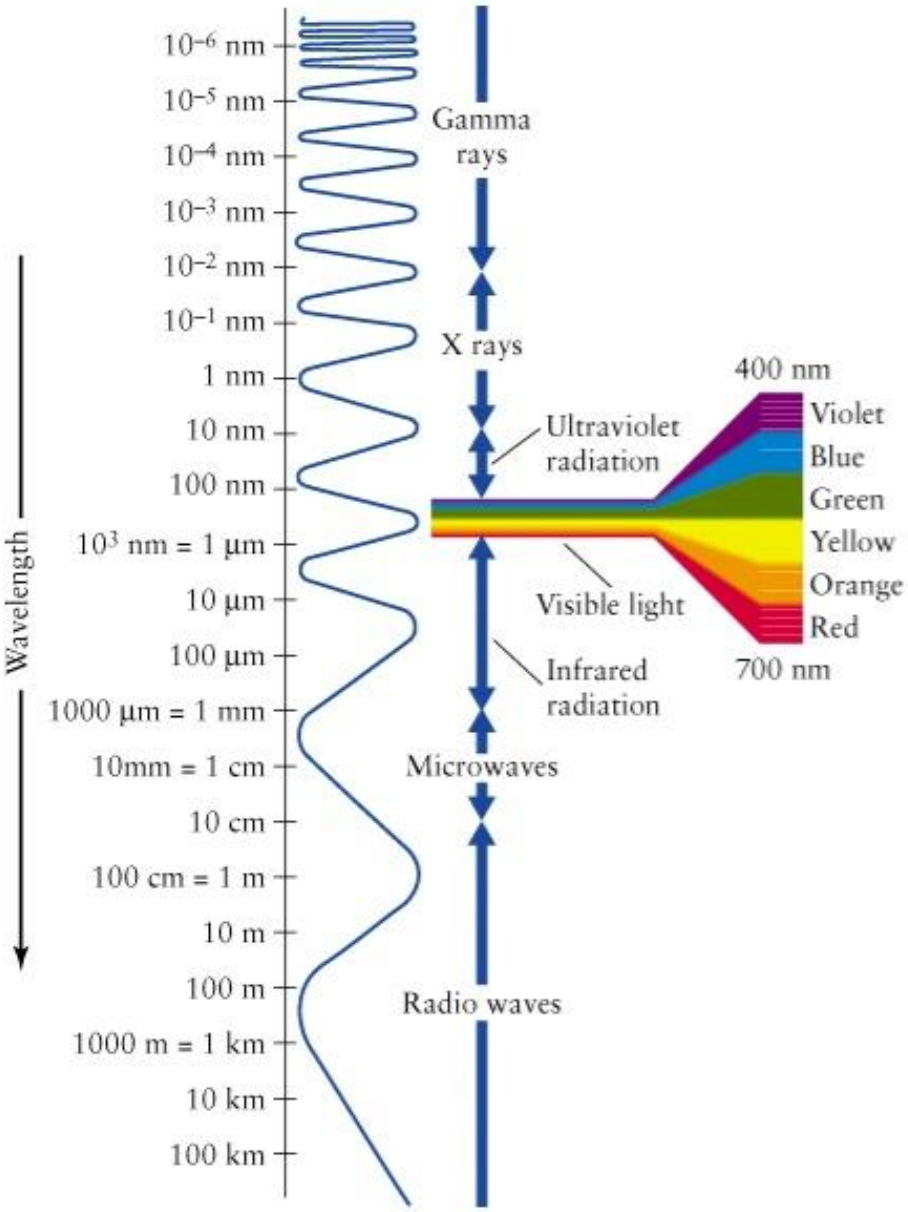

Figure 6 Wavelengths of the Electromagnetic Spectrum [45]

Emission spectroscopy works by identifying the lines that exist. Imagine the visible spectrum as a continuous wavelength scale changing from red to blue going left to right. Absorption spectroscopy looks at the lines that are missing to conclude which elements absorb the light blocking it from arriving. Emission spectroscopy is just the opposite. It looks at only the lines that are there. Figure 7 shows these differences.

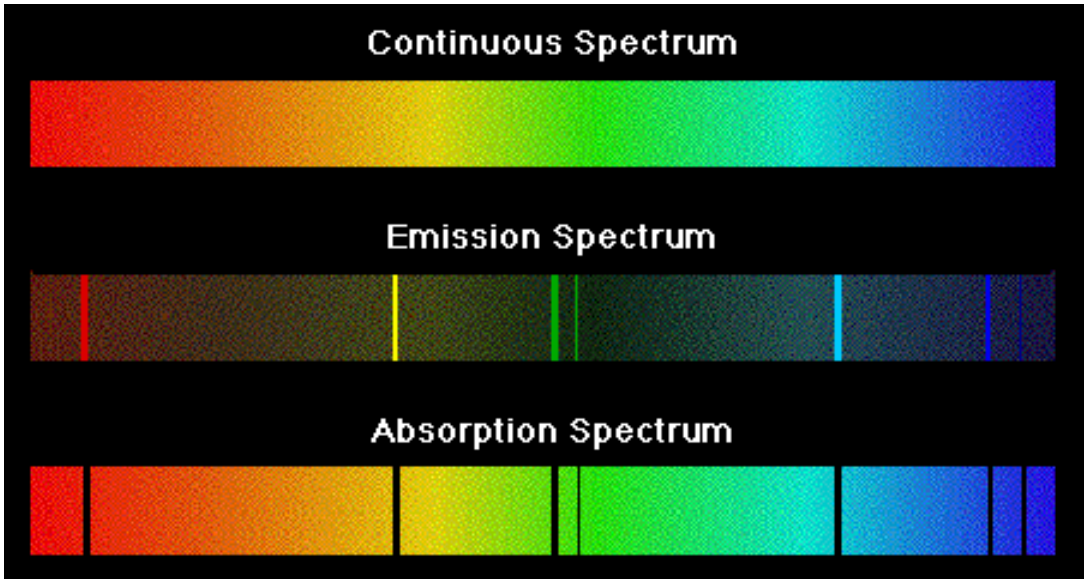

Figure 7 Spectroscopy on emission or absorption by atoms [46]

4. Spectral Line Analysis

All of this leads the LIBS experimenter to the collection of the spectrum from the plasma. From here analysis of the spectral lines yield information of the plasma and as a result the material the plasma was created from. In order for LIBS to be successful there must be a relationship between reproducible plasma properties and spectral line characteristics. The main characteristic of LIBS spectral lines are their widths. The widths of the lines are determined by the plasma temperature and the electron density within the plasma. Doppler width and Stark width are the most important contributions

to spectral line widths under nominal LIBS conditions. Natural lines widths can be neglected due to their small contribution, usually on the order of thousands of a nanometer. This is too small to resolve on most spectrometers used for LIBS.

4.1. Doppler Width

Doppler broadening is the broadening of the linewidth of atomic transitions caused by the random movements of atoms. Spectral line profiles resulting from Doppler broadening are Gaussian.[28, 43, 44] For example, if the atoms have a thermal velocity distribution with temperature *T*, the linewidth resulting from the Doppler effect is

$$\Delta\nu_D = \frac{2\nu_0}{c}\sqrt{2\ln 2 \cdot \frac{k_B T}{m}} \qquad \text{Equation 2.5}$$

where ν_0 is the mean optical frequency and *m* is the mass of the atoms. For this formula it is assumed that the Doppler broadening is much larger than the natural linewidth, which is typically the case for atoms in gases

Doppler broadening can place severe constraints on precise spectroscopic measurements. However, it can be eliminated in various ways. One way to reduce Doppler broadening is by reducing the temperature. From equation 2.5, Doppler widths depend on the temperature of the plasma and the atomic number of the emitting species [28]. Another method to reduce or eliminate Doppler broadening is to employing a measurement scheme which is intrinsically insensitive to Doppler broadening, such as *Doppler-free saturation spectroscopy* or the use of two-photon absorption with counter propagating beams can also eliminate the Doppler broadening. Doppler broadening is the dominant line broadening mechanism in gas lasers.[47]

4.2. Stark Width

Collision broadening occurs both in and outside of plasmas and can be seen in absorption lines that start in low energy levels. Usually these take place in neutral atoms or molecules. However; when the collisions occur with ions and electrons (charged particles) it is referred to as Stark broadening which results from the Stark effect. The Stark effect is the shifting and splitting of spectral lines of atoms and molecules due to the presence of an external static electric field. The amount of splitting and or shifting is called the Stark splitting or Stark shift. The splitting occurs on an energy level in the electric field creating sublevels. These sublevels are identified by the quantum number m_j. The electric field in LIBS experiments comes from the collisions of electrons, ions and the charged nature of the plasma. When there is a resolved series of sublevels, selection rules for the transitions of these levels allow for prediction of the spectral line intensities. [28, 43, 44] In all of our LIBS plasmas, Stark broadening is the dominant line-broadening mechanism.

4.3. Electron Density

Electron density is, as its name implies, the amount of electrons present in the plasma per unit volume. Calculation of this comes from the spectral line widths. Because the Stark broadening depends on the local electric field, it is proportion to the electron density in the plasma. Specifically, the Stark-broadened line width and the electron density are related by:

$$w_{total} \approx \left[1+1.75A(1-0.75r)n_e/10^{16}\right]w \qquad \text{Equation 2.6}$$

where w_{total} is the measured half-width at half maximum (HWHM), A is the ion contribution, r is the ratio of the mean distance between ions to the Debye radius, and w is the HWHM Stark width caused by the electron density.[28]

4.4. Plasma Opacity

Plasma opacity is another property that can be used as a diagnostic tool. Plasma opacity is determined by bound-bound transitions, bound-free transitions, electron scattering, and free-free transitions (Bremsstrahlung).[48] Optically thin plasmas provide better LIBS results due to a greater amount of radiation escaping the plasma along the length of the plasma. To be optically thin indicates that there is little absorption or scattering within the plasma. The radiation emitted from the plasma is given by:

$$I(\lambda) = [\varepsilon(\lambda)/\alpha(\lambda)]\{1 - \exp[-\alpha(\lambda)L]\} \qquad \text{Equation 2.8}$$

where $\varepsilon(\lambda)$ is the emissivity and $\alpha(\lambda)$ is the absorption coefficient. Plasma opacity can be determined from the widths of the spectral lines observed. The widths as discussed earlier can be determined from atomic physics. When re-absorption is seen in the spectral lines this can be indicative of more opaque plasmas as the lines are re-absorbing the emitted photons and thus saturate. The most intense lines will show this re-absorption first. The tops of the lines will be flattened or in extreme cases of saturation the line will have a dip at the peak. The self absorption poses a problem when measuring the area of the curve. The flattening or dip in the line introduces uncertainty in any area measurement that can be taken thus leaving the spectra unusable.

4.5. Plasma Temperature

Plasma temperature is a very important piece of information when it comes to plasmas. If there is thermodynamic equilibrium then a single plasma temperature, $T_{ion}=T_{electron}=T$, can be defined and certain properties can be determined from the temperature. The relative population of energy levels and distribution of the speed of the particles are just two such properties. However; complete thermodynamic equilibrium is rarely achieved. Instead, it is common to settle for equilibrium in a very small region around which the measurement is to be taken. It is possible for this equilibrium to vary from region to region therefore it is a local thermodynamic equilibrium (LTE). It is usually the case for a significant amount of collisions to have taken place to thermalize the plasma on this much smaller scale. It should be noted that thermal equilibrium is not achieved for all particles at the same time. Atoms and ions tend not to equilibrate as quickly as electrons. Particles of similar masses (atoms and ions) tend to share energy more equally. The more interaction between the particles the longer it takes to reach equilibrium. In the case of the LIBS experiments the temperature was not calculated for the plasma. The reason for this is because it is typically calculated from the intensity of multiple emission lines from a wide variety of uppers states plotted in a “Boltzmann plot”. However not enough lines were ever observed from any given atom in the LIBS spectra described here.[28]

Chapter 3 Data Collection Using LIBS

This chapter details all aspects of my experiment. First, I will describe the bacteria used and the methodology behind the choice of strains which I ablated. Second, I will discuss my experimental setup. I will discuss both specifics of my experiment as well as the theory behind what is happening. Finally, I will conclude with the procedures used to collect data.

1 Bacteria & Sample Preparation

This work describes laser-induced breakdown spectroscopy on two different types of bacteria: *Escherichia coli* and *Pseudomonas aeruginosa*. I will therefore start by describing these specific bacteria and why they are important for laboratory study, before detailing specifically how the spectroscopy was performed.

1.1 Bacterial Samples

1.1.1 Escherichia coli

Phylum: Proteobacteria

Class: Gamma Proteobacteria

Order: Enterobacteriales

Family: Enterobacteriaceae

Genus: *Escherichia*

Species: *coli*

E. coli is one of the main species of bacteria living in the lower intestines of mammals, known as gut flora. When located in the large intestine, it actually assists with waste processing, vitamin K production, and food absorption. It was discovered in 1885

by Theodor Escherich, a German pediatrician and bacteriologist [53]. *E. coli* is a gram-negative organism meaning it is unable to sporulate. Thus, any method that kills all the bacteria, such as pasteurization or boiling, is effective for their eradication. Gram-negative organisms have much thinner cell walls as compared to gram-positive organisms. Cell walls in Gram-negative bacteria only contain a few layers of peptidoglycan. In Gram-positive bacteria peptidoglycan is present in much higher levels. Another difference between negative and positive is in the outer membrane. Gram-negative cells are surrounded by an outer membrane containing lipopolysaccharide (which consists of Lipid A, core polysaccharide, and O-polysaccharide) outside the peptidoglycan layer. Gram-positive bacteria do not have this outer membrane.[54] This outer membrane plays a key role in our experiments.

E. coli plays a big role in disease. *E. coli* can generally cause several intestinal and extra-intestinal infections such as urinary tract infections, meningitis, peritonitis, mastitis, septicemia and Gram-negative pneumonia. The enteric *E. coli* are divided on the basis of virulence properties into enterotoxigenic (ETEC, causative agent of diarrhea in humans, pigs, sheep, goats, cattle, dogs, and horses), enteropathogenic (EPEC, causative agent of diarrhea in humans, rabbits, dogs, cats and horses); enteroinvasive (EIEC, found only in humans), verotoxigenic (VTEC, found in pigs, cattle, dogs and cats); enterohemorrhagic (EHEC, found in humans, cattle, and goats, attacking porcine strains that colonize the gut in a manner similar to human EPEC strains) and enteroaggregative *E. coli* (EAggEC, found only in humans). [57]

There are several different strains of *E. coli.* A "strain" of *E. coli* is a group with some particular characteristics that make it distinguishable from other *E. coli* strains.

These differences are often detectable only on the molecular level; however, they may result in changes to the physiology or lifecycle of the bacterium, for example leading to pathogenicity. Different strains of *E. coli* live in different kinds of animals, so it is possible to tell whether fecal material in water came from humans or from birds, for example. New strains of *E. coli* arise all the time from the natural biological process of mutation, and some of those strains have characteristics that can be harmful to a host animal. Although in most healthy adult humans such a strain would probably cause no more than a bout of diarrhea, and might produce no symptoms at all, in young children, people who are or have recently been sick, or in people taking certain medications, an unfamiliar strain can cause serious illness and even death.

A particularly virulent example of such a strain of *E. coli* is *E. coli* O157:H7.[57] In addition, *E. coli* and related bacteria possess the ability to transfer DNA via bacterial conjugation, which allows a new mutation to spread through an existing population. It is believed that this process led to the spread of toxin synthesis from *Shigella* to *E. coli* O157:H7.

Extended-Spectrum Beta-Lactamase (ESBL)–producing *E. coli* are antibiotic-resistant strains of *E. coli*. ESBL-producing strains are bacteria that produce an enzyme called extended-spectrum beta lactamase, which makes them more resistant to antibiotics and makes the infections harder to treat. In many instances, only two oral antibiotics and a very limited group of intravenous antibiotics remain effective.[59]

In our study we looked at four different strains of *E. coli*: two laboratory K-12 strains (HF4714 and AB), one environmental strain (NinoC) and one pathogenic strain

(EHEC). The two main strains that were focused on early in the experiments were Nino C and HF4714. These two strains were the basis of many experiments.

Nino C and K12, of which AB and HF4714 are a derivative, are nonpathogenic strains of *E. coli.* It should be noted that K-12 has been completely characterized genetically.[56] These strains are important to study since detection of certain nonpathogenic strains can indicate other more harmful strains of *E. coli.* These nonpathogenic strains are found mainly in the laboratory. The harmful strains such as EHEC are found in water and food which are consumed by humans.

EHEC are represented by a single strain (serotype O157:H7), which causes a diarrheal syndrome distinct from EIEC (and *Shigella*) in that there is copious bloody discharge and no fever. A frequent life-threatening situation is its toxic effects on the kidneys (hemolytic uremia). EHEC has recently been recognized as a cause of serious disease often associated with ingestion of inadequately cooked hamburger meat. Pediatric diarrhea caused by this strain can be fatal due to acute kidney failure (hemolytic uremic syndrome [HUS]). EHEC are also considered to be "moderately invasive". Nothing is known about the colonization antigens of EHEC but fimbriae are presumed to be involved. The bacteria do not invade mucosal cells as readily as *Shigella*, but EHEC strains produce a toxin that is virtually identical to the Shiga toxin. The toxin plays a role in the intense inflammatory response produced by EHEC strains and may explain the ability of EHEC strains to cause HUS. The toxin is phage encoded and its production is enhanced by iron deficiency.[55,60]

Different strains of *E. coli* can cause an impressive variety of diseases, including dysentery, hemolytic uremic syndrome (kidney failure), bladder infection, septicemia,

pneumonia, and meningitis. Therefore the ability to quickly and accurately identity particular strains of a given bacteria is a very important diagnostic tool to prevent or contain outbreaks caused by a particular strain.[57]

1.1.2 Pseudomonas aeruginosa

Phylum: Proteobacteria

Class: Gamma Proteobacteria

Order: Pseudomonadales

Family: Pseudomonadaceae

Genus: Pseudomonas

Species: aeruginosa

Pseudomonas aeruginosa is the epitome of an opportunistic pathogen of humans. The bacterium almost never infects uncompromised tissues, yet there is hardly any tissue that it cannot infect if the tissue defenses are compromised in some manner.

Pseudomonas aeruginosa is a Gram-negative, aerobic rod belonging to the bacterial family *Pseudomonadaceae*. The family includes other genera, which, together with certain other organisms, constitute the bacteria informally known as pseudomonads. These bacteria are common inhabitants of soil and water. They occur regularly on the surfaces of plants and occasionally on the surfaces of animals. The pseudomonads are well known to plant microbiologists because they are one of the few groups of bacteria that are true pathogens of plants. In fact, *Pseudomonas aeruginosa* is occasionally a pathogen of plants. But *Pseudomonas aeruginosa* and two former *Pseudomonas* species (now reclassified as *Burkholderia*) are pathogens of humans.[61]

Pseudomonas aeruginosa is an opportunistic pathogen, meaning that it exploits some break in the host defenses to initiate an infection. It causes urinary tract infections, respiratory system infections, dermatitis, soft tissue infections, bacteremia, bone and joint infections, gastrointestinal infections and a variety of systemic infections, particularly in patients with severe burns and in cancer and AIDS patients who are immunosuppressed. *Pseudomonas aeruginosa* infection is a serious problem in patients hospitalized with cancer, cystic fibrosis, and burns. The case fatality rate in these patients is 50 percent.

Pseudomonas aeruginosa is primarily a nosocomial pathogen. According to the CDC, the overall incidence of *P. aeruginosa* infections in US hospitals averages about 0.4 percent (4 per 1000 discharges), and the bacterium is the fourth most commonly-isolated nosocomial pathogen accounting for 10.1 percent of all hospital-acquired infections.[62] *P. aeruginosa* is an opportunistic pathogen capable of colonizing the skin and intestinal tract of humans and animals. *P. aeruginosa* is best known for it ability to infect burns and to cause complications in patients with cystic fibrosis (CF). CF patients typically develop persistent *P. aeruginosa* lung infections that lead to lung failure, followed by transplants or early death.[63]

1.2 Substrates

Substrates played a key role in the experiments. Once we had identified the organisms to be investigated and characterized with the LIBS technique, we needed a way to reproducibly sample a bacterial culture with our ablation laser, and efficiently collect emission light. The two substrates primarily used were Trypticase Soy agar (TSA) and Bacto agar. TSA was the growth medium for all of the *E. coli* samples. TSA was also sampled and analyzed by DFA. In chapter 5 data obtained from TSA is

frequently plotted with the bacteria data. The other substrate discussed, bacto agar, was key to the data collection process. The choice of agar as an ablation substrate afforded a very flat, large area substrate with a high-breakdown threshold due to its near-transparency.

1.2.1 Trypticase Soy Agar

Trypticase Soy Agar (TSA) is an enriched medium for isolating and cultivating several varieties of bacteria and organisms. TSA medium contains enzymatic digests of casein and soybean meal which provides amino acids and other nitrogenous substances making it a nutritious medium for a variety of organisms. Dextrose is the energy source. Sodium chloride maintains the osmotic equilibrium, while dipotassium phosphate acts as buffer to maintain pH. The medium may be supplemented with blood to facilitate the growth of more fastidious bacteria or antimicrobial agents to permit the selection of various microbial groups from mixed flora.[64] TSA is used for isolating and cultivating fastidious microorganisms and, with blood, in determining hemolytic reactions. [6] TSA was ideal for the growth of *E. coli* and *P. aeruginosa.* All samples were grown on this medium giving a consistent nutrient rich growth medium to grow bacteria for ablation. The formula for TSA is given below:

TSA Formula

- Tryptic Soy agar Formula Per Liter
- Tryptone . . (.Pancreatic Digest of Casein) 15 g
- Soytone . . . (.Papaic Digest of Soybean Meal . .) 5 g

- Sodium Chloride 5 g
- agar 15 g
- Final pH 7.3 ± 0.2 at 25°C

The TSA was prepared outside of our laboratory and made as follows: First 10.0 grams of TSA powder (containing NaCl, agar, casein and soybean meal) was added into a flask, containing 250 ml distilled water, inside water bath at 50 °C. Then the flask was kept inside an autoclave (120 °C) for approximately 45 minutes. Next the flask was transferred from the autoclave to water bath and after couple of minutes the solution was poured into a 9cm diameter sterile Petri dish and left for 1-2 minutes to dry at room temperature. Finally, the dish was placed inside the incubator (37 °C), for 90 minutes to remove the excess moisture on the lid. Then an inoculating loop was heated until red-hot, in order to sterilize the loop. After that one colony or a bit of a colony was picked up from a plate culture and was dragged on the surface of the TSA. Finally the TSA plate was kept inside the incubator for 24 hours to grow bacteria. Although I participated in the culturing of such samples, this was routinely done by Dr. Sunil Palchaudhuri, a Professor in the Department of Immunology and Microbiology or his assistant Dr. Ashan Habib.

Similar to TSA is Tryptic Soy Broth. As one would imagine the broth is a liquid as opposed to the agar which is solid. Both are used for the growth of bacteria. In our experiments we did investigate the bacteria grown in the broth.[64]

1.2.2 Tryptic Soy Broth

Tryptic Soy Broth is a general purpose medium used for isolating all types of microorganisms. Tryptic Soy Broth was originally developed for use without blood in determining the effectiveness of sulfonamides against pneumococci and other organisms. Tryptic Soy Broth is often used to support growth of non-typical isolates such as Brucella. Clostridia and non-sporulating anaerobes grow luxuriantly in this broth when incubated under anaerobic conditions. With the addition of 6.5% NaCl, TSB can be used for the selective growth of group D streptococci. TSB is recommended for testing bacterial contaminants in cosmetics and complies with established standards in the food industry. Tryptic Soy Broth w/o Dextrose, a modification of TSB, is a basal medium to which carbohydrates may be added for use in fermentation studies. agar may be added (0.5-1.0 grams/liter) to enhance anaerobic growth. Phenol red and other indicators may also be added. The formula and method of preparation is similar to TSA and is given below:

TSB Formula

- Tryptic Soy Broth Formula Per Liter
- Tryptone . . (.Pancreatic Digest of Casein) 15 g
- Soytone . . . (.Papaic Digest of Soybean Meal . .) 5 g
- Sodium Chloride 5 g

Method of Preparation

1. Suspend the medium in 1 liter distilled or deionized water:
    - Tryptic Soy Broth - 30 grams;

- Tryptic Soy Broth w/o Dextrose - 27.5 grams.

2. Dispense as desired

3. Autoclave at 121°C for 15 minutes. Cool to room temperature.

1.2.3 Bacto agar

Bacto agar is optimized for beneficial calcium and magnesium content. Detrimental ions such as iron and copper are reduced. agar is recommended for clinical applications, auxotrophic studies, bacterial and yeast transformation studies and bacterial molecular genetics applications. [64]

Agar was chosen as the ablation substrate in our experiments. Agar is optically transparent. This is critical to prevent ablation of the substrate. It also has a very small signature in terms of its contributing elements. We do see many of the elements also present in *E. coli*, however the amounts are significantly smaller. The agar is prepared at a concentration of 0.7%. The agar is prepared as follows:

1. The dry agar powder is mixed with distilled water and boiled for 15 minutes to completely dissolve the agar into solution.

2. The agar is then poured into 2.5” sample plates and put into a refrigerator to cool. This process, very similar to making jello, will create a flexible gelatinous substance which is sturdy enough to hold the bacteria.

3. Finally, in order to achieve the best results the agar is poured into the sample dish, filling it to the top, and placed in the refrigerator to solidify. The level of agar is poured slightly higher than the top lip, surface tension keeps the agar from overflowing the plate. Also, before completely solidifying the agar is scraped to

assist in creating a flat substrate. Lastly, a cover is placed on top to help prevent evaporation. When the agar substrate is allowed to setup without a cover we noticed that it would evaporate and create a concave meniscus within the sample dish.

1.3 Lab preparation of samples

All *E. coli* were cultured in the laboratory of our colleague, Dr. Sunil Palchaudhuri of the WSU Dept. of Immunology and Microbiology in his laboratory on the medical campus. The *E. coli* and substrates were delivered to the lab in individual Petri dishes. During each preparation standard microbiological precautions were taken to not contaminate the sample. Sterile utensils and gloves were used in each case. In addition masks were worn by the individuals preparing the sample. Typically, two *E. coli* samples were placed on a single agar substrate. The *E. coli* was removed from its Petri dish and spread onto the substrate in such a way as to replicate the original growth area. It should be noted that the application of the *E. coli* was different for each variety. Some of the *E. coli* samples spread easily onto the agar substrate while others tended to be a bit more 'sticky' making it much more difficult to spread from the utensil to the agar disk. Once the sample was ready it would then be moved to the experiment table for ablation. The samples were prepared immediately before collecting data. In addition each sample was cultured on the TSA substrate for approximately the same amount of time (24 hours) prior to LIBS analysis.

2 Experiment setup

The experimental setup consisted of the high-energy pulsed laser. A set of optics to deliver the beam to the collection microscope was used. Next, an optical fiber was used as a collection device which delivered the plasma light to the spectrometer. Finally, a data collection computer hooked to both the laser and the spectrometer was used to analyze data and to control timing for the laser and spectrometer. Figure 8 shows the experimental setup.

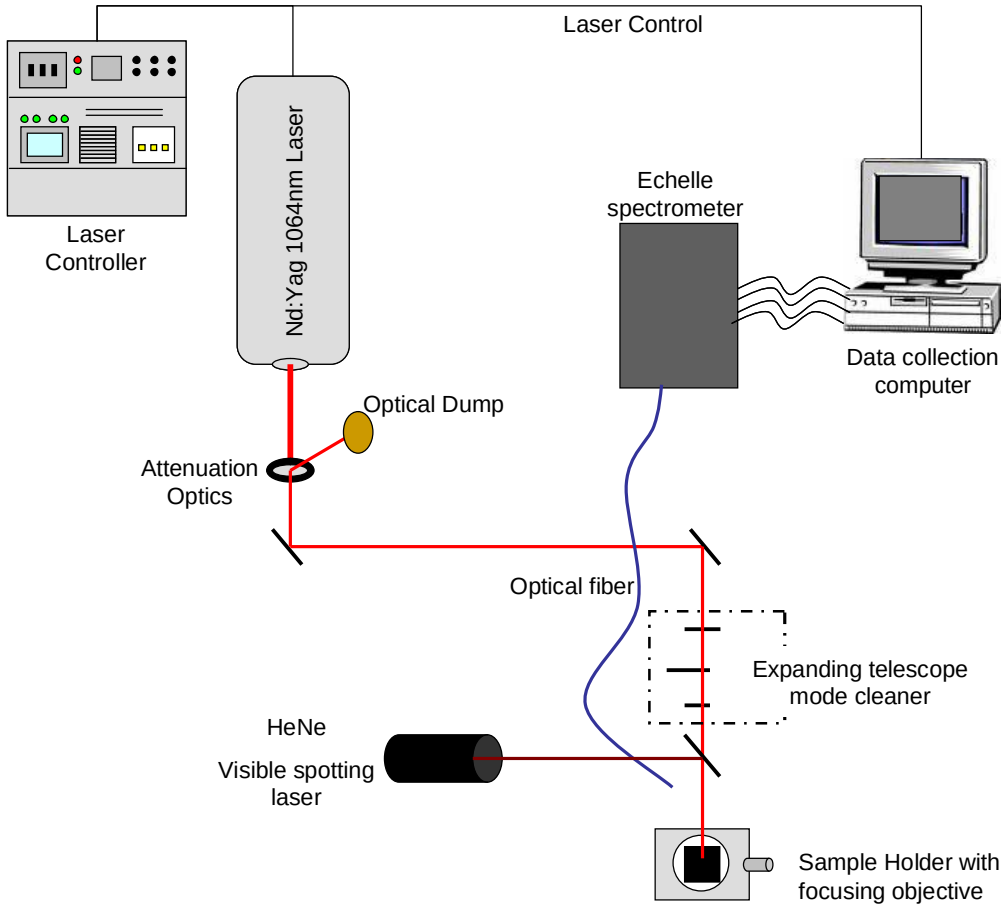

Figure 8 Experimental Setup

2.1 LASER

As discussed above a Q-Switched Nd:YAG laser was used as the energy source. The laser is a Spectra Physics, LAB-150-10. The laser was fired with 10ns pulses at 10Hz. The wavelength of the laser was 1064nm which is in the infrared portion of the electromagnetic spectrum. In comparison the visible portion is approximately 400nm to 700nm. It is also possible to do LIBS with other laser wavelengths. LIBS has been done with excimer (UV) lasers as well as visible (532 nm). In addition, femtosecond lasers at 810 nm have also been used.[51]

2.2 Optical Setup

2.2.1 Energy Attenuation Optics

The laser, Q-switched, does not have a way to regulate pulse energy. Instead the pulse energy is attenuated by optics outside the laser. As the vertically linearly polarized laser exited it passed through a half-wave plate, which allows us to produce a linear polarization of arbitrary orientation. It then entered a polarizing beam splitter which passed only vertical polarization and reflected out horizontal polarization. Because the waveplate makes the polarization of the incoming beam completely adjustable (always linear, but direction arbitrary), we could select what fraction of the beam makes it through the beam splitter. The pulse energy to be determined by how much of the beam is dumped. For the LIBS on bacteria experiments the power was set at 100 mJ/pulse. However this was not the final energy that was delivered to the sample. The final laser

energy was approximately 8mJ/pulse. The majority of this energy was lost in a “mode cleaner” which I describe later.

2.2.2 Mode Cleaning Telescope

A spatial mode cleaner consisting of a 3x telescopic beam expander was used to expand the beam from its nominal beam diameter of 9 mm to 27 mm prior to the final focusing lens. An iris with a 9 mm opening immediately following this beam-expander sampled the inner one-third of the beam diameter to obtain a more Gaussian transverse mode distribution. The LAB-150 specifies a >70% near-field (one meter) Gaussian fit to the actual spatial mode energy distribution, with this specification increasing to >95% in the far field (>6 m). The mode cleaner was located 1.3 m after the laser and transmitted approximately 15% of the energy incident upon it (100 mJ/pulse were obtained out of the laser, with 15 mJ in the pulse after the spatial filter.)

2.2.2.1 Gaussian Beam

In optics, a transverse Gaussian beam or spatial mode is a beam of electromagnetic radiation whose transverse electric field and intensity (irradiance) distributions are described by Gaussian functions. Many lasers emit beams with a Gaussian profile, in which case the laser is said to be operating on the *fundamental transverse mode*, or "TEM_{00} mode" of the laser's optical resonator. When refracted by a lens, a Gaussian beam is transformed into another Gaussian beam characterized by a different set of parameters.[69] The propagation of the laser through the optics is important to understand. It becomes important to utilize lenses and other optical elements to keep the beam as Gaussian as possible. In cases where the beam divergence

is small the paraxial approximation is used. This simplifies the propagation equation to a first order differential equation. A factor M^2 is used to describe the deviation of a beam from a theoretical Gaussian. This is called the M-squared factor. Theoretically $M^2 = 1$ in a true Gaussian beam. However, in real world cases $M^2 > 1$. As mentioned earlier the TEM_{00} mode is the fundamental transverse mode of the laser. As the beam exits a hypothetical laser it is a perfect plane wave with a Gaussian transverse profile shown in figure 9.

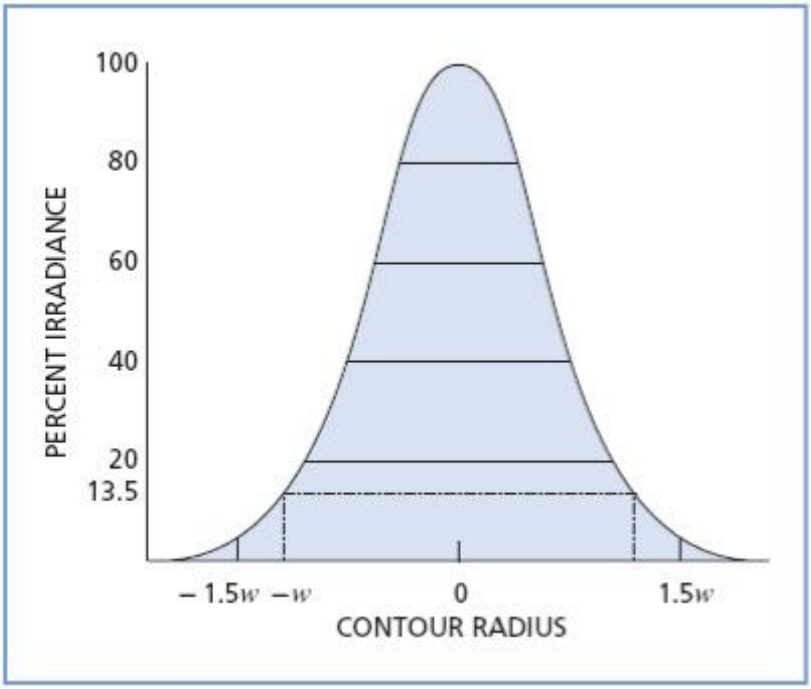

Figure 9 Gaussian profile of laser [68]

There are multiple ways to describe the diameter of the beam. The most common is to use the diameter where there intensity has fallen to $1/e^2$. Diffraction causes light waves to spread transversely as they propagate, and it is therefore impossible to have a perfectly collimated beam. The spreading of a laser beam is in precise accord with the

predictions of pure diffraction theory; aberration is totally insignificant in the present context. Under quite ordinary circumstances, the beam spreading can be so small it can go unnoticed. The following formulas accurately describe beam spreading, making it easy to see the capabilities and limitations of laser beams. Even if a Gaussian TEM_{00} laser-beam wavefront were made perfectly flat at some plane, it would quickly acquire curvature and begin spreading in accordance with:

$$R(z) = z\left[1+\left(\frac{\pi w_0^2}{\lambda z}\right)^2\right] \qquad \text{Equation 3.1}$$

and

$$w(z) = w_0\left[1+\left(\frac{\lambda z}{\pi w_0^2}\right)^2\right]^{1/2} \qquad \text{Equation 3.2}$$

where z is the distance propagated from the plane where the wavefront is flat, λ is the wavelength of light, w_0 is the radius of the $1/e^2$ irradiance contour at the plane where the wavefront is flat, $w(z)$ is the radius of the $1/e^2$ contour after the wave has propagated a distance z, and $R(z)$ is the wavefront radius of curvature after propagating a distance z. $R(z)$ is infinite at $z = 0$, passes through a minimum at some finite z, and rises again toward infinity as z is further increased, asymptotically approaching the value of z itself. The plane z=0 marks the location of a Gaussian waist, or a place where the wavefront is flat, and w_0 is called the beam waist radius.[68] Figure 10 shows propagation of a Gaussian beam. Our laser has its beam waist, w_0, located at the exit mirror with a beam diameter of 9 mm and a final divergence of <0.5 mrad.

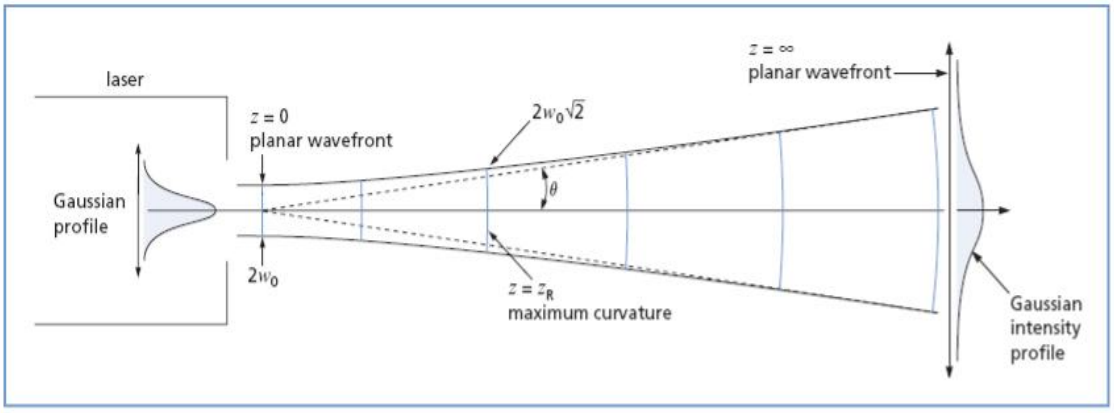

Figure 10 Beam expansion [68]

2.2.3 HeNe Alignment Laser

A helium-neon laser, usually called a HeNe laser, is a type of small gas laser. HeNe lasers have many industrial and scientific uses, and are often used in laboratory demonstrations of optics. Its usual operation wavelength is 632.8 nm, in the red portion of the visible spectrum.[72] The laser was used during the experiments as an overlay with the infra-red beam for spot visualization by using a beamsplitter (50:50 633 nm) for co-alignment. It gave a visual spot on the sample to indicate the location of ablation.

2.2.4 Collection Microscope

The beam next entered the collection telescope. Here the beam is focused through a high-damage threshold infinite-conjugate microscope objective. The setup is analogous to a laboratory microscope, light from the specimen travels through the objective to the user's eye. In the LIBS setup the light travels from the laser through the microscope and to the sample to be ablated. The focus is adjusted by correcting the height above the target sample. In the LIBS experiments the sample height was adjusted to the laser focus. Figure 11 shows different length objectives focusing the laser at different distances.

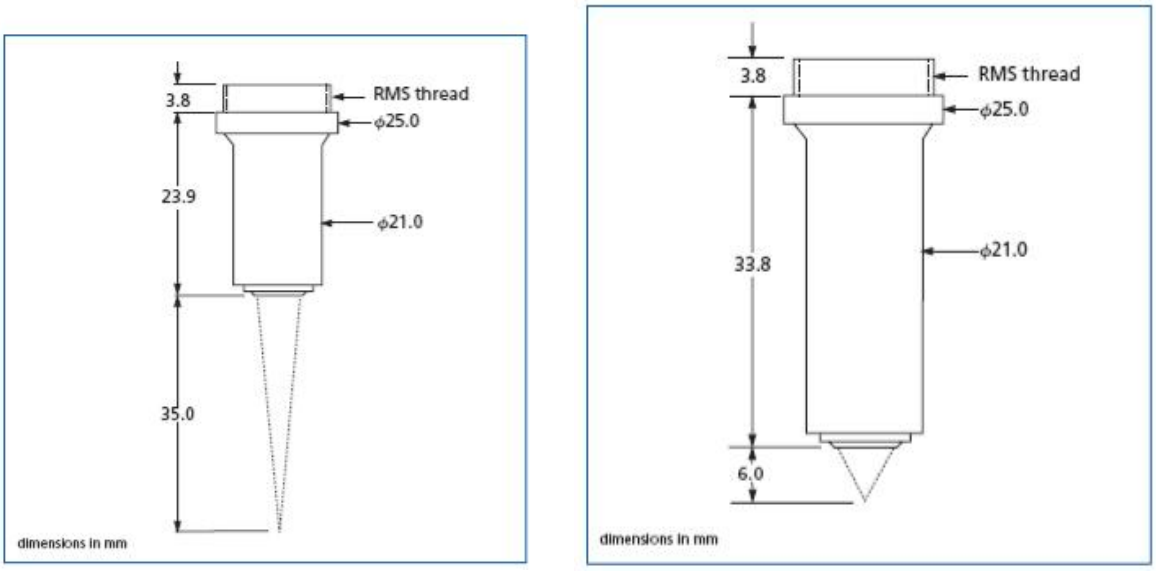

Figure 11 Focus of microscope objectives [67]

Regardless of focal length, a beam with a small waist radius is ideal. The beam waist of a laser beam is the size of the laser beam at a location along the propagation direction where the beam radius has a minimum and the wave fronts become flat. A small beam waist (more precisely, a beam waist with small waist radius) can be obtained by focusing a laser beam with large diameter with a lens which has a short focal length and high numerical aperture.[19] A beam of finite diameter is focused by a lens to obtain a smaller beam spot, as shown in Figure 12. In our experiments the laser was focused to a beam diameter of 100 μm.

If the diameter of the focused spot, d_0, is defined as the diameter which contains 86% of the focused energy, the focus spot size is determined by:

$$d_0 = \frac{2f\lambda}{D} \qquad \text{Equation 3.3}$$

where, *f* is the focal length of the focus lens, *D* is the entrance beam diameter, and λ is the wavelength.

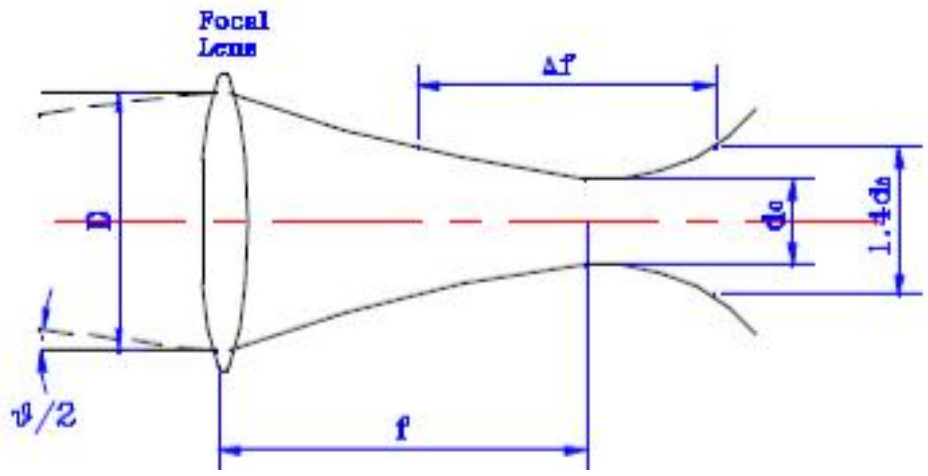

Figure 12 Focusing of a Gaussian beam

If the total beam divergence angle θ is known, the diameter of the focus spot size is given by equation 3.4.

$$d = f \bullet \theta \qquad \text{Equation 3.4}$$

It is obvious that the focus spot size is smaller if the beam divergence angle is smaller. In order to get a smaller focus spot size, a beam expander is used to reduce the beam divergence angle in most applications.

As the Gaussian beam focuses from a lens down to a waist and then expands, there is a need to define a depth of focus. Normally, it is defined as the distance between the $(2d_0)^{1/2}$ spot size points or 2 times Rayleigh range.[65,66] It can be written as:

$$\Delta f = 2Z_R \approx 2\pi\lambda F^2 \qquad \text{Equation 3.5}$$

or

$$\Delta f = \frac{2 f^2 \theta}{D} \qquad \text{Equation 3.6}$$

where F is the f- number of a focusing lens, which is defined as

$$F = \frac{f}{D} \qquad \text{Equation 3.7}$$

It is concluded from the above equations that a lens with a longer focal length gives a greater depth of focus and a larger focus spot size than a lens with a shorter focal length. Thus the focal length of the focus lens should be selected properly according to the application requirements.[65,66]

For our experiments the objective lens was selected to avoid a large depth of field. The focused ablation spot needed to be tight, and in one place. We had a limited focal length due to the experimental setup of the sample holder. The working distance beneath the objective needed to provide sufficient space in order to insert and remove samples. The objective chosen, LMH-5X-1064; Microspot Focusing Objective, has an aperture of 10mm and will give a nominal 6μm spot with 8-10mm beam and perfect alignment. The effective focal length of the objective is 40mm. The working distance from the objective was ~35mm. This allowed us to focus for best ablation, not smallest spot size, usually those are not the same place. Typically our spot size was ~12 μm. The objective has a numerical aperture of 0.13. The numerical aperture typically characterizes the range of angles the objective can receive or emit light and is given by equation 3.8. However, in laser physics θ is chosen to be the *divergence* of the beam. This is the far-field angle between the propagation direction and the distance from the beam axis for which the

irradiance drops to $1/e^2$ times the wavefront total irradiance. The NA of a Gaussian laser beam can also be related to the minimum spot size produced by the objective.[66]

$$NA = n \sin \theta \qquad \text{Equation 3.8}$$

2.3 Sample Holder

Data was collected in two configurations, in air and in argon. Both configurations used a translation stage with three moveable axes. The sample tray had .5" of travel in the X and Z directions and 1" in the Y direction. The tray had all 3 degrees of freedom to allow for adjustment of the sample in relation to the microscope objective. Replacing samples and collecting data was very straight forward. The sample was positioned in order to easily reach the thickest parts of the bacterial sample. The sample holder could easily be repositioned to collect other samples or adjust the sample thickness. Using the HeNe aligning laser the sample was positioned in the laser focus in a spot that allowed the maximum travel of the holder. Once the data collections were complete for the air configuration the sample holder was modified for collections in argon. The original translation stage was used however the sample holder was removed. A custom sample holder was fabricated from a clear plastic to hold the new samples. The front of the sample holder had an opening slightly larger than the sample trays. A door was also fabricated that would attach magnetically to the main body of the sample holder. Between the tray and the microscope objective a flexible boot is used to create an "air-tight" seal. The seal was not truly air-tight but created a chamber that could be continuously filled with a positive pressure of argon. The argon flushed all the air from the chamber allowing the bacterial samples to be ablated in argon.

2.4 Optical Collection

Optical emission from the LIBS microplasma was collected by a 1-m steel encased multimode optical fiber (core diameter = 600 μm, N.A. = 0.22) placed a distance of 23 mm from the ablation spot with no other light collection optics. This fiber was coupled to an Echelle spectrometer equipped with an intensified charge coupled device (ICCD) camera (LLA Instruments, Inc., ESA2000) which provided complete spectra coverage from 200 to 840 nm with a resolution of 0.005 nm in the UV. LIBS spectra were acquired at a delay time of 1 μs after the ablation pulse, with an ICCD intensifier gate width of 20 μs duration. Spectra from 10 laser pulses were accumulated on the CCD chip prior to readout. The sample was then translated 250 μm and another set of 10 laser pulses were averaged. 10 accumulations were averaged in this way, resulting in a spectrum comprised of 100 laser pulses that took approximately 40 seconds to obtain.

3 Data Collection

Collection of the data was methodical and straight forward. Typically two people would work in conjunction. Person A would work at the computer controlling the laser and examining the spectra. Person B would control the sample holder aligning the bacteria plate. As stated earlier the height of the sample holder was critical to the proper collection of data. Focus of the laser into the bacterial sample was important. If the sample holder was uneven, ablation of the substrate (if the sample was too high) or ablation in air could occur (sample was too low). Therefore each time a new dish was placed in the sample holder the height was adjusted. To do this a thin piece of metal shim stock was placed on the surface. The laser was focused onto the metal and LIBS spectra were obtained. This was compared with known spectra to determine the ideal

height where the focus was precisely on the surface. Next, the using the alignment laser to visualize the focus spot, the bacteria was aligned for proper sample ablation leaving enough travel of the sample plate to ensure 10 samples could be taken for each run. Once the sample was in place person A would start the flash lamps from the computer and then initiate the laser pulses. Ten groups of ten pulses were incident upon the bacteria for a total of 100 laser shots per run. Typically, there were 20-25 runs per bacterial sample. After the bacterial sample was spent (all available bacteria had been ablated) the next was placed into the sample holder and the process was repeated.

Chapter 4 Statistical Methods of LIBS

1. Statistical Principles

LIBS data collection can result in large amounts of data to analyze. Hundreds of spectra can be collected for each sample. To simply inspect each spectrum visually or reviewing the large amounts of numerical data is impractical. The differences in the spectrum of each sample can be very small. In order to identify patterns in the data and classify different samples a data analysis technique is needed. In this chapter I will first discuss several elementary statistical methods. This will set the ground work for larger statistical techniques. The elementary statistical methods discussed below are all used in the main analysis of the data. The two primary techniques discussed are principal component analysis and discriminant function analysis. Principal component analysis is a data reduction technique that can be used on many data sets. However; it was not applicable to our data. The technique I will focus primarily on is discriminant function analysis. This technique also reduces the dimension of the data but is more robust at classifying the data into groups.

1.1. Elementary Statistics

1.1.1. Standard Deviation

The standard deviation of a data set measures the spread of the measured values about the mean. In a normal distribution, 68% of the data will be within 1 standard deviation and 95% will be within 2 standard deviations of the mean.[70] The standard deviation is given by:

$$\sigma = \sqrt{\frac{1}{N-1}\sum\left(x_i - \bar{x}\right)^2} \qquad \text{Equation 4.1}$$

The standard deviation is calculated from the mean. The mean of a data set can tell several different stories. Are all the values the same? Are there large extrema to the data? Calculation of the standard deviation can shed light on these questions. For instance, if the standard deviation is zero then all of the data points are equal. The smaller the standard deviation the closer the data points are to the mean. Standard deviation can be represented graphically by thinking of a standard bell curve. Figure 13 shows a curve, which could be a histogram of measured values, with a very narrow peak representing a standard deviation of one.

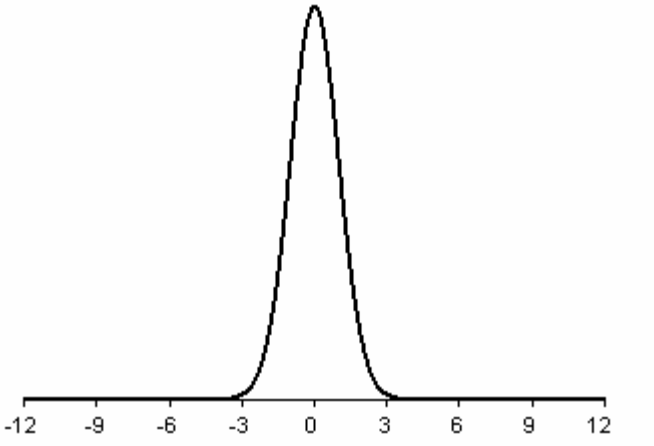

Figure 13 Curve with standard distribution of 1.

Figure 14 shows a curve with a standard distribution of 2. Notice that the data is more spread out than in Figure 13. As stated earlier, the standard deviation is a measure of how spread out the data is. Finally, Figure 15 shows a curve with standard deviation of 3. Here the data is much more spread out than the previous two figures. This indicates

that the measured values are more widely distributed about the mean of the measurements, although in all three cases, the mean is the same.[71]

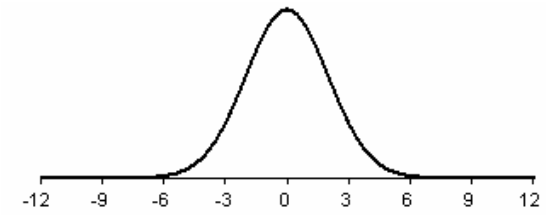

Figure 14 Curve with standard deviation of 2

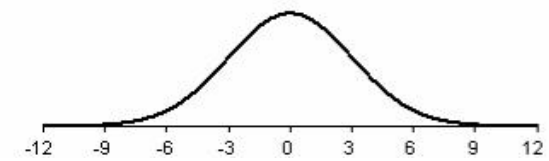

Figure 15 Curve with standard deviation of 3

1.1.2. Variance

Variance of a random distribution is the measure of its statistical dispersion. The variance indicates how much the values are spread out around the expected value. The variance is calculated from:

$$\sigma^2 = \frac{1}{N-1}\sum\left(x_i - \bar{x}\right)^2 \qquad \text{Equation 4.2}$$

The equation should look familiar, it is the square of the standard deviation. Variance is the measure of how much one variable differs from the expected value, covariance is the measure of how two random variables vary together. If two variables vary together then the covariance is positive. If for instance the variables differ in how they vary, one tends to be high while the other is below the expected value, the covariance is negative. Covariance is calculated from:

$$\mathrm{cov}(X,Y)=\sum_{i=1}^{N}\frac{(x_i-\bar{x})(y_i-\bar{y})}{N} \qquad \text{Equation 4.3}$$

Given a system with two variables X, Y the covariance is calculated from equation 4.3. From these values we can construct a covariance matrix which has all the possible combinations. In our case the matrix is 2x2, if we introduce another variable Z, the matrix will be 3x3.[71]

1.1.3. Correlation

Correlation describes the direction and strength of a straight-line relationship between two variables.[70] Typically in statistics correlation is represented by *r*. Correlation is either positive or negative and always between -1 and 1. Positive *r* represents a positive correlation between variables and negative *r* represents a negative correlation. The closer to -1 or 1 the correlation indicate that more of the points lie close to a straight-line. If *r* is 0 or near zero then there is little correlation and form a very weak straight-line relationship. Correlation is independent of the units of measure because *r* is calculated from the standard deviation. It is important to note that correlation is sensitive to a few outliers.[71]

1.1.4. Eigenvalues

Eigenvalues, sometimes referred to as characteristic roots, are a scalar values that are associated with the linear transform of a square matrix A. The ability to determine eigenvalues and eigenvectors is extremely important in physics. They also are key to DFA as they indicate the most significant discriminant functions. Eigenvalues, which are always paired with eigenvectors, can be found by decomposition of a square matrix A.

For example, let A be a square matrix representing a linear transformation. If there is a vector X such that:

$$AX = \lambda X \qquad \text{Equation 4.4}$$

then λ is an eigenvalue of the system and **X** is an eigenvector.

Letting A be a *kxk* square matrix

$$\begin{bmatrix} a_{11} & a_{12} & \mathsf{K} & a_{1k} \\ a_{21} & a_{22} & \mathsf{L} & a_{2k} \\ \mathsf{M} & \mathsf{M} & \mathsf{O} & \mathsf{M} \\ a_{k1} & a_{k2} & \mathsf{L} & a_{kk} \end{bmatrix} \qquad \text{Equation 4.5}$$

with eigenvalue λ, then the corresponding eigenvectors satisfy

$$\begin{bmatrix} a_{11} & a_{12} & \mathsf{K} & a_{1k} \\ a_{21} & a_{22} & \mathsf{L} & a_{2k} \\ \mathsf{M} & \mathsf{M} & \mathsf{O} & \mathsf{M} \\ a_{k1} & a_{k2} & \mathsf{L} & a_{kk} \end{bmatrix} \begin{bmatrix} x_1 \\ x_2 \\ \mathsf{M} \\ x_k \end{bmatrix} = \lambda \begin{bmatrix} x_1 \\ x_2 \\ \mathsf{M} \\ x_k \end{bmatrix} \qquad \text{Equation 4.6}$$

which is equivalent to the homogeneous system

$$\begin{bmatrix} a_{11} - \lambda & a_{12} & \mathsf{K} & a_{1k} \\ a_{21} & a_{22} - \lambda & \mathsf{L} & a_{2k} \\ \mathsf{M} & \mathsf{M} & \mathsf{O} & \mathsf{M} \\ a_{k1} & a_{k2} & \mathsf{L} & a_{kk} - \lambda \end{bmatrix} \begin{bmatrix} x_1 \\ x_2 \\ \mathsf{M} \\ x_k \end{bmatrix} = \begin{bmatrix} 0 \\ 0 \\ \mathsf{M} \\ 0 \end{bmatrix} \qquad \text{Equation 4.7}$$

equation 4.7 can be written as: (A- λI)X = 0; where I is the identity matrix. The solutions of this equation can be found from:

$$\det(A - \lambda I) = 0 \qquad \text{Equation 4.8}$$

Equation 4.8 is known as the characteristic equation of the system.[73]

1.2. Principal Component Analysis

Principle Component Analysis (PCA) is a data reduction technique to allow for analysis of data with high dimension. PCA is a method to find similarities and differences in data. By reducing the number of dimensions, without reducing the amount of information, it is possible to find patterns in the data that otherwise couldn't be detected. PCA combines several elementary statistical techniques to achieve this reduction and allow for a graphical plot of the data. Standard deviation, variance and covariance matrices are some of the said techniques and were discussed earlier. PCA consists of 5 steps discussed below.

1. Find mean and subtract it from each data value. This produces a new data set whose mean is zero.
2. Calculate the covariance matrix
3. Calculate the eigenvalues and eigenvectors of the covariance matrix.
4. Reduce the number of data dimensions by selecting the eigenvectors with the largest eigenvalues. The eigenvector with the largest eigenvalue is the principal component. By selecting only the highest eigenvalues we are reducing the number of dimensions of the data. It should be noted that some information is lost by throwing out the smallest of eigenvalues. However; typically this is less than 1% of the information. Using the largest eigenvectors a feature vector can be chosen. From this feature vector a matrix of vectors can be constructed by putting the eigenvectors in the columns.

5. Lastly, derive a new data set using the feature vector and multiply its transpose on the left of the transposed original data set. This will give a new data set with the same dimension as the original.

PCA has many advantages in data analysis. The ability to easily reduce the dimension of large data sets is the greatest advantage of PCA. However; in our experiments PCA didn't give enough discrimination between samples. It was possible to derive some patterns in the data, but it wasn't definitive. Another technique was needed to provide greater discrimination within the data.

2. Discriminant Function Analysis (DFA)

Discriminant function analysis is a multivariate analysis of variance. DFA attempts to determine membership in naturally occurring groups. To predict the group memberships DFA uses the independent variables (predictors) instead of the dependent variables. By creating discriminant functions, DFA can find small commonalities in the variances of the dependent variables. It then can classify each dependent variable by giving it a score. The scores are then plotted. From the plots measurements of confidence can be made on the group predictions. DFA is similar to other statistical classification techniques including Principle Component Analysis, Multiple Regression and MANOVA (Multivariate analysis of variance). In fact the first two parts of DFA are identical to MANOVA (only in reverse) in terms of the computations. Where DFA differs is in the group prediction. Note: the information below was derived from the software documentation from the software package used in this analysis, SPSS V15.0, SPSS Inc..

2.1. Finding Discriminant Functions

To construct the discriminant functions we first look at the variability within the independent variables. We can create two matrices, one with the total variance. The total variance does not discriminate among the dependent variables. The second matrix is constructed from the within group variance. Equation 4.9 describes the discriminant function. The discriminant scores are found to maximize the ratio between the group variances.

$$D_i = b_0 + \sum_{k=1}^{p} b_k X_k \qquad \text{Equation 4.9}$$

Equation 4.9 is used to determine the discriminant functions using the known variables and unknown which we solve for. The *X* variable in equation 4.9 represents the experimentally determined data. These values are the areas under the peaks of the chosen spectral lines. In our case *p* is equal to 19, because we analyzed the intensity of 19 emission lines. The *b* values are the coefficients calculated during DFA. Together they form *D* which is the discriminant function. The discriminant function, also called a *canonical root*, is a latent variable which is created as a linear combination of discriminating (independent) variables, such that D = b0 + b1x1 + b2x2 + ... + bnxn, where the *b's* are discriminant coefficients, the x's are discriminating variables, and *b0* is a constant. The *b's* are discriminant coefficients which maximize the distance between the means of the criterion (dependent) variable. The maximum number of discriminant functions is equal to one less than the number of dependent variables. For example, calculating the mean discriminant function coefficient will give you the centroid for each

group. When plotted the separation in the centroids will show the dimensions along which the groups differ.

2.2. Testing for Significance

2.2.1. Statistically Significant

The second step of DFA is to test the discriminant functions for statistical significance. Statistical significance is the likelihood that a result did not occur by 'chance'. Statistical significance indicates that there is a difference between results regardless of how large or small it is. However; it should be noted that because a result did not occur by chance tells nothing of it. It does not indicate that the result is good or has any decision-making ability.

Performing a significance tests involves comparing a test value to a value that was calculated to some critical statistic. In our case we calculate the Wilks lambda in two different manners which allows us to compare the results thus generating a statistic of significance. In general however it doesn't matter what type of statistic we are calculating (e.g., a t-statistic, a chi-square statistic, an F-statistic, etc.), the procedure to test for significance is the same.

1. Decide on the critical alpha level you will use (i.e., the error rate you are willing to accept).
2. Conduct the research.
3. Calculate the statistic.
4. Compare the statistic to a critical value obtained from a table.

If your statistic is higher than the critical value from the table:

- Your finding is significant.
- You reject the null hypothesis.
- The probability is small that the difference or relationship happened by chance, and p is less than the critical alpha level ($p < alpha$).

If your statistic is lower than the critical value from the table:

- Your finding is not significant.
- You fail to reject the null hypothesis.
- The probability is high that the difference or relationship happened by chance, and p is greater than the critical alpha level ($p > alpha$).

The null hypothesis states, in our case, that there are no differences between the groups of data being analyzed. If the data is indeed statistically significant then the null hypothesis is rejected. Modern computer software can calculate exact probabilities for most test statistics. If you have an exact probability from computer software, simply compare it to your critical alpha level. If the exact probability is less than the critical alpha level, your finding is significant, and if the exact probability is greater than your critical alpha level, your finding is not significant. Using a table is not necessary when you have the exact probability for a statistic.

2.2.2. DFA Significance Test

DFA also uses tests of significance to disprove the null hypothesis. Discriminant function analysis provides the null hypothesis that all the data is sampled from a single normal distribution with mean μ and variance σ^2. In DFA we test for significance through several variables and statistical tests including: Wilks' Lambda and F-Test for significance.

2.2.2.1. F-Test for Significance

F-Statistic determines the significance of means between groups. The F statistic also tests the null hypothesis that the values are sampled from a single normal distribution. To determine differences the matrix of total variances and covariances is compared to the within-group matrix of variances and covariances.

From these matrices we can determine the sum-of-squares-and-cross-products-matrix (SS) for the within-group and between group matrices. The total is simply the sum of each.

$SS_{bg} \equiv$ between group matrix

$SS_{wg} \equiv$ within-group matrix

$SS_{total} = SS_{bg} + SS_{wg}$

The determinants of the various SS matrices are found and ratios between them are used to test hypotheses about the effects of the independent variables on linear combination(s) of the dependent variables. In the case of DFA it determines if there is significant difference in the means of the sampled groups. If the F-Statistic, which is a

function of the Wilks' lambda, is ~1 then there are no significant differences among the group means.

2.2.2.2. Wilks' Lambda

Wilks' lambda is used to test the null hypothesis that the groups have identical means within the distribution. Wilks' lambda is $= \frac{SS_{within\_groups}}{SS_{total}}$, so the smaller the Wilks' lambda the more doubt cast upon that null hypothesis. We can determine how much of the variance in the grouping variable is explained by our predictor variables by subtracting the Wilks' lambda from one. [15]

2.2.3. DFA Eigenvalues

In order to determine which discriminant function has the most weight the eigenvalues are used. Each discriminant function has an eigenvalue associated with it. The eigenvalues, also referred to as a characteristic roots or singular values, assess relative importance because they reflect the percents of variance explained in the dependent variable, cumulating to 100% for all functions. That is, the ratio of the eigenvalues indicates the relative discriminating power of the discriminant functions. If the ratio of two eigenvalues is 1.4, for instance, then the first discriminant function accounts for 40% more between-group variance in the dependent categories than does the second discriminant function.[16] The eigenvalues are determined from the covariance matrix. The eigenvectors associated with the eigenvalues are orthogonal with ensures that the discriminant functions do not correlate with one another. Two other values associated with the discriminant function eigenvalues are the relative percentage and the canonical correlation, R*.

The relative percentage of a discriminant function equals a function's eigenvalue divided by the sum of all eigenvalues of all discriminant functions in the model. Thus it is the percent of discriminating power for the model associated with a given discriminant function. Relative % is used to tell how many functions are important. Typically, in data such as ours, one may find that only the first two or so eigenvalues are of importance.

The canonical correlation, R*, is a measure of the association between the groups formed by the dependent and the given discriminant function. When R* is zero, there is no relation between the groups and the function. When the canonical correlation is large, there is a high correlation between the discriminant functions and the groups. Note that relative % and R* do not have to be correlated. R* is used to tell how much each function is useful in determining group differences. An R* of 1.0 indicates that all of the variability in the discriminant scores can be accounted for by that dimension. Note that for two-group DA, the canonical correlation is equivalent to the Pearsonian correlation of the discriminant scores with the grouping variable.

2.3. Classification

Classification sets DFA apart from other multivariate analysis techniques. If the F-Tests indicates that there is significant difference in the group variance it is then possible to classify the groups. Using the most significant discriminant function, determined by the largest eigenvalue, the discriminant function scores can be determined. The discriminant coefficients (b_k from equation 4.9) are than used to calculate correlations between the entries and the discriminant scores. Classification score CS_j for group j is found by multiplying the raw score on each predictor (x) by its associated classification function coefficient (c_j), summing over all predictors and adding a constant, c_{j0}

$$CS_j = c_{j0} + c_{j1}x_1 + \mathsf{L} + c_{jp}x_p \qquad \text{Equation 4.10}$$

The coefficients are found by taking the inverse of the within-group covariance matrix SS_{wg} and multiplying it by the predictor means:

$$C_j = W^{-1}M_j \qquad \text{Equation 4.11}$$

And the intercept is found by:

$$c_{j0} = \left(-\frac{1}{2}\right)C_j M_j \qquad \text{Equation 4.12}$$

Using the discriminant functions and classifications scores as a model we can classify/predict each group. Consider the following approach:

- Calculate the probability that a subject belongs to a certain group using the estimated discriminant model.
- Do this for all groups.
- Classification rule: subject is assigned to group it has the highest probability to fall into.

3. Application to LIBS bacteria Experiments

3.1. Spectral Lines

In our LIBS bacteria experiment we used 19 spectral lines, see Table 1 in Chapter 5 for details on each line. To determine the intensity of these 19 lines, spectra from 2 different *E. coli* samples, HF4714 and Nino C, and the substrate (agar) were collected

and analyzed using the Esawin software suite. Figure 16 is a typical spectrum from an *E. coli* sample.

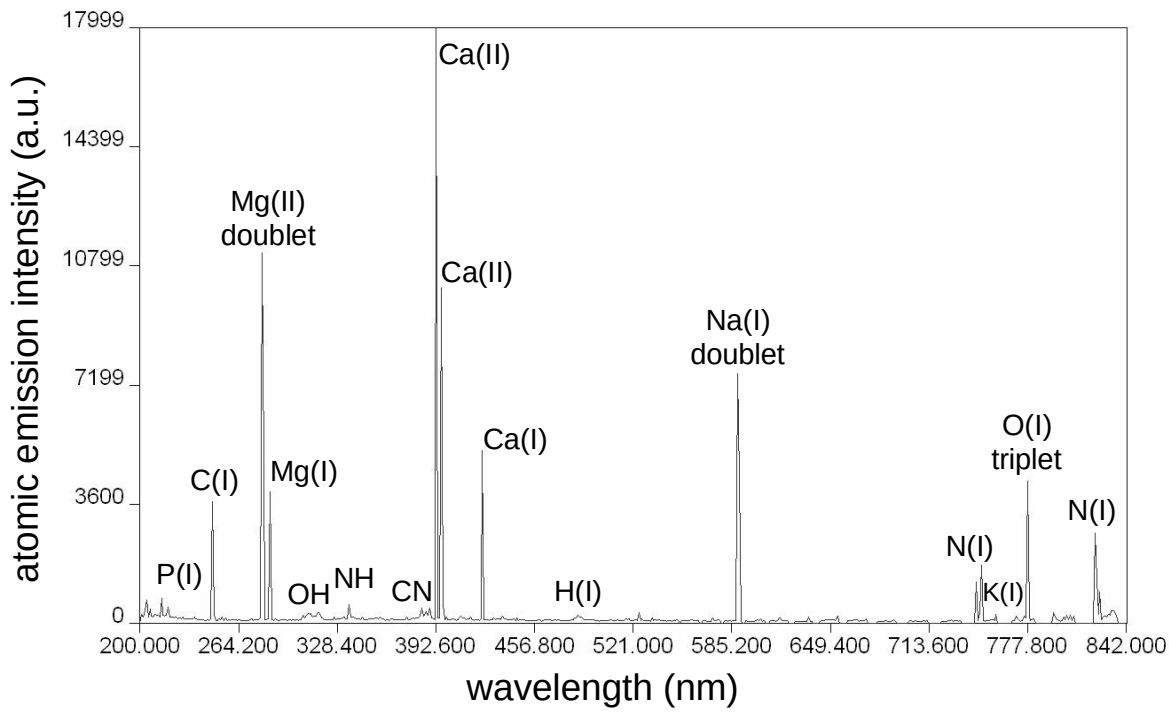

Figure 16 Typical E. coli spectrum

Each peak was examined to determine if it was a true peak or simply noise. Several parameters can be adjusted within the software that effect the spectral signatures. The gate delay, τ_d is the time interval before measurement begins following the laser pulse. The detector gate width, τ_w is the time during which the emission is integrated. These timing parameters, as well as the amplification, were not fully optimized initially, but were chosen based on preliminary observations to provide relatively intense elemental line emission while minimizing background continuum emission.

The spectral peaks are related to 6 elements: carbon (C), calcium (Ca), phosphorous (P), magnesium (Mg), sodium (Na) and potassium (K). The areas under the

curve for these 19 lines represent the independent variables in the discriminant function analysis. Note that all the lines are not equal and some contribute to the analysis more than others. By examining the output from the discriminant function analysis we can determine which lines contribute and how much. In order to determine the area under the peak of each emission line the Esawin software performs a non-linear least squares fit of a Lorentzian lineshape to each emission line. This value, which is defined to be the intensity, is then utilized as the single independent predictor variable in our analysis.

Standardized Canonical Coefficients are one of the statistics provided as output of the analysis. The standardized coefficients allow you to compare variables measured on different scales. Coefficients with large absolute values correspond to variables with greater discriminating ability. Figure 17 shows the independent variable coefficients associated with each of the 19 specific emission peaks for each of 4 discriminant functions .

Standardized Canonical Discriminant Function Coefficients

	Function			
	1	2	3	4
P213.618	.455	.342	1.801	1.340
P214.914	.561	.299	1.136	1.050
P247.856	1.148	1.832	4.017	2.734
P253.566	-.029	.138	.105	.769
P279.553	.566	.188	.951	1.289
P280.271	.382	.077	1.008	1.123
P285.213	.103	-.316	1.262	.706
P373.690	.153	.117	.406	.715
P383.231	.411	.165	.585	1.078
P383.829	.046	.357	.129	.699
P393.366	.204	1.347	2.924	2.116
P396.847	.625	.662	1.022	.859
P422.673	-.254	.190	1.310	.779
P430.253	.371	.253	1.311	1.223
P518.361	.146	.117	.390	.599
P585.745	-.079	-.022	.250	.612
P588.995	1.462	.775	1.883	2.076
P589.593	1.045	.291	1.596	.965

Figure 17 Discriminant Function Coefficients

In addition to the standardized canonical coefficients the structure matrix shows the correlation of each predictor variable with the discriminant function. The ordering in the structure matrix is the same as that suggested by the tests of equality of group means and is different from that in the standardized coefficients table. Figure 18 is an example of a structure matrix where discriminant function one is most strongly defined by the two lines of sodium at 589.593 and 588.995. This is the defining difference between our substrates (which are sodium rich) and the bacteria (which are relatively sodium poor). Although the spectra from substrates and bacteria are different, it is the presence, or relative size of the sodium peaks, which perform most of the discrimination between

them. Notice how function two (as denoted by the asterisks,) is most importantly defined by the magnesium lines at 279.553, this function is used to discriminate between bacteria.

Structure Matrix

	Function			
	1	2	3	4
P589.593	.661*	-.083	.311	-.123
P588.995	.553*	-.062	.115	.152
P285.213	-.185	-.678*	.285	-.008
P279.553	-.215	-.342*	-.176	-.147
P280.271	-.186	-.316*	-.125	-.170
P247.856	-.087	.279*	-.261	-.020
P393.366	-.202	.207	.352*	-.144
P422.673	-.124	-.178	.299*	.087
P253.566	-.034	.051	-.254*	.212
P214.914	-.040	-.021	-.197*	.001
P769.896 [a]	-.019	-.206	-.405	-.444*
P383.829	-.030	.100	-.207	.436*
P383.231	-.048	.060	-.131	.409*
P585.745	-.025	.019	-.078	.370*
P396.847	-.169	.202	.113	-.291*
P518.361	-.029	.029	.061	.278*
P373.690	-.030	.145	-.256	.256*
P430.253	-.014	.016	.038	.111*
P213.618	-.037	-.043	.074	.081*

Pooled within-groups correlations between discriminating variables and standardized canonical discriminant functions
Variables ordered by absolute size of correlation within function.

*. Largest absolute correlation between each variable and any discriminant function

a. This variable not used in the analysis.

Figure 18 DFA Structure Matrix - The structure matrix shows which elements contributed the most to discrimination

Chapter 5 Results

1 Data Preparation

To analyze the data collected during the experiments it is necessary to be able to get at the spectra raw data. Using software it is possible to enter the measured line intensities from spectra and generate statistics and graphs. In chapter 4, figure 16 shows a typical LIBS spectrum from an *E. coli* sample. As observed by Baudelet *et al*.,[50] the *E. coli* spectrum is dominated by singly ionized and neutral Mg and Ca.[51] From these and other dominant emission lines, 19 were selected to be analyzed by nonlinear least squares fitting of a Lorentzian line shape to each emission peak.[52] Table 1 show the 19 lines used in the analysis. In addition, Table 1 shows a specific spectrum sampled from the data collected. The fraction of total spectral power and Wilks' Lambda are specific for this given spectrum, however the concepts can be used on all of the experimental data.

wavelength (nm)	line identification	fraction of total spectral power	Wilks' Lambda
213.618	P I	0.023	.619
214.914	P I	0.013	.492
247.856	C I	0.086	.521
253.560	P I	0.005	.771
279.553	Mg II	0.201	.040
280.271	Mg II	0.109	.061
285.213	Mg I	0.097	.037
373.690	Ca II	0.002	.909
383.231	Mg I	0.008	.782
383.829	Mg I	0.006	.588
393.366	Ca II	0.081	.034
396.847	Ca II	0.035	.060
422.673	Ca II	0.031	.062
430.253	Ca I	0.001	.803
518.361	Mg I	0.003	.773
585.745	Ca I	0.001	.920
588.995	Na I	0.182	.020
589.593	Na I	0.103	.022
769.896	K I	0.012	.931

Table 1 Identification, relative strength (for a given spectrum), and importance to discriminant functions of nineteen atomic and ionic emission lines used in the spectral fingerprinting of bacteria.

Using the Esawin software provided with the spectrometer it is possible to get the measured line intensities of each spectral line collected. From these values it is necessary to normalize the data for consistent values across the 19 lines. Some spectra were larger than others, analysis of such data would result in skewed outcomes due to a few large spectra. Normalization strategies were discussed before two were settled on for testing. The first method used the largest line, carbon, as a normalization line, and all line intensities were divided by the intensity of this line. However, it did not yield the consistency needed. The second method utilized the total spectral power. The total spectral power was calculated from the sum of the intensities of all 19 lines. Once the normalized values for each emission line are known they are put into a 1x19 array and entered into SPSS and the Discriminant Function Analysis (DFA) was performed. This analysis was described in detail in Chapter 4. It is the relative strengths of these 19 lines

that form the basis of discrimination. From the DFA statistics, SPSS generates graphs of the discriminant function scores for each of the samples. Each function is optimized such that the first function provides the most overall discrimination and second provides the second most, etc. The sections below will show the graphical output of the DFA analysis on different bacterial samples.

2 *E. coli*

2.1 HF4714 & Nino C

Initial bacterial experiments began with investigation of two strains of *E. coli*. Starting with just two strains the goal was to be able to discriminate between the two with a high degree of confidence. The initial two strains chosen were nonpathogenic HF4714 and Nino C. These two strains will be used as a basis for comparison through out the bacteria experiments.

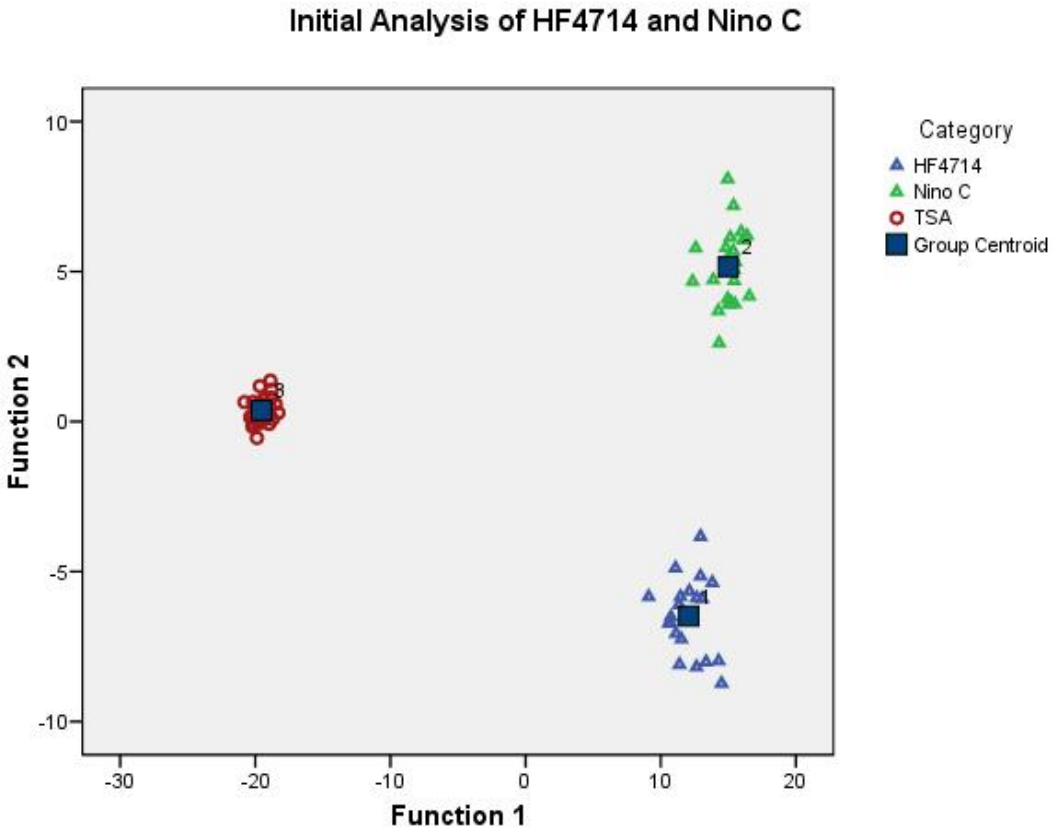

Figure 19 Initial discrimination results

Figure 19 shows a DFA plot of HF4714, Nino C and TSA. This type of graph will be used throughout this chapter to show results from the LIBS bacterial analysis. Each colored object in the graph represents a single data point representing an entire spectrum. This point is the plot of the spectrum's discriminant function one (DF1) score verses its DF2 score. The legend in the upper right of each of the graphs indicates which colored object is associated with each bacteria, yeast, substrate etc. The group centroid, the mean of the group, is shown as a blue square. Notice how the spectra from a single type of *E. coli* are clustered around the group centroid, but clearly away from the other samples. In the above graph HF4714 is represented by the blue triangle, Nino C by the

green triangle and the TSA substrate by the red circle. Using the SPSS software we can determine the total variance expressed in each DF, the separation between centroids of each group and finally the prediction percentage of group membership for each sample plotted. Recall from chapter 4 that most of the information is contained in Function 1. The output from the SPSS DFA analysis reports that 93.1% of the variance is expressed in function 1 as opposed to 6.9% in function 2. In the figure above there is a difference of 34.54 and 31.61 between the centroids of TSA and the *E. coli* samples respectively. This indicates that there is significant discrimination between the TSA and the *E. coli*. This is not shocking as we would expect large similarities between the different strains of *E. coli*. However; if we look at Function 2 there is a separation between HF4714 and Nino C. This is significant. Although there is a small amount of information in Function 2 it is still able to determine a difference between the strains of *E. coli*. The separation values are relative to the samples being investigated. They do however make sense in the scope of the graph presented. In Function 1 the difference was around 35. In Function 2, the one that discriminates the *E. coli*, the separation is smaller, around 10, which we would expect.

DFA was able to predict group membership 100% of the time. The cross-validation of each group showed that 95% of the HF4714 predicted correctly and 95.7% of Nino C predicted correctly. Table 2 shows each group (bacteria sample or TSA) shown as columns. Group 1 is HF4714, Group 2 is Nino C and Group 3 is TSA. They are listed in the same order as shown in the Figure 19. Along the rows are the counts for each of the samples. For example, in Table 2 Count 1 Group 1 has a value of 20. This indicates that 20 HF4714 samples were predicted as HF4714. The next row shows that 23 Nino C

spectra were grouped as Nino C and similarly 30 TSA were predicted to be in group 3 (TSA). Below the counts are the percentage that were placed in each group. Ideally, as in this case, all the spectra will be correctly predicted.

SPSS can also cross-validate the data. Here SPSS removes the given group identification for each spectra to classify it freely. In this case nearly all spectra were correctly predicted. What it shows for both HF4714 and Nino C is that when not associated with a group two spectra will be incorrectly classified. This is significant as it shows that given a database of values it is possible to put in an unknown sample and predict rather accurately the group membership and thus the strain of bacteria.

Classification Results[b,c]

			Predicted Group Membership			
		Category	1	2	3	Total
Original	Count	1	20	0	0	20
		2	0	23	0	23
		3	0	0	30	30
	%	1	100.0	.0	.0	100.0
		2	.0	100.0	.0	100.0
		3	.0	.0	100.0	100.0
Cross-validated[a]	Count	1	19	1	0	20
		2	1	22	0	23
		3	0	0	30	30
	%	1	95.0	5.0	.0	100.0
		2	4.3	95.7	.0	100.0
		3	.0	.0	100.0	100.0

a. Cross validation is done only for those cases in the analysis. In cross validation, each case is classified by the functions derived from all cases other than that case.

b. 100.0% of original grouped cases correctly classified.

c. 97.3% of cross-validated grouped cases correctly classified.

Table 2 Classification Results

Agar, the ablation substrate, was initially not included in the analysis. Agar which was chosen for many of its optical properties has some of the same elemental

constituents as the bacteria. It is statistically different and is shown in Figures 20 and 21. Figure 20 shows its place with the HF4714, Nino C and TSA. As you can see it is similar to the bacteria as illustrated by its Function 1 score. In Function 2 it is most similar to HF4714 but still clearly different. To investigate this further, Figure 21 shows the same data with TSA removed. This figure illustrates discrimination among samples. The relative scale of the discriminant functions is similar but the groupings are more clearly visible.

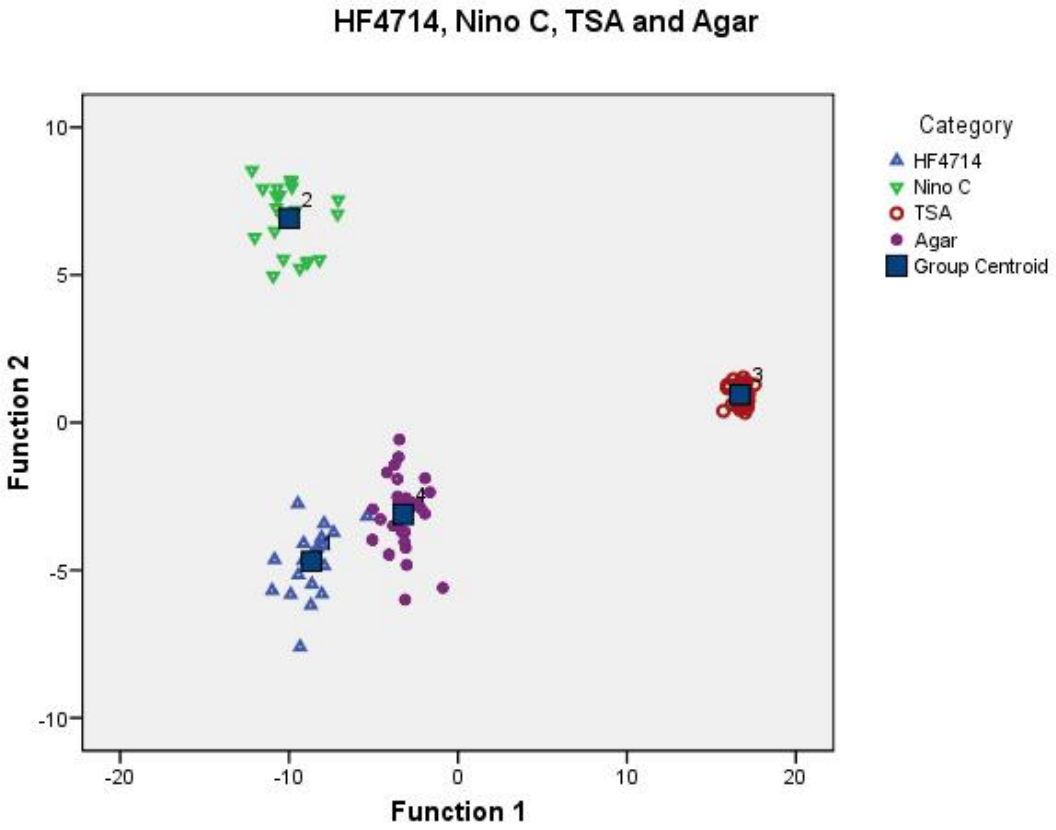

Figure 20 HF4714, Nino C, TSA and agar

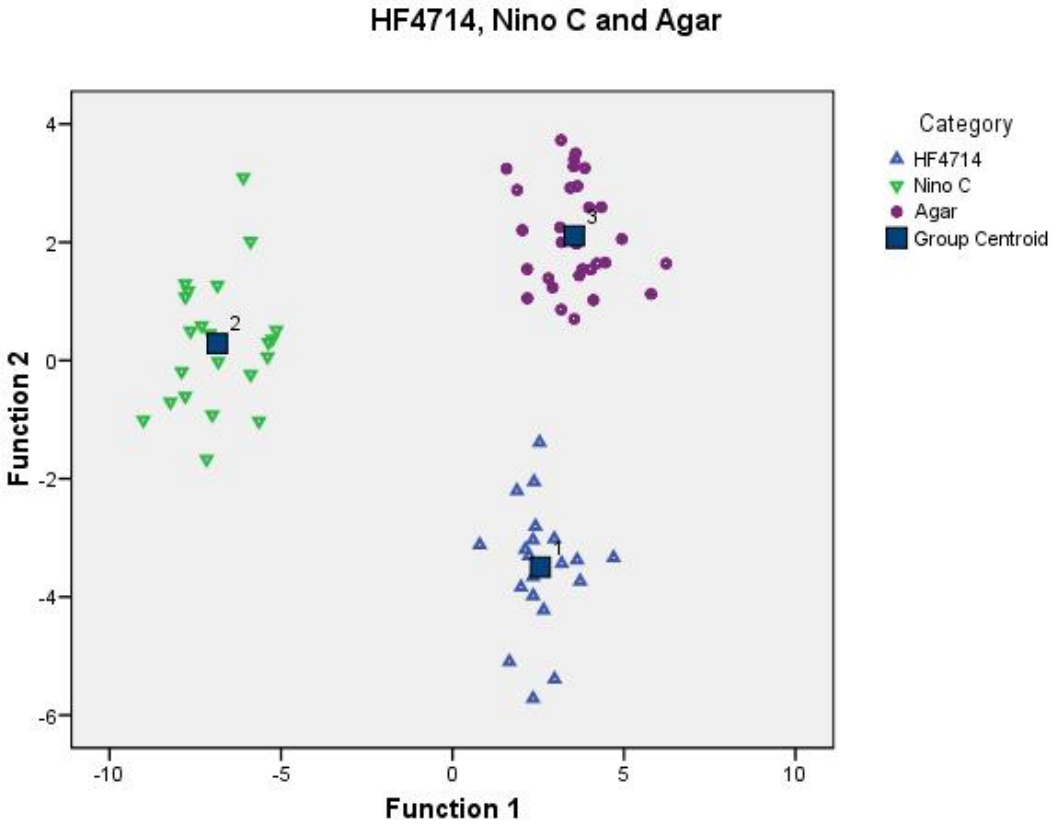

Figure 21 HF4714, Nino C and agar

To statistically quantify the prediction ability of the agar graphs DFA was able to predict group membership 100% of the time for each group. Cross-validation showed that HF4714 and Nino C predicted 95% and 95.7% accurately and agar with 100% accuracy, Table 3.

Classification Results[b,c]

		Category	Predicted Group Membership 1	2	3	Total
Original	Count	1	20	0	0	20
		2	0	23	0	23
		3	0	0	30	30
	%	1	100.0	.0	.0	100.0
		2	.0	100.0	.0	100.0
		3	.0	.0	100.0	100.0
Cross-validated[a]	Count	1	19	0	1	20
		2	1	22	0	23
		3	0	0	30	30
	%	1	95.0	.0	5.0	100.0
		2	4.3	95.7	.0	100.0
		3	.0	.0	100.0	100.0

a. Cross validation is done only for those cases in the analysis. In cross validation, each case is classified by the functions derived from all cases other than that case.

b. 100.0% of original grouped cases correctly classified.

c. 97.3% of cross-validated grouped cases correctly classified.

Table 3 Classification Results

These initial results were encouraging. Next, more data was collected on the same strains in order to develop a database for future comparison. Post collection of new HF4714 and Nino C data, analysis showed discrepancies in the data as compared with our initial findings. Much of the new HF4714 data grouped as Nino, Figure 22. Upon further inspection of the samples it was shown that the agar substrate was not prepared in the same fashion as the first. Also, there was believed to be some contamination within the lab in which the *E. coli* samples were grown. This was significant due to the fact that the results identified these discrepancies. It should be noted that it is impossible for us to identify what the contamination was or how it occurred. It is only significant that the detection of an anomaly is possible with this technique.

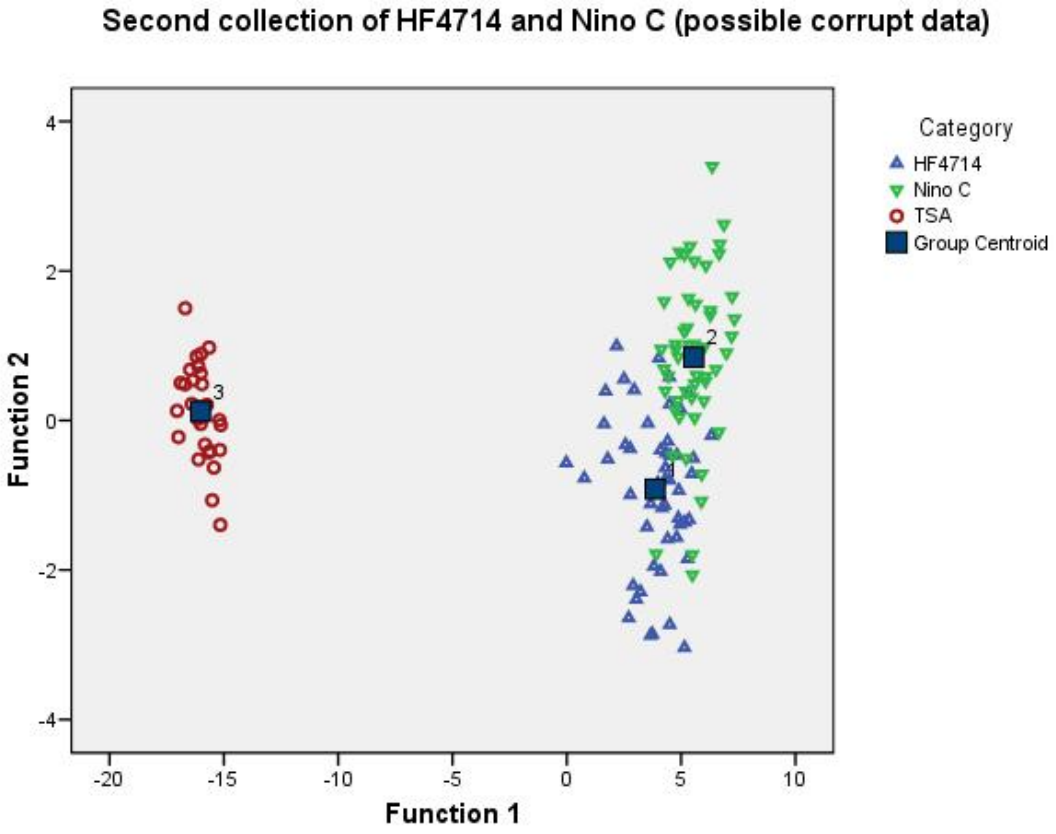

Figure 22 Second collection of data. Possible contamination.

If we remove the suspect HF4714 the Figure 23 is now similar to Figure 19 in terms of the separation between TSA and the bacteria as well as the separation within the bacteria. From this we can conclude that indeed the data collected was suspect.

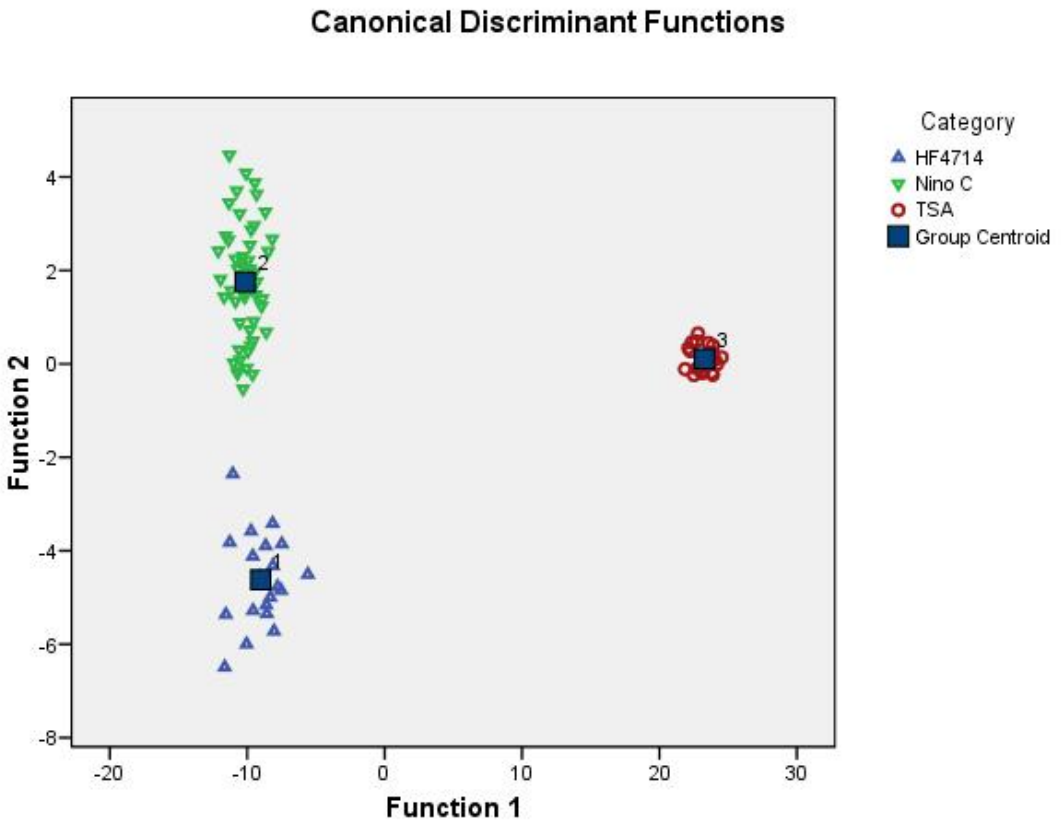

Figure 23 Removing the suspect HF4714 sample

Once we determined that we had suspect HF4714 data we turned to collecting more data, keeping the emphasis on HF4714 and Nino C. As shown in all figures the growth medium, TSA, is clearly different from the bacteria. To investigate this further data was collected from the same two strains of *E. coli*, but grown differently from the previous collection. As discussed in chapter 3 there are two growth mediums we investigated, TSA and TSB. HF4714 and Nino C were grown in the TSB and transferred to the agar (ablation substrate) via micropipette. This created a uniform area of bacteria for ablation. Figure 23 shows the two strains compared against the TSA for consistency.

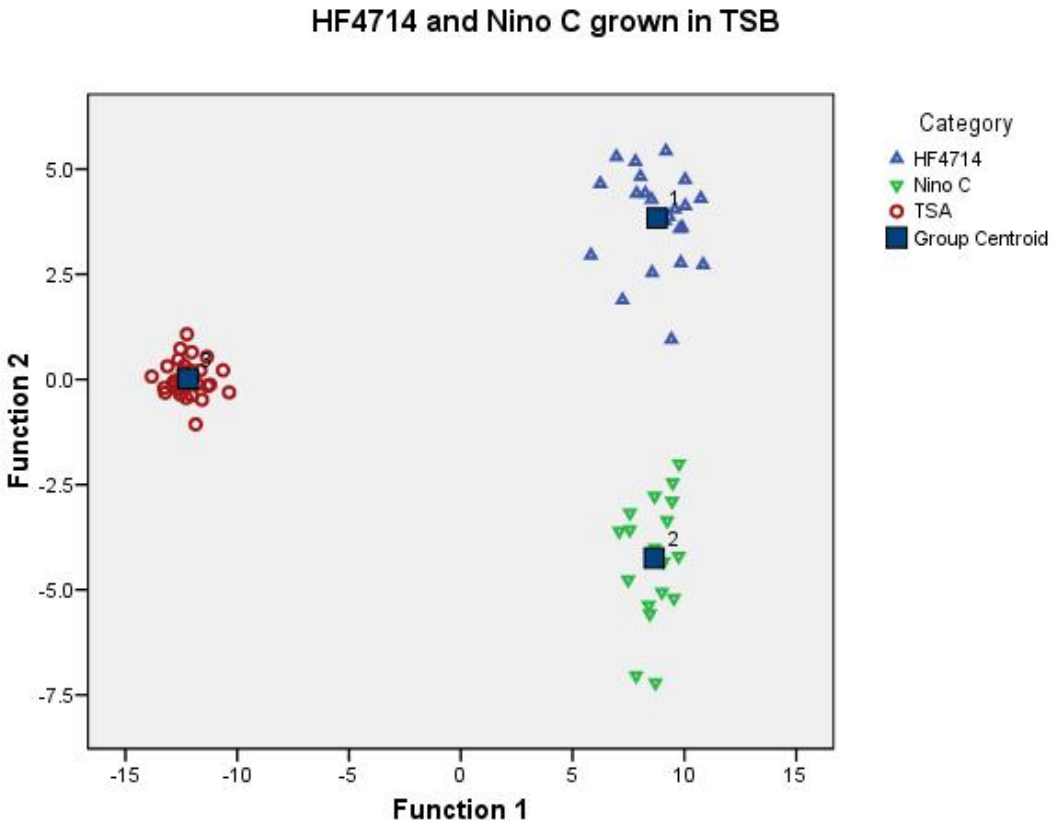

Figure 24 HF4714 and Nino C grown in TSB

Figure 24 shows HF4714 and Nino C grown in the broth. The data plot is very similar to Figure 19. From this we can conclude that growth media does not immediately effect the discrimination of the bacteria strains. Next, additional *E. coli* samples will be investigated.

2.2 Additional Strains of E. coli

2.2.1 AB

Once we had a spectral library built we could then introduce other bacterial samples to investigate the ability of LIBS to discriminate among more than two strains. The introduction of two *E. coli* strains would allow for possible discrimination of four *E.*

coli strains. EHEC and AB were prepared for ablation in an identical manner as the HF4714 and the Nino C. Each strain was ablated and the spectrum collected. Figure 25 shows three of the *E. coli* strains (HF4714, Nino C and AB) plotted with TSA. It is obvious from the plot that the bacterial samples are very similar to each other in comparison to the TSA. The near vertical alignment of the three strains indicates that their function 1 scores are nearly the same. With 90.2% of the variance in function 1 it clearly indicates that the discrimination between the bacteria and the TSA is the greatest difference.

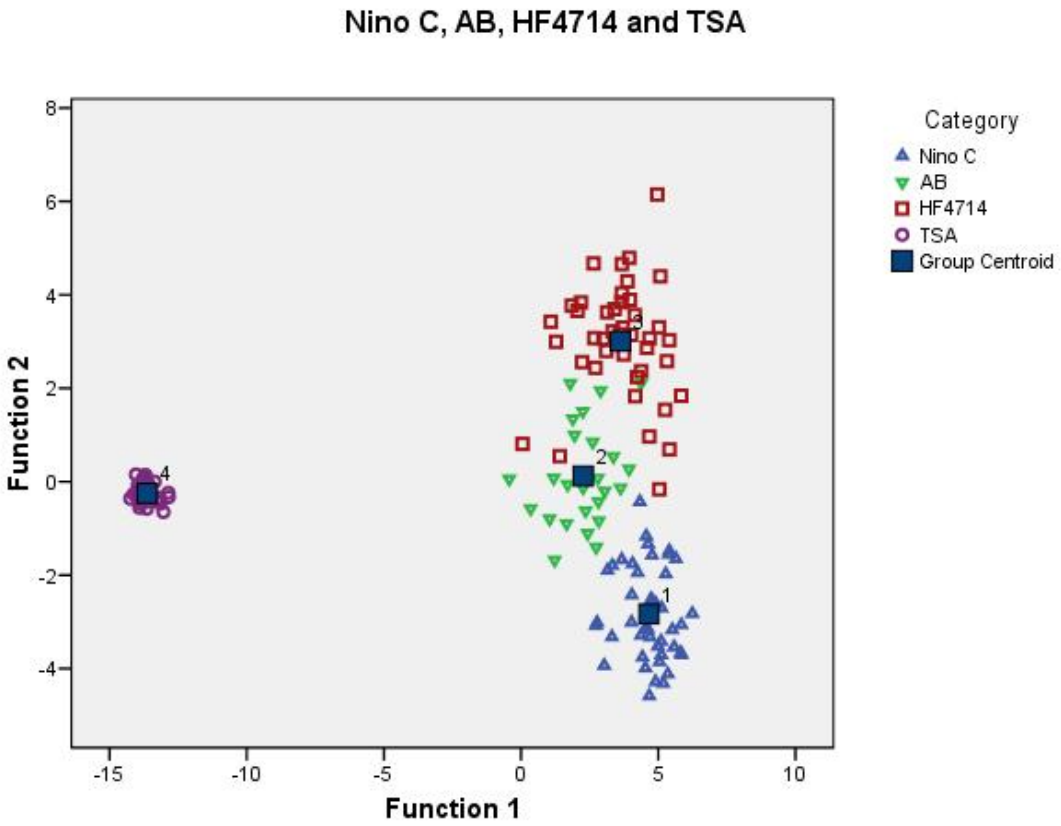

Figure 25 Three *E. coli* strains

Figures 26 and 27 show AB plotted with each of the previous strains. In each case the analysis was able to discriminate between strains. In figure 26, DFA was able to predict group membership of AB 92.0% of the time and HF4714 97.6% of the time. Cross-validation of the same data showed 84.0% of the AB predicted correctly and 83.3% of the HF4714 predicted correctly. An interesting note, HF4714 is a derivative of the AB (K-12) strain. Something the analysis indeed bears out. In figure 27, AB and Nino C, DFA was able to correctly predict group membership 100% of the time for all samples. Cross-validating the data shows 92.0% and 90.7% of AB and Nino C respectively, predicted group membership correctly.

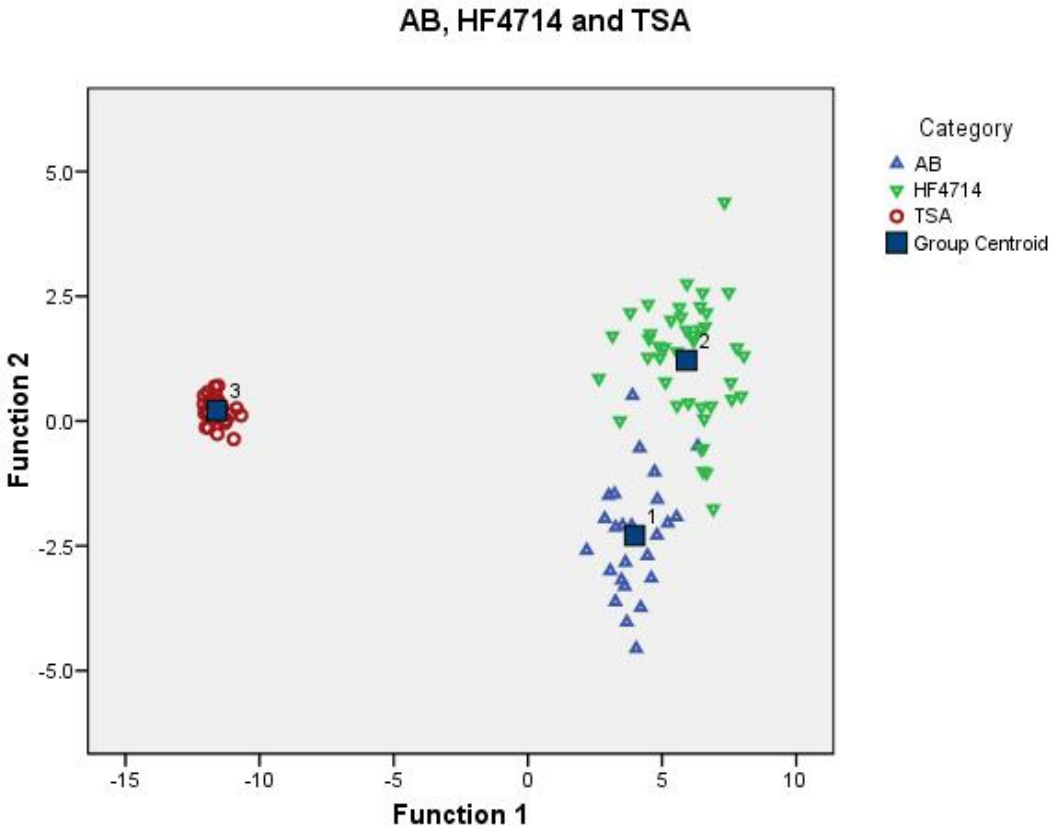

Figure 26 AB, HF4714 and TSA

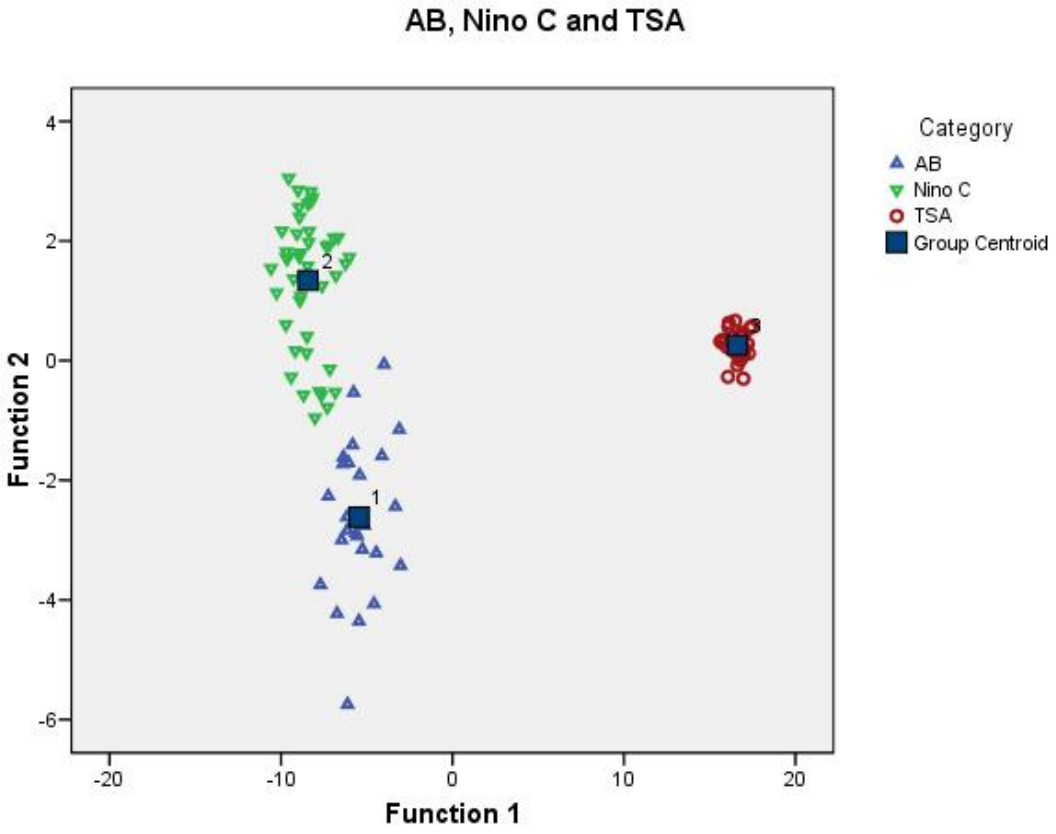

Figure 27 AB, Nino C and TSA

Figure 28 shows the comparison of all three *E. coli* strains. Notice that both AB and HF4714 have positive function 1 scores. With 85.8% of the variance between groups represented by function 1 this clearly indicates that AB and HF4714 are more similar.

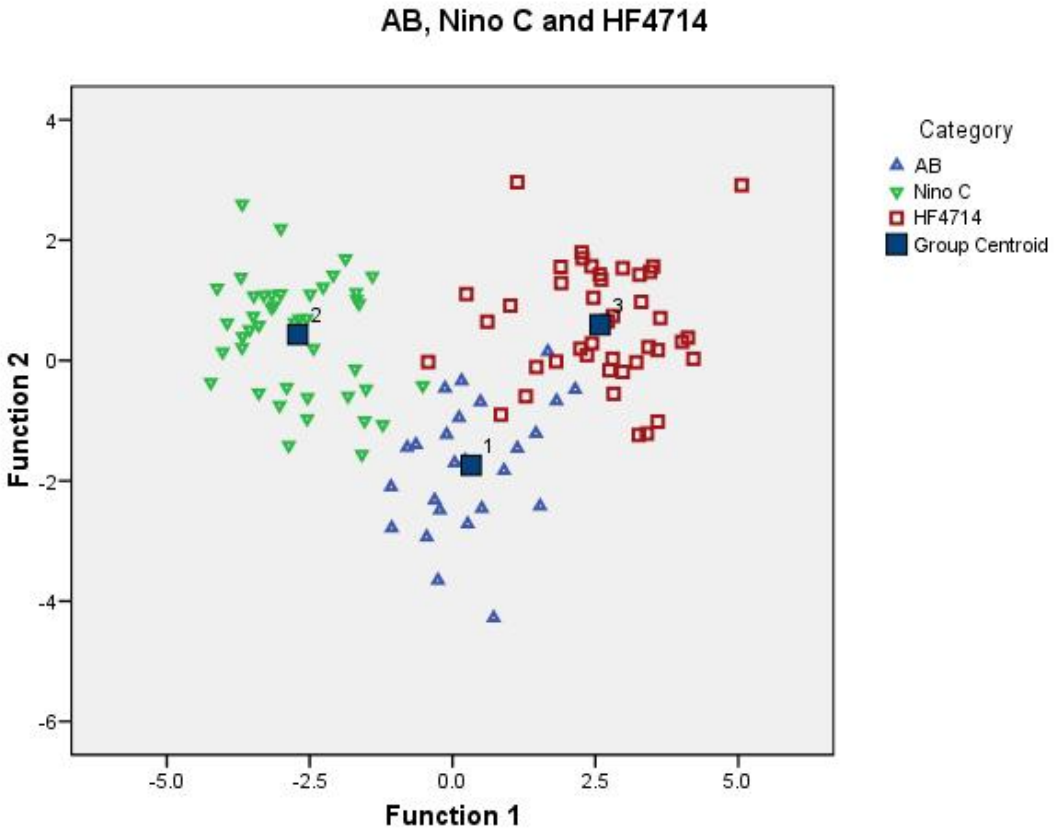

Figure 28 All three *E. coli* strains

Finally, a fourth strain of *E. coli* was analyzed. This strain however was different from the previous three. Up until this point only nonpathogenic strains were used. Next, a pathogenic strain will be investigated.

2.2.2 EHEC

The ability to discriminate between laboratory and environmental strains of *E. coli* is important to the success of further discrimination. Up to this point all strains have been nonpathogenic. Next, we prepared and collected data from a pathogenic strain of *E. coli*, 0157:H7 (EHEC). Like previous samples EHEC were prepared by removing the

bacteria from the TSA growth plate and spread onto an agar plate for ablation. Spectra were analyzed and compared to previous strains HF4714, Nino C and AB. The results shown below indeed show discrimination among the pathogenic and nonpathogenic strains. Figure 29 shows all four bacterial strains plotted against TSA. Not surprising the greatest discrimination is between the growth media and the bacteria.

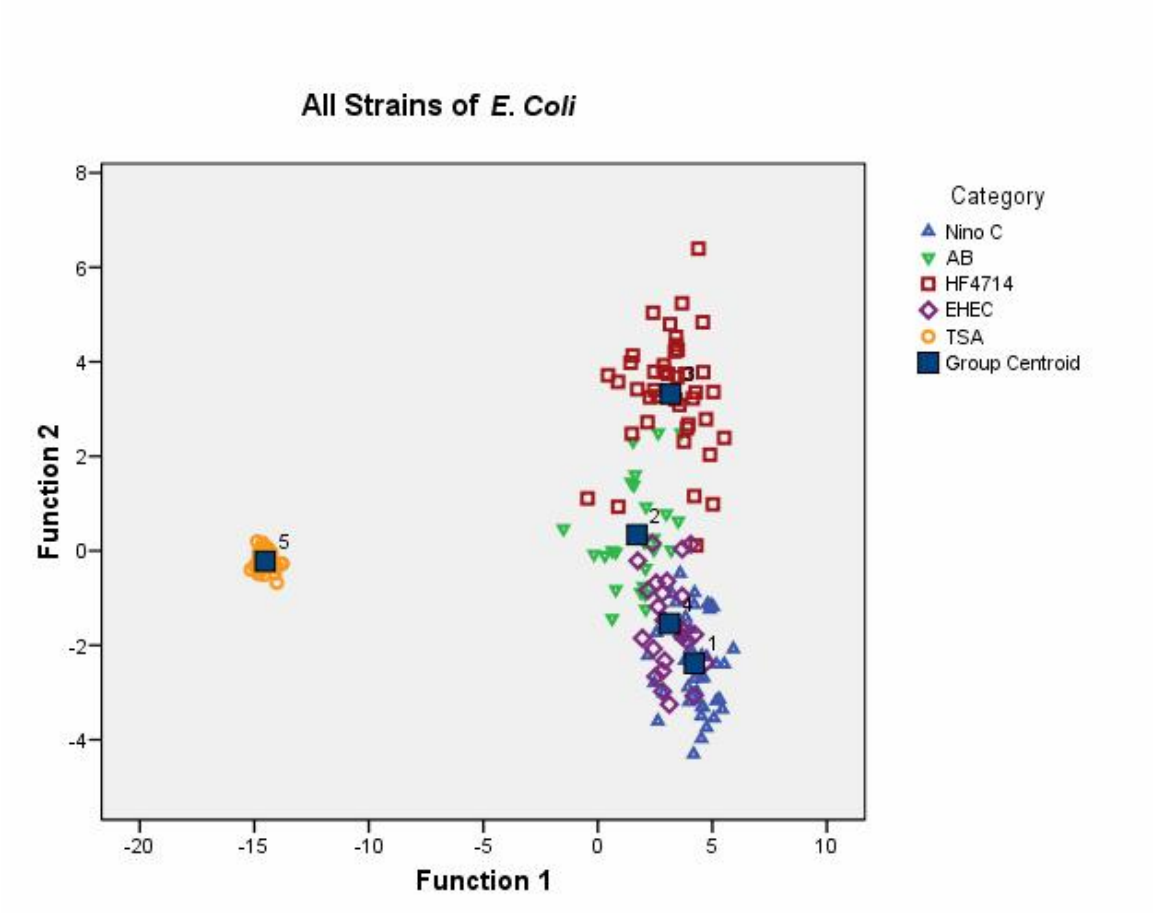

Figure 29 All strains of *E. coli*

Figure 30 shows three groups of data: nonpathogenic strains (HF4714, AB, Nino C), pathogenic (EHEC) and the growth medium (TSA). DFA correctly predicted group membership of the nonpathogenic strains 90.9% of the time with cross-validation

between groups at 90%. The pathogenic strain predicted group membership correctly 88.0% and cross-validation between groups at 72%.

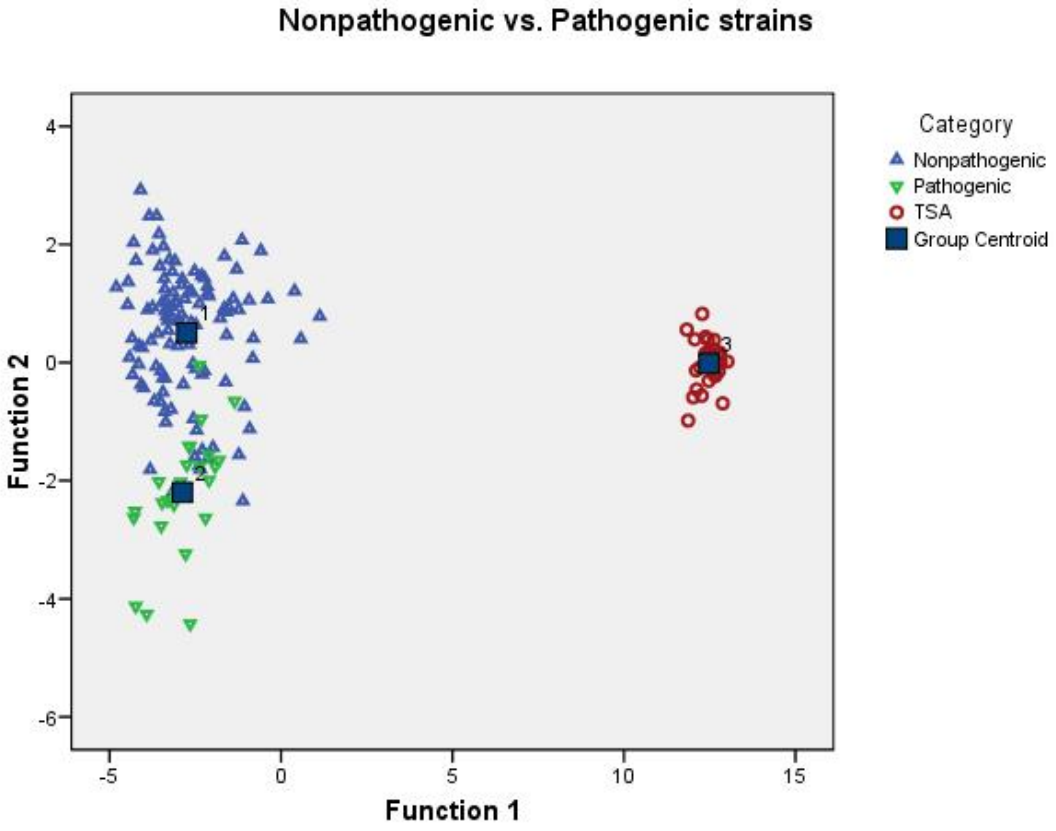

Figure 30 Pathogenic vs Nonpathogenic strains of *E. coli*

Lastly, it is important to show two environmental strains. Nino C and EHEC are two strains potentially found in the environment. So far I've shown both several laboratory strains as well as the environmental. Discrimination between two environmental strains is closer to the real world applications these experiments were designed to push toward. Nino C is a non-pathogenic strain as compared to EHEC, pathogenic, which can cause sickness. Figure 31 shows the two strains plotted against each other. Once again DFA was able to show significant discrimination between the

two strains. As given by Table 4, EHEC is classified correctly 100% of the time and Nino C 93.0%. Cross-validation showed that 84.0% and 88.4% of EHEC and Nino C classified correctly.

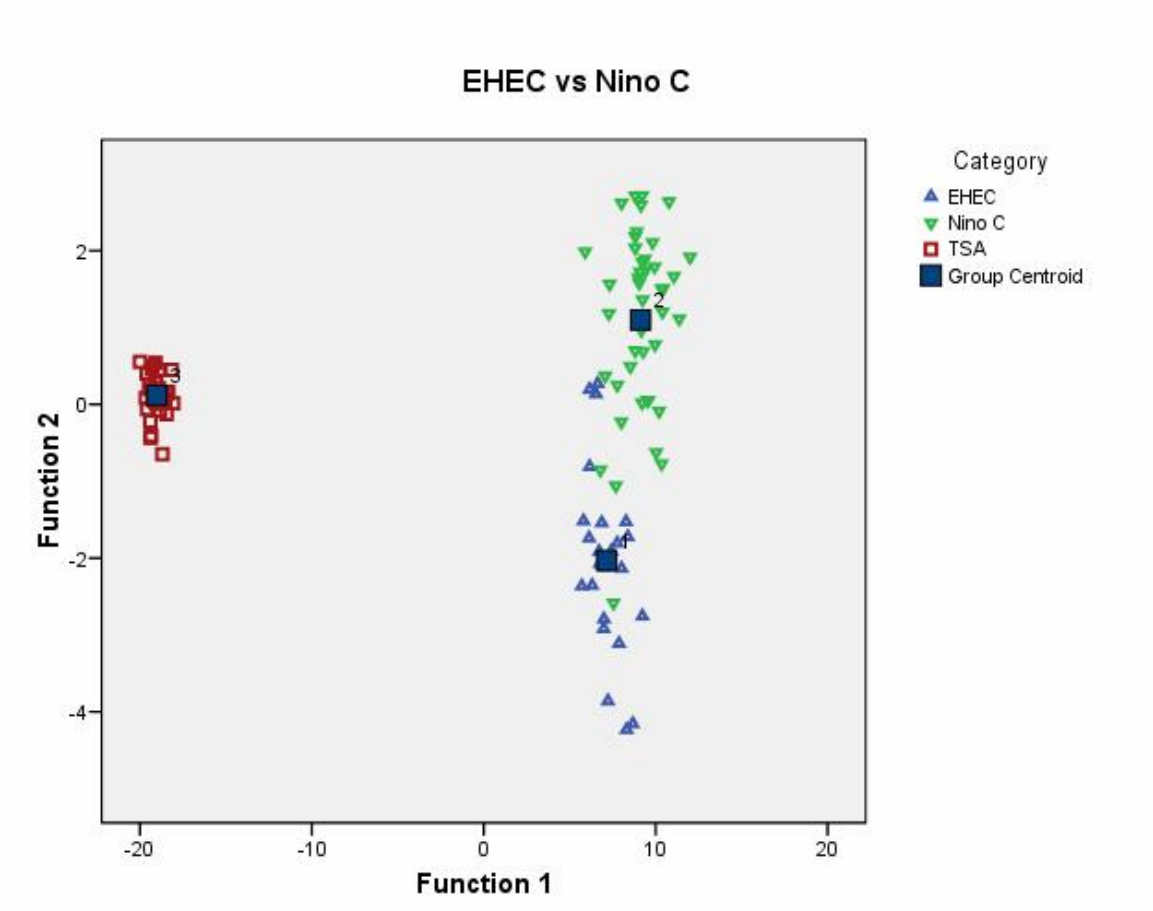

Figure 31 EHEC (environmental pathogenic strain) vs Nino C (environmental non-pathogenic strain of *E. coli*.

Classification Results[b,c]

		Category	Predicted Group Membership 1	2	3	Total
Original	Count	1	25	0	0	25
		2	3	40	0	43
		3	0	0	30	30
	%	1	100.0	.0	.0	100.0
		2	7.0	93.0	.0	100.0
		3	.0	.0	100.0	100.0
Cross-validated[a]	Count	1	21	4	0	25
		2	5	38	0	43
		3	0	0	30	30
	%	1	84.0	16.0	.0	100.0
		2	11.6	88.4	.0	100.0
		3	.0	.0	100.0	100.0

a. Cross validation is done only for those cases in the analysis. In cross validation, each case is classified by the functions derived from all cases other than that case.

b. 96.9% of original grouped cases correctly classified.

c. 90.8% of cross-validated grouped cases correctly classified.

Table 4 Classification of EHEC and Nino C

2.3 Pseudomonas

In addition to *E. coli*, *P. aeruginosa* was also studied. The experiments on *P. aeruginosa* were to show the ability of LIBS to discriminate between two different bacteria. In addition to bacterium discrimination, the effect of growth medium was also studied. *P. aeruginosa* was grown on TSA, MacConkey agar (MAC), and Blood agar Plate (BAP). MAC has bile salts which inhibit the growth of Gram positive bacteria. The addition of bile salts is important. Detection of *P. aeruginosa* on MAC has many applications in the medical industry where bacteria are present in bile salts. Figure 32 shows *P. aeruginosa* grown on each substrate plotted with the spectra from the growth substrates themselves. Table 5 shows the predicted group memberships along with the cross-validation percentages for all six samples.

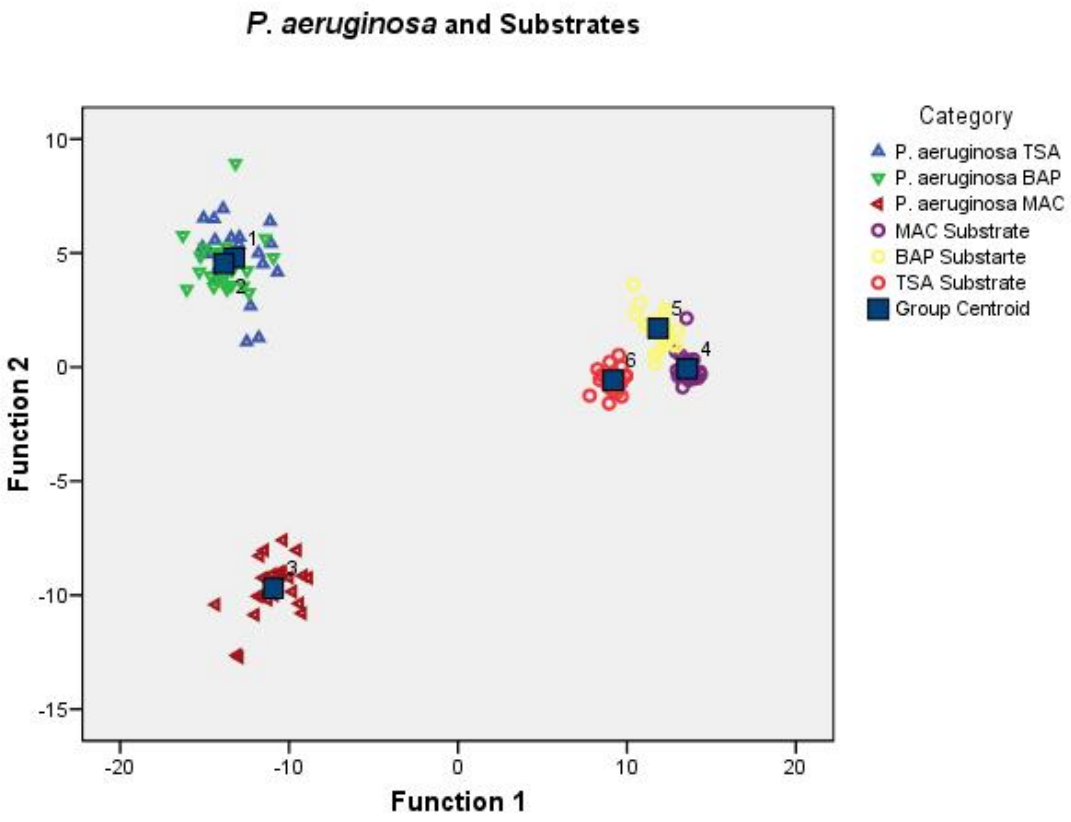

Figure 32 *P. aeruginosa* grown on multiple substrates

Classification Results[b,c]

			Predicted Group Membership						
		Category	1	2	3	4	5	6	Total
Original	Count	1	22	1	0	0	0	0	23
		2	1	23	0	0	0	0	24
		3	0	0	25	0	0	0	25
		4	0	0	0	24	1	0	25
		5	0	0	0	5	20	0	25
		6	0	0	0	0	0	30	30
	%	1	95.7	4.3	.0	.0	.0	.0	100.0
		2	4.2	95.8	.0	.0	.0	.0	100.0
		3	.0	.0	100.0	.0	.0	.0	100.0
		4	.0	.0	.0	96.0	4.0	.0	100.0
		5	.0	.0	.0	20.0	80.0	.0	100.0
		6	.0	.0	.0	.0	.0	100.0	100.0
Cross-validated[a]	Count	1	17	6	0	0	0	0	23
		2	3	21	0	0	0	0	24
		3	0	0	25	0	0	0	25
		4	0	0	0	24	1	0	25
		5	0	0	0	8	17	0	25
		6	0	0	0	0	0	30	30
	%	1	73.9	26.1	.0	.0	.0	.0	100.0
		2	12.5	87.5	.0	.0	.0	.0	100.0
		3	.0	.0	100.0	.0	.0	.0	100.0
		4	.0	.0	.0	96.0	4.0	.0	100.0
		5	.0	.0	.0	32.0	68.0	.0	100.0
		6	.0	.0	.0	.0	.0	100.0	100.0

a. Cross validation is done only for those cases in the analysis. In cross validation, each case is classified by the functions derived from all cases other than that case.

b. 94.7% of original grouped cases correctly classified.

c. 88.2% of cross-validated grouped cases correctly classified.

Table 5 Results of DFA on *P. aeruginosa* and growth substrates

DFA was able to very accurately discriminate between the *P. aeruginosa* grown on MAC from *P. aeruginosa* grown on TSA and BAP. BAP and TSA are very similar in composition. Blood agar plates are made by enriching TSA plates with blood. Thus, bacterial growth on these plates will not show as many differences as compared to bacteria grown on a substrate with bile salts added. This is significant because substrates, although highly different, all look similar to DFA. The bacteria however tell a different story. The TSA and BAP samples are nearly identical. Thus it may be possible to identify bacteria grown in different areas of the body i.e. bacteria grown in your bloodstream, in your mouth, etc. In addition the spectrum from bacteria grown on MAC

is different due to the detergent action of the bile salts on the outer membrane of the bacteria. These bacteria are actually chemically altered. We are sensitive to this alteration (i.e. an interaction between the bacteria and their environment) and it shows up through the DFA.

Figure 33 compares *P. aeruginosa* to *E. coli* plotted against TSA. The two *E. coli* strains used in this comparison were Nino C and EHEC. These represent the two environmental strains of *E. coli.* There is a noticeable separation of bacteria to the right and left of the dashed line. In addition, the strains of *E. coli* discriminate as well as the *P. aeruginosa* grown on different substrates.

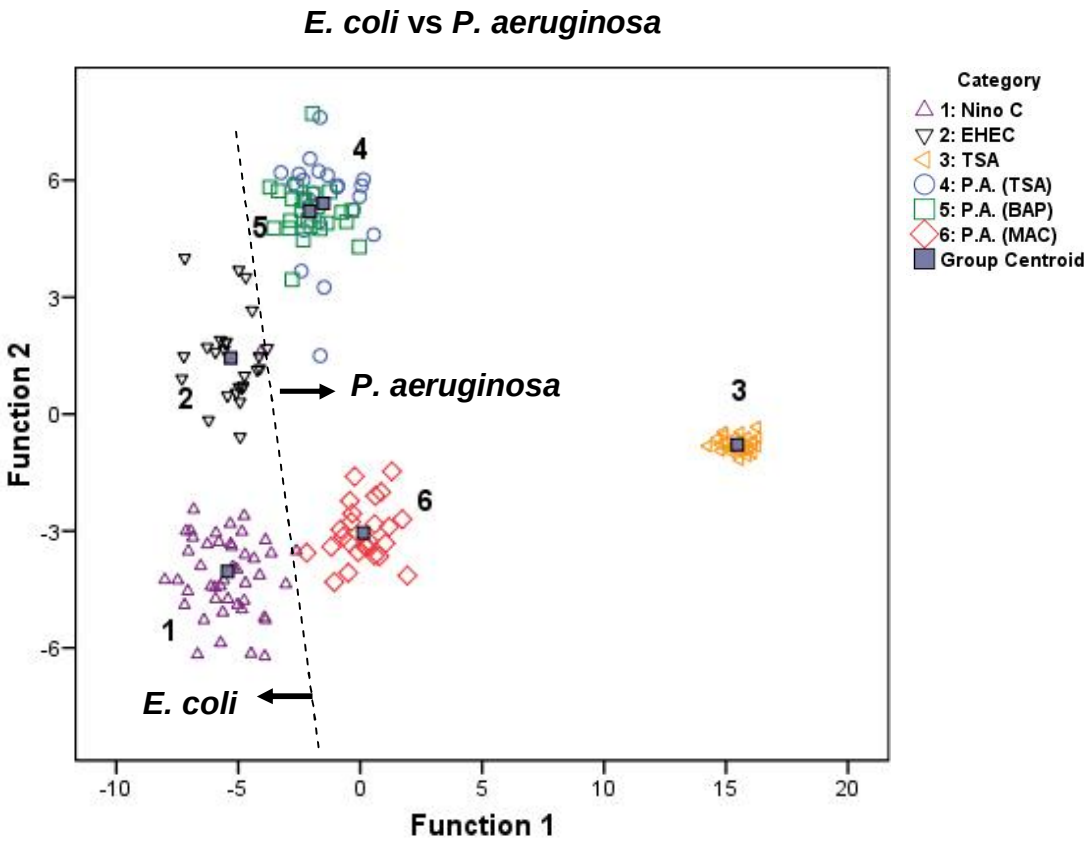

Figure 33 *E. coli* and *P. aeruginosa*

2.4 Other Samples

Finally, LIBS was used to analyze non bacterial samples. An environmental mold and the *Candida albicans* yeast were grown on TSA, prepared on agar and ablated using LIBS. Analyses of the spectrums are shown in Figure 34.

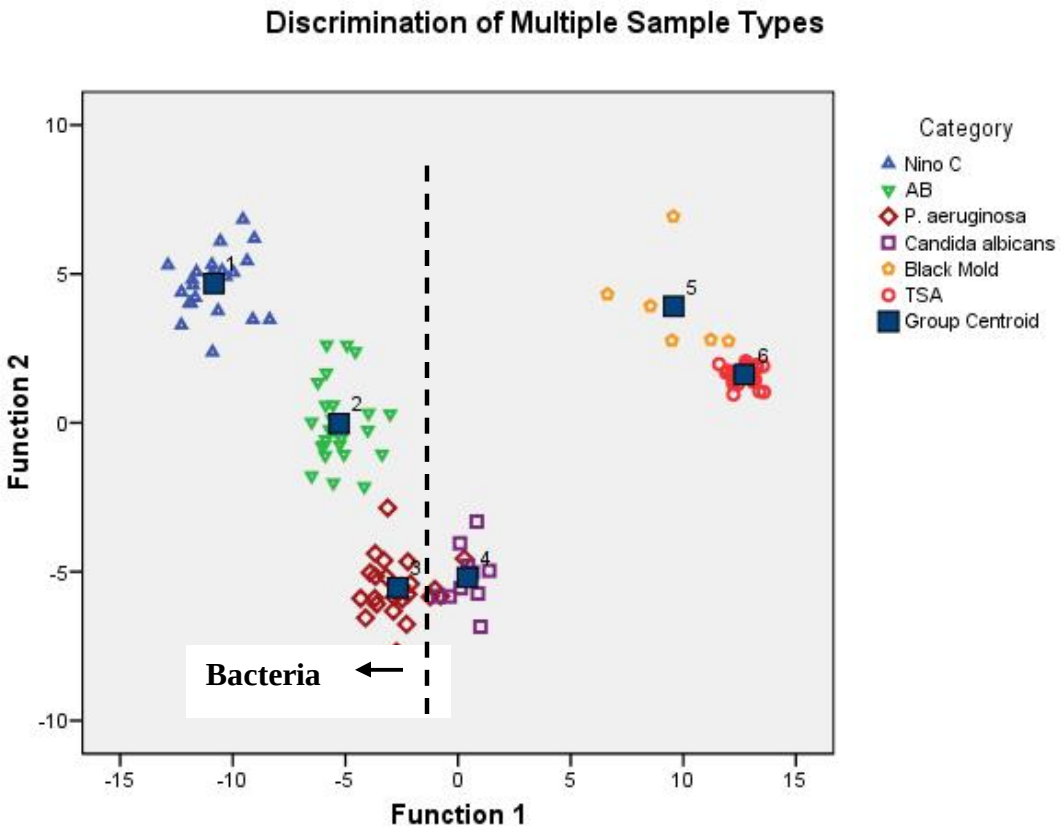

Figure 34 DFA discrimination of multiple sample types

Discrimination among all the samples is apparent from the plot. The two *E. coli* samples are separate from all the others as expected. Also, all three bacteria samples are have negative function 1 scores. Discrimination function 1 is responsible for 74.4% of the between group variance. DFA was able to predict group memberships 100% of the time for all groups plotted as shown in Table 6. The cross-validation of the groups shows

that Nino C, *Candida albicans* and TSA all grouped 100% correctly. AB, *P. aeruginosa* grouped correctly greater than 90% of the time and black mold 83.3% of the time. A possible reason for the lower grouping percentage on black mold is the sample size. Black mold had only 6 data points.

Classification Results[b,c]

			Predicted Group Membership						
		Category	1	2	3	4	5	6	Total
Original	Count	1	23	0	0	0	0	0	23
		2	0	25	0	0	0	0	25
		3	0	0	23	0	0	0	23
		4	0	0	0	10	0	0	10
		5	0	0	0	0	6	0	6
		6	0	0	0	0	0	30	30
	%	1	100.0	.0	.0	.0	.0	.0	100.0
		2	.0	100.0	.0	.0	.0	.0	100.0
		3	.0	.0	100.0	.0	.0	.0	100.0
		4	.0	.0	.0	100.0	.0	.0	100.0
		5	.0	.0	.0	.0	100.0	.0	100.0
		6	.0	.0	.0	.0	.0	100.0	100.0
Cross-validated[a]	Count	1	23	0	0	0	0	0	23
		2	1	24	0	0	0	0	25
		3	0	2	21	0	0	0	23
		4	0	0	0	10	0	0	10
		5	0	0	0	0	5	1	6
		6	0	0	0	0	0	30	30
	%	1	100.0	.0	.0	.0	.0	.0	100.0
		2	4.0	96.0	.0	.0	.0	.0	100.0
		3	.0	8.7	91.3	.0	.0	.0	100.0
		4	.0	.0	.0	100.0	.0	.0	100.0
		5	.0	.0	.0	.0	83.3	16.7	100.0
		6	.0	.0	.0	.0	.0	100.0	100.0

a. Cross validation is done only for those cases in the analysis. In cross validation, each case is classified by the functions derived from all cases other than that case.

b. 100.0% of original grouped cases correctly classified.

c. 96.6% of cross-validated grouped cases correctly classified.

Table 6 DFA Prediction of all samples

The results presented here were submitted for peer-review in three different journals. The first article, published in Applied Physics Letters (Appendix B) described only the initial discrimination of biotypes and between two strains. The second article, published in Journal of Applied Physics (Shown in Appendix C) described the discrimination of pathogenic from non-pathogenic strains and added the growth in TSB

media. The third article, published in Spectrochimica Acta Part B, (Shown in Appendix D) described all of the analysis of the *P. aeruginaosa* bacterium.

2.5 Collection in Argon

As shown in the above plots and prediction tables, DFA is able to take the spectrum data from each of the samples and very accurately predict group membership of each sample. DFA has been able to predict between environmental samples, between bacterial species, and strains of the same bacteria. However, to improve upon discrimination more data was collected using an argon bath to purge the air from the collection tray. The goal was two fold. First, remove the oxygen and nitrogen that lines that result from the atmosphere. With this it may be possible to add additional lines to the analysis giving better discrimination. Second, the argon would increase plasma temperature giving a better spectral signature for each sample. Figure 35 shows the spectra in air compared to the spectra from argon. Notice the increased response in addition to the additional lines.

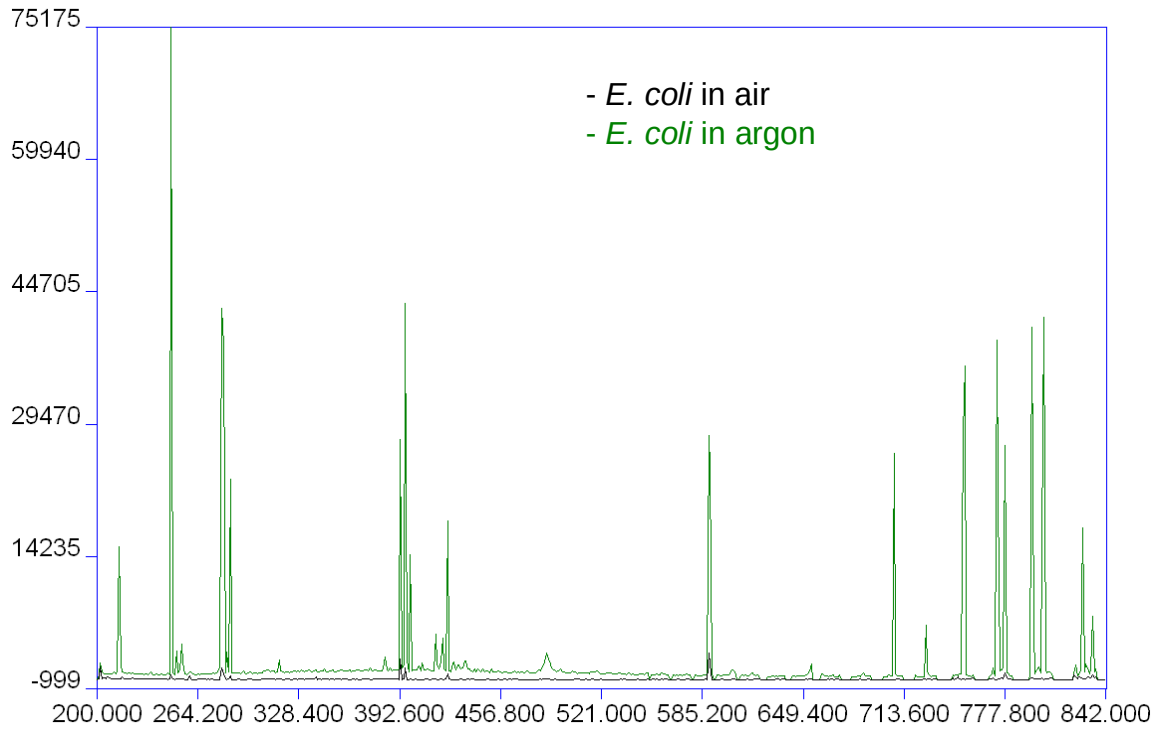

Figure 35 LIBS spectrum collected in air overlaid with a spectrum from argon.

The increased spectral response would hopefully help DFA discriminate among the bacteria. The initial results, taken only on *E. coli*, only show discrimination similar to data collected in atmosphere. It should be noted that the data presented is the preliminary data. More extensive work was done in argon but was not part of this research.

Figure 36 shows *E. coli* plotted with TSA. The data collected was ablated in an argon bath. As illustrated in the graph the bacteria is still distinguished from the growth media. Table 7 shows the DFA group memberships. Although it appears that all four *E. coli* samples are tightly grouped DFA was still able to distinguish group membership more than 70% of the time. However, on cross-validation the results were not as good on an individual basis. Note though that on a whole 80.2% of cross-validated grouped cases correctly classified.

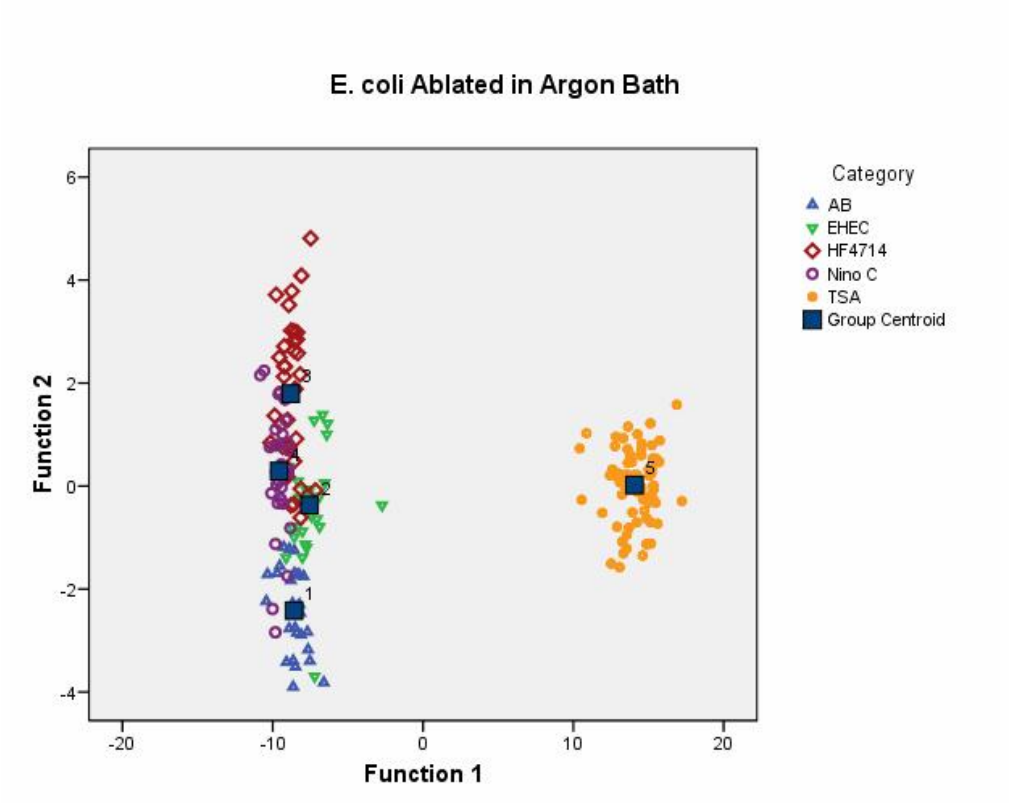

Figure 36 *E. coli* ablated in argon bath

Classification Results[b,c]

			Predicted Group Membership					
		Category	1	2	3	4	5	Total
Original	Count	1	27	0	0	2	0	29
		2	1	26	0	0	0	27
		3	0	2	34	3	0	39
		4	3	1	4	22	0	30
		5	0	0	0	0	77	77
	%	1	93.1	.0	.0	6.9	.0	100.0
		2	3.7	96.3	.0	.0	.0	100.0
		3	.0	5.1	87.2	7.7	.0	100.0
		4	10.0	3.3	13.3	73.3	.0	100.0
		5	.0	.0	.0	.0	100.0	100.0
Cross-validated[a]	Count	1	20	3	0	6	0	29
		2	4	21	2	0	0	27
		3	3	3	27	6	0	39
		4	4	2	7	17	0	30
		5	0	0	0	0	77	77
	%	1	69.0	10.3	.0	20.7	.0	100.0
		2	14.8	77.8	7.4	.0	.0	100.0
		3	7.7	7.7	69.2	15.4	.0	100.0
		4	13.3	6.7	23.3	56.7	.0	100.0
		5	.0	.0	.0	.0	100.0	100.0

a. Cross validation is done only for those cases in the analysis. In cross validation, each case is classified by the functions derived from all cases other than that case.

b. 92.1% of original grouped cases correctly classified.

c. 80.2% of cross-validated grouped cases correctly classified.

Table 7 Classification results from *E. coli* in argon.

Figure 37(a) and (b) shows discrimination between the samples (AB, Nino C and HF4714) about zero in function 1. AB and a derivative HF4714 have positive function 1 scores, Nino C has a negative function 1 score. In the argon there is more separation between Nino C and the other two strains in function 1. This indicates that argon enhances the differences between strains.

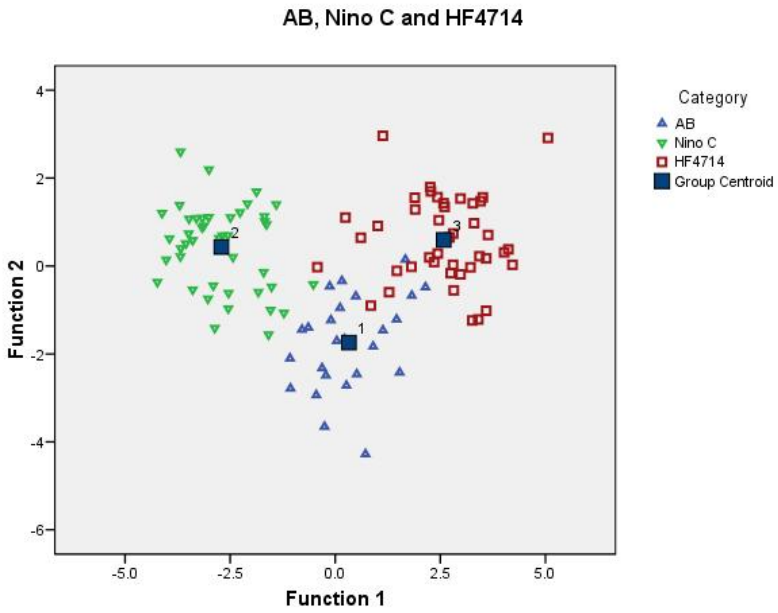

(a)

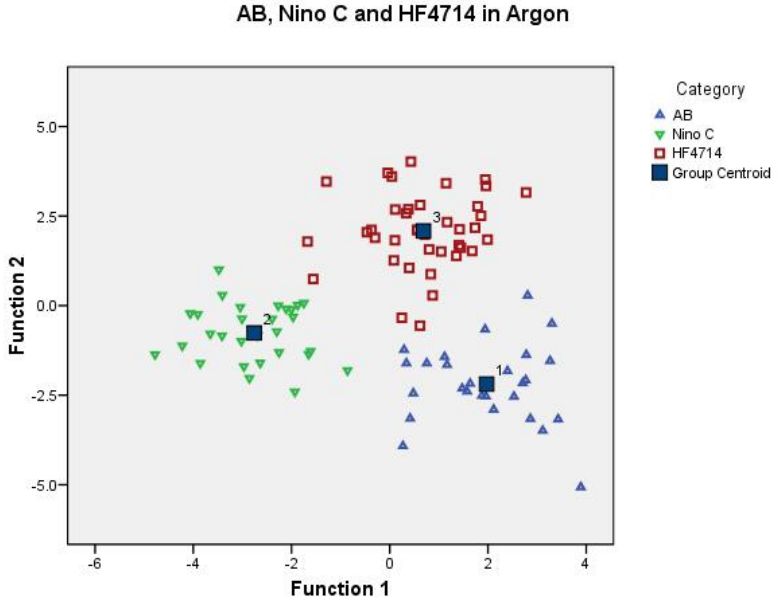

(b)

Figure 37 (a) *E. coli* ablated in atmosphere. 5.19(b) *E. coli* ablated in argon

Chapter 6 Conclusions

In this thesis I investigated the ability of LIBS to detect and discriminate different strains of a given bacterium. Using *E. coli* as the primary bacteria, several experiments were conducted and data collected using LIBS. A data analysis technique called Discriminant Function Analysis was used to statistically discriminate and classify the different bacterial samples. I showed in chapter 5 the ability of LIBS to discriminate between *E. coli* and *P. aeruginosa,* two bacteria, other environmental substances and the growth substrate upon which all were grown. Further, it was demonstrated that LIBS was successful in discriminating between different strains of *E. coli.* Nino C, HF4714, AB and EHEC - all strains of *E. coli* - *were* successfully classified with accuracies greater than 90%. It is also important to note that within the different strains of *E. coli* pathogenic and nonpathogenic strains were used. I also investigated the ability of LIBS to discriminate and correctly classify. DFA was able to correctly predict the group membership of the nonpathogenic strains more than 90.0% of the time and the pathogenic strain 88.0% of the time. This is significant to possible future applications to detect pathogenic strains of *E. coli* that could be harmful to humans.

It was also demonstrated that the use of argon was initially successful in the enhancement of the spectra which lead to greater discrimination between the samples. However; the argon data was preliminary and more data must be collected to in order to make further conclusions on the advantages of argon.

Path Forward

The path forward holds many exciting opportunities. The use of Argon is only the beginning of the possibilities for further discrimination. I envision 3 categories of future work.

First, additional collections in multiple atmospheres are necessary in order to determine the best gas for collection. Argon, Helium and other inert gases should be investigated. In addition to other atmospheres investigation of bacteria grown in several substrates is also important. Saliva, blood, water and other substrates should be investigated to determine the probability of detection within multiple substrates.

Second, further data collections need to be done in order to create a predictable method to accurately collect data. Reproducibility is extremely important. Refinement of the methods and apparatus can lead to more reliable data collection. The translation stage can be upgraded to accommodate a more secure boot. The boot is used to trap the gas inside of the sample chamber. The current version allowed too much gas to escape. For heavier gases this wasn't much of a problem. However, lighter gases such as helium will need more secure seals. The one major obstacle to reproducible collections was determination of the microscope objective's location above the sample. If the focus was too high the spark would be in the air, too low and ablation occurs in the substrate. Preparation of extremely flat ablation substrates is important. In addition to the substrate the sample itself needs to be homogeneous in height. To accomplish this moving to bacteria grown in a broth would allow a more uniform spot on the substrate.

Lastly, moving beyond *E. coli* and onto other bacteria will broaden the impact of LIBS. I've demonstrated that it is possible to discriminate between multiple strains *E. coli*. The technique used on the *E. coli* can be used on other bacteria. Investigation of bacteria like *Staphylococcus aureus* could lead to breakthroughs in many areas of medicine, military technology and public safety.

Appendix A – Reuse statements

Appendix B reused with permission from Jonathan Diedrich, Steven J. Rehse, and Sunil Palchaudhuri, Applied Physics Letters, 90, 163901 (2007). Copyright 2007, American Institute of Physics.

Appendix C reused with permission from Jonathan Diedrich, Steven J. Rehse, and Sunil Palchaudhuri, Journal of Applied Physics, 102, 014702 (2007). Copyright 2007, American Institute of Physics.

Appendix D reused with permission from Jonathan Diedrich, Steven J. Rehse, and Sunil Palchaudhuri, Spectrochimica Acta Part B: Atomic Spectroscopy, 62, 1169-1176 (2007). Copyright 2007, Elsevier.

Appendix B – Article 1 (Applied Physics Letters)

APPLIED PHYSICS LETTERS 90, 163901 (2007)

Escherichia coli identification and strain discrimination using nanosecond laser-induced breakdown spectroscopy

Jonathan Diedrich and Steven J. Rehse[a)]
Department of Physics and Astronomy, Wayne State University, Detroit, Michigan 48201

Sunil Palchaudhuri
Department of Immunology and Microbiology, Wayne State University, Detroit, Michigan 48201

(Received 26 January 2007; accepted 15 March 2007; published online 16 April 2007)

Three strains of *Escherichia coli*, one strain of environmental mold, and one strain of *Candida albicans* yeast have been analyzed by laser-induced breakdown spectroscopy using nanosecond laser pulses. All microorganisms were analyzed while still alive and with no sample preparation. Nineteen atomic and ionic emission lines have been identified in the spectrum, which is dominated by calcium, magnesium, and sodium. A discriminant function analysis has been used to discriminate between the biotypes and *E. coli* strains. This analysis showed efficient discrimination between laser-induced breakdown spectroscopy spectra from different strains of a single bacteria species.
 [DOI: 10.1063/1.2723659]

Laser-induced breakdown spectroscopy (LIBS) is a time-resolved spectroscopic analysis technique based on optical emission following pulsed laser ablation of a sample. The technique has numerous advantages stemming from its flexibility, which has allowed it to be utilized to a wide variety of applications.[1,2] In the past three years, several research efforts related to the detection and identification of microbiological samples have been reported.[3–5] These early works were concerned primarily with investigating the ability to discriminate particular microorganisms (usually bacteria used as surrogate of pathogenic bioagents) from "background" biological organisms, often of different biotypes (pollen, molds, etc.) The underlying motivation for most of these studies was the development of a practical, real-time early-warning technology to protect against incidents of bioterrorism.[6–9]

Recent results have shown the utility of using LIBS with femtosecond laser pulses, specifically to identify the *Escherichia coli* bacterium.[10–12] *E. coli* is an ideal candidate for initial studies due to its complete genetic characterization, nonpathogenicity, and ease of preparation. These studies have mostly avoided the issue of realistic sample preparation by analyzing samples which have been harvested from culture, washed, aspirated onto filters, washed again, and then dried to ensure a high signal-to-noise ratio. Only one instance of performing LIBS on an actual *E. coli* bacterial colony has been reported.[13]

While *E. coli* has many nonpathogenic strains, it also has many strains which can be very harmful to humans. Different *E. coli* strains can cause an impressive variety of diseases including dysentery, hemolytic uremic syndrome (kidney failure), bladder infection, septicemia, pneumonia, and meningitis. In general, different strains are associated with different diseases. Therefore the ability to identify particular strains is very important so that outbreaks caused by a particular strain can be identified.[14]

In this letter, we report on the use of LIBS as a technology to differentiate not only between bacterial species and other biotypes but also between strains of a single bacterial species. In particular, discrimination is shown between three strains of *E. coli* prepared in an identical manner and tested with no sample preparation other than transfer to a suitable ablation substrate. Discrimination is also shown between the *E. coli* strains, an environmental mold, and the *Candida albicans* yeast.

10 ns laser pulses from a Nd:YAG (yttrium aluminum garnet) laser (Spectra Physics, LAB-150-10) operating at 10 Hz at its fundamental wavelength were focused by a 5× high-damage threshold microscope objective to a beam waist diameter of 100 μm. The laser mode was made more Gaussian with an expanding telescope mode cleaner and the resulting laser pulse energy at the beam waist was 8 mJ/pulse. Optical emission from the LIBS microplasma was collected by a 1 m steel encased multimode optical fiber (core diameter=600 μm, numerical aperture=0.22) placed at a distance of 23 mm from the ablation spot with no other light collection optics. This fiber was coupled to an Echelle spectrometer equipped with an intensified charge coupled device (ICCD) camera (LLA Instruments, Inc., ESA3000), which provided complete spectra coverage from 200 to 840 nm with a resolution of 0.005 nm in the UV.

E. coli and *C. albicans* samples were prepared in the following way: colonies were grown on a trypticase soy agar (TSA) growth medium for 24 h, and then transferred to the surface of a 0.7% agar plate with a very thin smear. TSA is a rich bacteriological growth medium containing pancreatic digest of casein, soybean meal, NaCl, dextrose, and dipotassium phosphate. The environmental mold was prepared by exposure of a blank TSA plate to environmental conditions until a blackish-looking mold developed. Agar was chosen as a substrate for laser ablation due to its ease of preparation, lack of nutrients which would effect bacterial growth, and relatively high optical breakdown threshold due to optical transparency.

LIBS spectra were acquired for three strains of *E. coli*: a laboratory strain of K-12 (AB) which is completely characterized genetically,[15] a derivative of the same strain termed HF4714, and an environmental strain, *E. coli* C (Nino C), used for the assay of bacteriophage ΦX174. The purity of the cultures of all bacterial strains used in this study was rou-

a)Electronic mail: rehse@wayne.edu

Appendix C – Article 2 (Journal of Applied Physics)

JOURNAL OF APPLIED PHYSICS 102, 014702 (2007)

Pathogenic *Escherichia coli* strain discrimination using laser-induced breakdown spectroscopy

Jonathan Diedrich and Steven J. Rehse[a)]
Department of Physics and Astronomy, Wayne State University, Detroit, Michigan 48201

Sunil Palchaudhuri
Department of Immunology and Microbiology, Wayne State University, Detroit, Michigan 48201

(Received 7 February 2007; accepted 28 May 2007; published online 5 July 2007)

A pathogenic strain of bacteria, *Escherichia coli* O157:H7 (enterohemorrhagic *E. coli* or EHEC), has been analyzed by laser-induced breakdown spectroscopy (LIBS) with nanosecond pulses and compared to three nonpathogenic *E. coli* strains: a laboratory strain of K-12 (AB), a derivative of the same strain termed HF4714, and an environmental strain, *E. coli* C (Nino C). A discriminant function analysis (DFA) was performed on the LIBS spectra obtained from live colonies of all four strains. Utilizing the emission intensity of 19 atomic and ionic transitions from trace inorganic elements, the DFA revealed significant differences between EHEC and the Nino C strain, suggesting the possibility of identifying and discriminating the pathogenic strain from commonly occurring environmental strains. EHEC strongly resembled the two K-12 strains, in particular, HF4714, making discrimination between these strains difficult. DFA was also used to analyze spectra from two of the nonpathogenic strains cultured in different media: on a trypticase soy (TS) agar plate and in a liquid TS broth. Strains cultured in different media were identified and effectively discriminated, being more similar than different strains cultured in identical media. All bacteria spectra were completely distinct from spectra obtained from the nutrient medium or ablation substrate alone. The ability to differentiate strains prepared and tested in different environments indicates that matrix effects and background contaminations do not necessarily preclude the use of LIBS to identify bacteria found in a variety of environments or grown under different conditions.
 [DOI: 10.1063/1.2752784]

I. INTRODUCTION

The rapid detection and identification of microbiological organisms, particularly bacteria, has been an active area of research in the past several years, particularly with the threat of biological warfare attacks and frequently recurring outbreaks of illness caused by food-borne pathogens. Laser-induced breakdown spectroscopy (LIBS) has recently been considered as a candidate for rapid real-time detection of the microbes responsible for such illness both in the field and in a laboratory setting. LIBS is a time-resolved spectroscopic analysis technique based on optical emission following pulsed laser ablation of a sample. The technique has numerous advantages, primarily stemming from its flexibility which allows it to be utilized in a wide variety of applications.[1,2] In the past three years, several research efforts related to the detection and identification of microbiological, particularly bacterial, samples have been reported.[3–5] These early works were concerned primarily with investigating the ability to discriminate particular microorganisms (usually bacteria used as surrogates of pathogenic bioagents) from "background" biological organisms, often of a different biotype (pollen, molds, etc.). The underlying motivation for many of these studies was the development of a practical, real-time early-warning technology to protect against incidents of bioterrorism.[6–9]

Recent results have shown the utility of using LIBS with both nanosecond and femtosecond laser pulses to identify the *Escherichia coli* bacterium.[10–12] *E. coli* is an ideal candidate for initial studies due to its complete genetic characterization, nonpathogenicity, and ease of preparation.[13] As observed by Baudelet *et al.*,[12] *E. coli* is a nonsporulating, Gram-negative bacterium with a specific outer membrane which contains divalent cations, such as Mg^{+2} and Ca^{+2}.[14] Thus the dominant spectral features in the LIBS spectrum of the *E. coli* bacterium are ionized and neutral Mg and Ca emission lines. The creation of a "spectral fingerprint" or full spectral identification of a particular bacterium results from the measurement of emission lines from these and other trace inorganic elements, such as iron, potassium, sodium, manganese, and phosphorus, among others. It is important to note that it is not a genetic difference detected by the LIBS analysis (the typical LIBS analysis does not rely heavily on the elements which comprise DNA or proteins such as carbon, nitrogen, hydrogen, and oxygen), it is rather the differences in the chemical composition of the outer membrane which is detected and which varies between bacterial species as a function of the genetic variation between those species.

These studies performed hitherto have mostly avoided the issue of realistic sample preparation, instead relying on techniques which ensure high-repeatability and high signal-to-noise spectra. For example, *Bacillus globigii* has been grown as spores, harvested by suspension, followed by centrifugation to pelletize the spores then vacuum filtrated

a)Electronic mail: rehse@wayne.edu

Appendix D – Article 3 (Spectrochimica Acta)

ELSEVIER

Spectrochimica Acta Part B 62 (2007) 1169 – 1176

SPECTROCHIMICA ACTA PART B

www.elsevier.com/locate/sab

Identification and discrimination of *Pseudomonas aeruginosa* bacteria grown in blood and bile by laser-induced breakdown spectroscopy

Steven J. Rehse [a,*], Jonathan Diedrich [a,1], Sunil Palchaudhuri [b,2]

[a] *Department of Physics and Astronomy, Wayne State University, Detroit, MI 48201, USA*
[b] *Department of Immunology and Microbiology, Wayne State University, Detroit, MI 48201, USA*

Received 23 May 2007; accepted 23 July 2007
Available online 1 August 2007

Abstract

Pseudomonas aeruginosa bacteria colonies have been analyzed by laser-induced breakdown spectroscopy using nanosecond laser pulses. LIBS spectra were obtained after transferring the bacteria from a nutrient-rich culture medium to a nutrient-free agar plate for laser ablation. To study the dependence of the LIBS spectrum on growth and environmental conditions, colonies were cultured on three different nutrient media: a trypticase soy agar (TSA) plate, a blood agar plate, and a medium chosen deliberately to induce bacteria membrane changes, a MacConkey agar plate containing bile salts. Nineteen atomic and ionic emission lines in the LIBS spectrum, which was dominated by inorganic elements such as calcium, magnesium and sodium, were used to identify and classify the bacteria. A discriminant function analysis was used to discriminate between the *P. aeruginosa* bacteria and two strains of *E. coli*: a non-pathogenic environmental strain and the pathogenic strain enterohemorrhagic *E. coli* 0157:H7 (EHEC). Nearly identical spectra were obtained from *P. aeruginosa* grown on the TSA plate and the blood agar plate, while the bacteria grown on the MacConkey plate exhibited easily distinguishable differences from the other two. All *P. aeruginosa* samples, independent of initial growth conditions, were readily discriminated from the two *E. coli* strains.

Keywords: Laser-induced breakdown spectroscopy (LIBS); Bacteria identification; Biological; Discriminant function analysis (DFA); *P. aeruginosa*; *E. coli*

1. Introduction

Laser-induced breakdown spectroscopy (LIBS) is a time-resolved spectroscopic analysis technique based on optical emission following pulsed-laser ablation of a sample. The technique, which has been utilized in a wide variety of applications, has numerous advantages over other competing spectrochemical analysis techniques [1,2]. A short list of these advantages includes: minimal or no sample preparation is required; very rapid measurements are possible (potentially in under 1 s); a high spatial resolution on the target can be obtained (under 10 μm is possible, although under 100 μm is more common); and the analysis detects all elements without bias, including those present in molecules (which are atomized during the process). Two advantages specific to the application of LIBS in microbiologically important systems are that measurements can be preformed remotely allowing the safe analysis of hazardous, highly-contagious, or pathogenic targets and that the analysis can be computerized, removing the requirement of the expertise of a trained microbiologist for the identification of bacteria or bio-agents.

In the past three years the use of LIBS as a practical detection and identification technology for biological samples, particularly bacteria, has been investigated by several research groups. These early works were concerned primarily with investigating the ability to discriminate particular microorganisms (usually bacteria used as simulants of pathogenic bio-agents) from "background" biological organisms, often of a different bio-type (pollen, molds, etc.). For example, in preliminary experiments performed in 2003, Morel et al. investigated the detection of six strains of bacteria and two pollens [3]. They placed particular emphasis on *Bacillus globigii* which acts as a non-pathogenic

* Corresponding author. Tel.: +1 313 577 2411; fax: +1 313 577 3932.
E-mail addresses: rehse@wayne.edu (S.J. Rehse), jon.diedrich@gd-ais.com (J. Diedrich), spalchau@med.wayne.edu (S. Palchaudhuri).
[1] Fax: +1 313 577 3932.
[2] Tel.: +1 313 577 1313.

0584-8547/$ - see front matter © 2007 Elsevier B.V. All rights reserved.
doi:10.1016/j.sab.2007.07.008

References

[1] S. Morel, M. Leone, P. Adam, and J. Amouroux, “Detection of bacteria by time-resolved laser-induced breakdown spectroscopy,” Appl. Opt. 42, 6184-6191 (2003).

[2] A.C. Samuels, F.C. DeLucia, Jr., K.L. McNesby, and A.W. Miziolek, “Laser-induced breakdown spectroscopy of bacterial spores, molds, pollens, and protein: initial studies of discrimination potential,” Appl. Opt. 42, 6205- 6209 (2003).

[3] J.D. Hybl, G.A. Lithgow, and S.G. Buckley, “Laser-induced breakdown spectroscopy detection and classification of biological aerosols,” Appl. Spect. **57**, 1207-1215 (2003).

[4] F.C. DeLucia, Jr., A.C. Samuels, R.S. Harmon, R.A. Walter, K.L. McNesby, A. LaPointe, R.J. Winkel, Jr., and A.W. Miziolek, “Laser-induced breakdown spectroscopy (LIBS): a promising versatile chemical sensor technology for hazardous material detection,” IEEE Sens. Jour. **50**, 681-689 (2005).

[5] P.B. Dixon and D.W. Hahn, “Feasibility of detection and identification of individual bioaerosols using laser-induced breakdown spectroscopy,” Anal. Chem. **77**, 631-638 (2005).

[6] C.A. Munson, F.C. DeLucia Jr., T. Piehler, K.L. McNesby, A.W. Miziolek, “Investigation of statistics strategies for improving the discriminating power of laser-induced breakdown spectroscopy for chemical and biological warfare agent simulants,” Spect. Acta B 60, 1217-1224 (2005).

[7] D.C.S. Beddows and H.H. Telle, “Prospects of real-time single-particle biological aerosol analysis: A comparison between laser-induced breakdown spectroscopy and aerosol time-of-flight mass spectrometry,” Spectrochim. Acta B 60, 1040-1059 (2005).

[8] Versalovic J, Lupski JR., ” Molecular detection and genotyping of pathogens: more accurate and rapid answers.” Trends in Microbiology Volume 10, Issue 10, 1 October 2002, Pages s15-s21

[9] Rüssmann H, Kothe E, Schmidt H, Franke S, Harmsen D, Caprioli A, Karch H, “Genotyping of Shiga-like toxin genes in non-O157 Escherichia coli strains associated with haemolytic uraemic syndrome.” The Journal of Medical Microbiology, Vol **42**, Issue 6 404-410

[10] Baron EJ (1996). *Classification. In: Baron's Medical Microbiology* (Baron S et al, eds.), 4th ed., Univ of Texas Medical Branch. ISBN 0-9631172-1-1.

[11] Ryan KJ; Ray CG (editors) (2004). *Sherris Medical Microbiology*, 4th ed., McGraw Hill. ISBN 0-8385-8529-9.

[12] L. Durso, J. Bono, James, J. Keen, “Molecular Serotyping of Escherichia Coli O26:h11” Applied and Environmental Microbiology, August 2005, p. 4941-4944, Vol. 71, No. 8

[13] M. Harz, P. Ro¨sch, K.-D. Peschke, O. Ronneberger, H. Burkhardtb and J. Popp, “Micro-Raman spectroscopic identification of bacterial cells of the genus Staphylococcus and dependence on their cultivation conditions” The Royal Society of Chemistry Analyst, 2005, **130**, 1543–1550

[14] R. Jarvis, R. Goodacre, “Ultra-violet resonance Raman spectroscopy for the rapid discrimination of urinary tract infection bacteria” FEMS Microbiology Letters **232** (2004) 127-132.

[15] R. Jarvis, R. Goodacre, “Discrimination of Bacteria Using Surface-Enhanced Raman Spectroscopy” Analytical Chemistry, Vol. **76**, No. 1, January 1, 2004

[16] R. Jarvis, A. Brooker, R. Goodacre, “Surface-Enhanced Raman Spectroscopy for Bacterial Discrimination Utilizing a Scanning Electron Microscope with a Raman Spectroscopy Interface” Analytical Chemistry, Vol. **76**, No. 17, September 1, 2004

[17] M. Zourob, S. Mohr, B.Treves Brown, P. Fielden, M. McDonnell, N. Goddard, “Bacteria detection using disposable optical leaky waveguide sensors” Biosensors and Bioelectronics Volume **21**, Issue 2, 15 August 2005, Pages 293-302

[18] M. Mehrvar, C. Bis, J. Scharer, M. Moo-Young, “Fiber Optic Biosensors-Trends and Advances” Analytical Sciences July 2000, Vol. **16**

[19] D. Hage, “Immunoassays” Analytical Chemistry, Vol. **67**, No. 12, June 15, 1995

[20] W. Agger, D. Maki, “Efficacy of Direct Gram Stain in Differentiating Staphylococci from Streptococci in Blood Cultures Positive for Gram-Positive Cocci,” JOURNAL OF CLINICAL MICROBIOLOGY, Feb. 1978, p. 111-113

[21] R. Gleckman, J. DeVita, D. Hibert, C. Pelletier, R. Martin, “Sputum Gram Stain Assessment in Community-Acquired Bacteremic Pneumonia,” JOURNAL OF CLINICAL MICROBIOLOGY, May 1988, p. 846-849

[22] D. Stokes, G. D. Griffin, T. Vo-Dinh, “Detection of *E. coli* using a microfluidics-based antibody biochip detection system,” Fresenius' Journal of Analytical Chemistry Volume **369**, Numbers 3-4 / February, 2001 295-301

[23] M. Marazuela, M. Moreno-Bondi, “Fiber-optic biosensors - an overview” Analytical and Bioanalytical Chemistry Volume **372**, Numbers 5-6 / March, 2002 p.664-682

[24] T. Geng, J. Uknalis, S. Tu, A. Bhunia. “Fiber-Optic Biosensor Employing Alexa-Fluor Conjugated Antibody for Detection of *Escherichia coli* O157:H7 from Ground Beef in Four Hours” *Sensors* 2006, **6**, 796-807

[25] D. Meadows, J. Schultz,. (1988/02)."Fiber-optic biosensors based on fluorescence energy transfer." Talanta 35(2): 145-150. http://hdl.handle.net/2027.42/27414

[26] http://www.chemistry.mcmaster.ca/faculty/brennan/fiber.html

[27] T. Kim, Z.G. Specht, P.S. Vary, and C.T. Lin, "Spectral fingerprints of bacterial strains by laser-induced breakdown spectroscopy," J. Phys. Chem. B 108, 5477-5482 (2004).

[28] D.A. Cremers and L.J. Radziemski, *Handbook of Laser-Induced Breakdown Spectroscopy*,1st ed. (John Wiley & Sons Ltd., Chichester, 2006).

[29] A. W. Miziolek, V. Palleschi, and I. Schechter, *Laser Induced Breakdown Spectroscopy*, 1st ed. (Cambridge University Press, Cambridge, 2006).

[30] J. Blacic, D. Pettit, D. Cremers, "Preliminary LIBS analysis of Yucca Mountain manganese oxide minerals" Publication Date 1996 Jan 01 OSTI Identifier OSTI ID: 176765; Legacy ID: DE96004207

[31] D. Cremers "The Analysis of Metals at a Distance Using Laser-Induced Breakdown Spectroscopy" Applied Spectroscopy, Vol. 41, Issue 4, pp. 572-579

[32] A. Ciucci, V. Palleschi, S. Rastelli, R. Barbini, F. Colao, R. Fantoni, A. Palucci, S. Ribezzo and H. J. L. van der Steen, "Trace pollutants analysis in soil by a time-resolved laser-induced breakdown spectroscopy technique" Applied Physics B: Lasers and Optics Volume **63,** Number 2 / August, 1996 p.185-190

[33] F. DeLucia Jr., A.C. Samuels, R.S. Harmon, R.A. Walters, K.L. McNesby, A. LaPointe, R.J. Winkel Jr., A.W. Miziolek, "Laser-induced breakdown spectroscopy (LIBS): a promising versatile chemical sensor technology for hazardous material

detection" Sensors Journal IEEE. Publication Date: Aug. 2005 Volume: **5**, Issue: 4 On page(s): 681- 689

[34] F. Rull, P. Martinez-Frias, J. Martinez-Frias, "Raman Spectroscopy Goes to Mars" Vol 18 NO. 1 (2006) www.spectroscopyeurope.com

[35] I. Cravetchi, M. Taschuk, Y. Tsui, R. Fedosejevs, "Scanning microanalysis of Al alloys by laser-induced breakdown spectroscopy" Spectrochimica Acta Part B **59** (2004) 1439–1450

[36] P. Lucena, J. M. Vadillo, and J. J. Laserna, "Compositional Mapping of Poisoning Elements in Automobile Three-Way Catalytic Converters by Using Laser-Induced Breakdown Spectrometry" Applied Spectroscopy Volume **55**, Number 3, 2001

[37] M. Mateo, S. Palanco, J. M. Vadillo, and J. J. Laserna. "Fast Atomic Mapping of Heterogeneous Surfaces Using Microline-Imaging Laser-Induced Breakdown Spectrometry" Applied Spectroscopy Volume 54, Number 10, 2000

[38] K. Maquelin, C. Kirschner, L.-P. Choo-Smith, N. van den Braak, H.Ph. Endtz , D. Naumann, G.J. Puppels, "Identification of medically relevant microorganisms by vibrational spectroscopy" Journal of Microbiological Methods 51 (2002) 255– 271

[39] R. Noll, H. Bette, A. Brysch, M. Kraushaar, I. onch, L. Peter, V. Sturm, "Laser-induced breakdown spectrometry - applications for production control and quality assurance in the steel industry" Spectrochimica Acta Part B **56** (2001) 637_649

[40] A. Yariv, *Quantum Electronics* 3rd Edition, (Wiley 1989)

[41] W. Koechner, *Solid-State Laser Engineering*, 2nd Edition, (Springer-Verlag 1988)

[42] F. Sears, G Salinger, *Thermodynamics, Kinetic Theory, and Statistical Thermodynamics*, 3rd Edition (Addison-Wesley 1986)

[43] I.H. Hutchinson, *Principles of Plasma Diagnostics*, 2nd Edition (Cambridge University Press 2002)

[44] R. Huddlestone, S. Leonard, *Plasma Diagnostic Techniques*, (Academic Press 1965)

[45] Derived from http://fuse.pha.jhu.edu/outreach/kit1/em.html

[46] Derived from http://www.cartage.org.lb/en/themes/sciences/astronomy/Modenastronomy/Interactionoflight/AtomicAbsorption/AtomicAbsorption.htm

[47] R. Paschotta, *Encyclopedia of Laser Physics and Technology* http://www.rp-photonics.com/encyclopedia.html

[48] Weisstein, Eric W. "Plasma Opacity" *Eric Weisstein's World of Physics.* http://scienceworld.wolfram.com/physics/PlasmaOpacity.html

[49] A.L. Peratt, "Advances in Numerical Modeling of Astrophysical and Space Plasmas" Astrophysics and Space Science, v. 242, Issue 1/2, p. 93-163 (1996)

[50] M. Baudelet, L. Guyon, J. Yu, J.-P. Wolf, T. Amodeo, E. Frejafon, and P. Laloi, "Spectral signature of native CN bonds for bacterium detection and identification using femtosecond laser-induced breakdown spectroscopy," Appl. Phys. Lett. 88, 063901-1-3 (2006).

[51] M. Baudelet, L. Guyon, J. Yu, J.-P. Wolf, T. Amodeo, E. Frejafon, and P. Laloi, "Femtosecond time-resolved laser-induced breakdown spectroscopy for detection and identification of bacteria: A comparison to the nanosecond regime," J. Appl. Phys. 99, 084701-4—9 (2006).

[52] P. Singleton, *Bacteria in Biology, Biotechnology and Medicine*, 4th ed. (Wiley, Chichester, England, 1997).

[53] Feng P, Weagant S, Grant, M (2002-09-01). "Enumeration of *Escherichia coli* and the Coliform Bacteria" *Bacteriological Analytical Manual (8th ed.)*.

[54] K. Nill, *Glossary of Biotechnology Terms*, 3rd ed. (CRC Press, 2002)

[55] K. Todar, *Online Textbook of Bacteriology* University of Wisconsin-Madison Department of Bacteriology

[56] F.R. Blattner, G. Plunkett, C.A. Bloch, N.T. Perna, V. Burland, M. Riley, J. ColladoVides, J.D. Glasner, C.K. Rode, G.F. Mayhew, J. Gregor, N.W. Davis, H.A. Kirkpatrick, M.A. Goeden, D.J. Rose, B. Mau, and Y. Shap, Science **277**, 1453 (1997)

[57] A.A. Salyers, D.D. Whitt, *Bacterial pathogenesis*, second ed., (ASM Press, Washington D.C., 2002).

[58] M. Sussman, *Escherichia coli Mechanisms of Virulence*, (Cambridge University Press, 1997)

[59] E. Lautenbach, J.B. Patel, W.B. Bilker, P.H. Edelstein, N.O. Fishman, "Extended-spectrum beta-lactamase-producing Escherichia coli and Klebsiella pneumoniae: risk factors for infection and impact of resistance on outcomes." Clinical infectious diseases 2001 Apr 15;32(8):1162-71. Epub 2001 Mar 26.

[60] *P.I. Tarr*, "Escherichia coli O157:H7: clinical, diagnostic, and epidemiological aspects of human infection." Clinical infectious diseases 1995 Jan;20(1):1-8; quiz 9-10.

[61] A.L. Baltch, R.P. Smith, Pseudomonas Aeruginosa: Infections and Treatment (Informa Health Care 1994).

[62] T. Kim, Z.G. Specht, P.S. Vary, C.T. Lin, "Spectral fingerprints of bacterial strains by laser-induced breakdown spectroscopy," J. Phys. Chem. B 108 (2004) 5477-5482.

[63] N. Hoiby, "*P. aeruginosa* in Cystic Fibrosis patients Resists Host Defenses, Antibiotics," Microbe 1 (2006) 571-576.

[64] R.M. Atlas, J.W. Snyder, *Handbook of Media for Clinical Microbiology (CRC Press, 2006)*

[65] W.T. Silfvast, *Laser Fundamentals* (Cambridge University Press, 2004)

[66] M. Bass, *Handbook of Optics*, 2nd ed. (McGraw-Hill, 1994)

[67] Images from Melles Griot website. Application Note: Microscope Objectives.

[68] Website: Melles Griot. Application Note Gaussian Beam Optics

[69] E. A Bahaa Saleh,. and C.M. Teich, *Fundamentals of Photonics*. (John Wiley & Sons., 1991)

[70] J. Taylor, *An Introduction To Error Analysis: The study of uncertainties in physical measurements*, (University Science Books, Sausalito, 1997)

[71] D. Moore *Statistics: concepts and controversies*, 4th ed. (W.H. Freeman and Company, 1996)

[72] International Union of Pure and Applied Chemistry. "helium–neon laser". *Compendium of Chemical Terminology* Internet edition.

[73] G. Williams, *Linear Algebra*, 3rd ed. (Wm. C. Brown, 1996)

ABSTRACT
LASER-INDUCED BREAKDOWN SPECTROSCOPY
ON BACTERIAL SAMPLES

BY

JONATHAN DIEDRICH

December 2007

Advisor: Dr. Steven J. Rehse

Major: Physics

Degree: Master of Science

Laser-Induced Breakdown Spectroscopy (LIBS) has many applications in medicine, industry and even the military. This research focuses on using LIBS to differentiate between different strains of the same bacterial species and between species of two similar bacteria. LIBS works by using a pulsed laser to ablate a sample material. During ablation a plasma is created which emits light from the excited atoms. The light is collected using a spectrometer and recorded. This information is then analyzed to determine the atomic composition of the sample.

I have identified 19 emission lines arising from six elements present in the bacteria in the LIBS spectra from Gram-negative bacteria. Using this information and a data analysis technique called Discriminant Function Analysis, I have shown for the first time that LIBS provides a fast, accurate method to differentiate between multiple strains of *E. coli*, including, most importantly, the pathogenic strain EHEC (*E. coli* 0157:H7) responsible for illness and death in humans. In addition, I describe the investigation of the ability to discriminate *E. coli* from the pathogenic bacterium *Pseudomonas*

aeruginosa. I also describe the effect that culturing the bacteria on various growth media has on this discrimination.

Lastly, I suggest several ways in which these results could be made more reproducible, more sensitive, and more applicable to a wider range of bacteria in future applications.

AUTOBIOGRAPHICAL STATEMENT

JONATHAN DIEDRICH

In addition to the MS degree I will be receiving from the Wayne State University I also hold a BS degree in Applied Mathematics. I received this degree in 2000 from the University of Toledo. Since then I have been employed by General Dynamics Advanced Information Systems as a Principal Engineer. I work in the EOIR (Electro Optics and Infrared) sensing group in Ypsilanti, Michigan. Here my work primarily focuses on polarimetric imaging for military applications. This new technology is incredibly interesting and has given me the opportunity to hopefully make a small difference in securing our nation. My current program has won several awards and been recognized for its impact on the global war on terrorism.

I enjoy a few hobbies including baseball and home brewing. Baseball has always been a passion of mine. I plan to use some of the data analysis techniques in this thesis and apply them to baseball statistics. I am also a member of the Society of American Baseball Research (SABR). Above all I enjoy spending time with my family.